116 p
hc - 4.00
mf - 0.25

COPY 2 of 3 COPIES

INVESTIGATION TOWARD OBTAINING SIGNIFICANTLY HIGHER MECHANICAL PROPERTIES OF AS-WELDED JOINTS IN HIGH-STRENGTH, HEAT-TREATABLE ALUMINUM ALLOYS

By

James R. Terrill

Contract No. DA-36-034-ORD-3237A
DA Project No. 1-H-0-24401-A-11-01
Final Report

July 30, 1964
Report 2-64-16

Signed *James R. Terrill* Date *July 30, 1964*
Project Engineer
Process Metallurgy Division

Approved *Fred R. Collins* Date *July 30, 1964*
Assistant Chief
Process Metallurgy Division

Approved *Allen [illegible] Russell* Date *July 30, 1964*
Chief
Process Metallurgy Division

Aluminum Company of America
Alcoa Research Laboratories
New Kensington, Pennsylvania

TABLE OF CONTENTS

Abstract 1

Introduction 3

Materials and Equipment. 5

Welding Procedure. 7

Testing

Non-Destructive Tests 8
Tensile Tests 8
Bulge Tests 8
Cracking Tests. 9
Corrosion Tests 10

Discussion

Local Heat Treatment. 11

Weld Bead Contour
Producing Nipple-Shaped Weld Beads . . 12
Nipple Beads in 1/8-in. Sheet. 18

Copper-Free Al-Zn-Mg Alloys 20

Conclusions. 26

Appendix

Local Heat Treatment of Welds 28
Weld Bead Contour 34
Nitrogen-Cooled Welds 37

References 40

Table 1 - Nominal Composition of Aluminum Base and Filler Metals 41

Table 2 - Actual Composition of Base and Filler Metals. 42

Table 3 - Mechanical Properties of DCSP-GTA Welds in 1/8-in. 71/8-T6 Sheet (X5180 Filler) Locally Heat-Treated in Horizontal Position with Infrared Heating Lamps. 43

Table 4 - Properties of Frankford and Early Alcoa-Made DCRP-GMA Welds. 44

Table 5 - Mechanical Properties of .090-in. 2014-T6 Sheet DCRP-GMA Welded (716 Filler) With Various Ar-He Mixtures 45

Table 6 - Weld Bead Dimensions of DCRP-GMA Welds in .090-in. 2014-T6 Sheet. 46

Table 7 - Mechanical Properties of 1/8-in. 7178-T6 Sheet (716 Filler) DCRP-GMA Welded with Different Ar-He Shielding Gas Mixtures 47

Table 8a - Mechanical Properties of 1/8-in. High-Strength Alloy Sheet DCRP-GMA Welded with Conditions that Produced Pronounced Nipple-Shaped Beads 48

Table 8b - Welding Conditions Used in DCRP-GMA Welding 1/8-in. Sheet to Achieve Pronounced Bead Contour 50

Table 9 - Cracking Tests of Experimental Copper-Free Al-Zn-Mg Alloys. 51

Table 10 - General Correlation of Weld Cracking Results With Anticipated Difficulty in Welding. . . . 52

Table 11 - Base Metal Mechanical Properties for M791 and M793 (.128") Sheet 53

Table 12 - Weld Cracking Tests on M791 and M793 Alloys . 54

Table 13 - Mechanical Properties of DCSP-GTA Welded 1/8-in. M791 and M793 Sheet. 55

Table 14 - Stress Corrosion Results on Post-Weld Aged M791 and M793-T6 Sheet 56

Table 15 - Weld Cracking Tests of Cu-Free Al-Zn-Mg Alloys Containing Zirconium 56

Table 16 - Mechanical Properties of DCSP-GTA Welded 1/8-in. Sheet of Cu-Free Al-Zn-Mg Alloys Containing Zirconium 57

Table 17 - Comparison of Properties of DCSP-GTA And DCRP-GMA Welded 1/8-in. Al-Zn-Mg Alloy Sheet 58

Table 18 - Properties of Reheated DCSP-GTA Welds In 1/8" 7178-T6 Sheet - X5080 Filler 59

Table 19 - Properties of Reheated DCSP-GTA Welds In 1/8" 7178-T6 Sheet - X5080 Filler 60

Table 20 - Mechanical Properties of DCSP-GTA Welds In 1/8-in. 7178-T6 Sheet (X5080 Filler) Reheated to 870 F with Quartz Infrared. . . . Lamps and Water Quenched. 61

Table 21 - Mechanical Properties of DCSP-GTA Welds in 1/8-in. 7178-T6 Sheet (X5080 Filler) Reheated with Quartz Infrared Lamps Then Aged 8 hrs at 212 F + 3 hrs at 325 F. 62

Table 22 - Comparison of Mechanical Properties of Infrared Locally-Heated DCSP-GTA Welds in 1/8-in. 7178-T6 sheet (X5080 Filler) 63

Table 23 - Mechanical Properties of DCRP-GMA Welds in .090-in. 2014-T6 Sheet Made at Various Travel Speeds on Steel Backing Bar 64

Table 24 - Mechanical Properties of DCRP-GMA Welds in .090-in. 2014-T6 Sheet Made at Various Travel Speeds on Copper Backing Bar 64

Table 25 - Mechanical Properties of DCRP-GMA Welds in .090-in. 2014-T6 Sheet (716 Filler) Welded with Decreasing Arc Current at Constant Travel Speed. 65

Table 26 - Mechanical Properties of .090-in. 2014-T6 Sheet DCRP-GMA Welded (716 Filler) on a Liquid Nitrogen-Cooled Backing Bar. 66

Figure 1 - Equipment for DCRP-GMA welding panels for bead contour studies

Figure 2 - Close-up of welding table showing close positioning of hold-down plates

Figure 3 - Welded panel from which tensile and bulge test specimens were removed

Figure 4 - Types of tensile failures. Symbols A, B and C are used in the Tables

Figure 5 - Types of failure of sheet specimens in bulge test

Figure 6a - Weld cracking specimen

Figure 6b - Welding procedure for cracking test

Figure 7 - Schematic diagram of horizontal infrared lamp heating unit

Figure 8 - Horizontal infrared heating apparatus with a 14 x 16 welded 1/8-in. 7178-T6 panel in position

Figures 9 - DCRP-MIG welds in .090-in. 2014-T6 sheet
10

Figure 11 - Properties of DCRP-GMA welds in .090-in. 2014-T6 sheet made with various Ar-He gas mixtures

Figures 12 - DCRP-GMA welds in .090-in. 2014-T6 sheet
13

Figures 14 - DCRP-GMA welds in .090-in. 2014-T6 sheet
15

Figures 16 - DCRP-GMA welds in .090-in. 2014-T6 sheet
17

Figures 18 - DCRP-GMA welds in .090-in. 2014-T6 sheet
19

Figure 20 - Microstructure of the partially-melted zone in the DCRP-GMA weld in .090-in. 2014-T6 sheet

Figure 21 - DCRP-GMA welds in 1/8-in. sheet made with conditions that produced pronounced nipple-shaped weld beads

Figure 22 - Hot short cracking in X7006/X5080 combination

No cracking with X7106/X5180, which contains Zr

Figure 23 - 1/8-in. M791-T6 sheet DCSP-GTA welded with 9Zn-3Mg filler

Figure 24 - 1/8-in. M793-T6 sheet DCSP-GTA welded with 9Zn-2Mg filler

Figure 25 - 1/8-in. M793-T6 sheet DCSP-GTA welded with 9Zn-2Mg filler. Weld bead shaved flush.

Figure 26 - Oxyacetylene flame heating apparatus for local heat treating of welds

Figure 27 - Schematic illustrating the principal components of the above flame heating apparatus

Figure 28 - DCSP-GTA welds in 1/8-in. 7178-T6 sheet

Figure 29 - Hinged multiple-element quartz infrared heaters positioned above a water quench tank

Figure 30 - Welded panel being locally heat treated. The supporting wire was snipped to drop the panel into the water.

Figure 31 - Properties of DCSP-GTA welded 1/8-in. 7178-T6 sheet locally heat treated with quartz infrared heaters mounted vertically

Figure 32 - Temperature profile of 1/8 x 14 x 16-in. panel locally heat treated vertically between two banks of infrared heaters

Figure 33 - DCRP-GMA welds in .090-in. 2014-T6 made at 160, 140 and 130 amps at 26 volts, 55 ipm, 17Ar-33He

Figure 34 - Shows the change in bead shape of DCRP-GMA welds in .090-in. 2014-T6 sheet made with decreasing gas flow

Figure 35 - DCRP-GMA welds in .090-in. 2014-T6 sheet showing changes in bead shape with increasing weld travel speed

Figure 36 - DCRP- IA welds in .090-in. 2014-T6 sheet showing change in bead shape with 100% Ar shielding and decreasing weld travel speed

Figure 37 - DCRP-GMA welds in .090-in. 2014-T6 sheet made with 10Ar-65He cfh shielding gas mixture

Figure 38 - Frankford DCRP-GMA welds in .090-in. 2024-T86 sheet made on a liquid nitrogen-cooled and room-temperature backing bar. Notice the difference in width of the heat-affected zones.

Figure 39 - Frankford DCRP-GMA welds in .090-in. 2014-T6 sheet

Figure 40 - Shows the difference in cell size in the weld nugget and in the width of the partially-melted zone between welds in .090-in. 2024-T86 made on a liquid nitrogen-cooled and room-temperature backing bars.

Figure 41 - DCRP-GMA welds in .090-in. 2014-T6 sheet showing the smaller cell size and narrower partially-melted zone in a liquid nitrogen-cooled weld than in a weld made on a room-temperature backing bar.

IMPROVEMENT OF MECHANICAL PROPERTIES IN WELDED, HIGH-STRENGTH, HEAT-TREATABLE ALUMINUM ALLOYS

By

James R. Terrill

ABSTRACT

This report describes the third phase(1,2) of an investigation to improve welds in high-strength aluminum alloys such as 7178 and 2014.

Local heat treatment of welds for 10 minutes at 885 F followed by cold water quenching and artificial aging markedly improved mechanical properties of welded 7178-T6 sheet.

Nipple-shaped beads characteristic of DCRP-GMA welds made by Frankford with brine cooling were reproduced in .090-in. 2014-T6 sheet without a refrigerated backing bar by proper balance of energy input and shielding gas flow during welding. Narrow heat-affected zones that followed bead contour were achieved by positioning hold-down plates close to the sheet edges being welded. Use of 5-20 per cent argon in the argon-helium shielding gas mixture decreased root bead angle and increased tensile properties from 5 to 7 ksi.

Copper-free Al-Zn-Mg alloys DCSP-GTA welded with compatible fillers and post-weld artificially aged developed

---

1. Collins, F.R., "Investigation Toward Obtaining Significantly Higher Mechanical Properties of As-Welded Joints in High-Strength, Heat-Treatable Aluminum Alloys," DA Project 593-32-005, Sept. 6, 1961

2. Collins, Fred R., "Investigation Toward Obtaining Significantly Higher Mechanical Properties of As-Welded Joints in High-Strength, Heat-Treatable Aluminum Alloys," DA Project No. 1-H-0-24401-A-111-01, Sept. 20, 1963

remarkably high strengths with excellent longitudinal ductility but high susceptibility to stress corrosion cracking. With bead reinforcement intact, tensile failures occurred in base metal 1/4 to 1/2 inch from the weld. The best combination, based on both strength and ductility, was Al-6.5Zn-2.5Mg base metal welded with Al-9Zn-2Mg filler. For many service environments, more compatible fillers are needed for these high-strength alloys.

INTRODUCTION

In Phase II of this investigation, the results of initial attempts to locally heat treat welds using heat from a low-current arc were reported. Brown and Adams(3) showed that weld beads could be solution heat treated in a very short time because of their small dendritic cell size. Locally applied arc heating was tried in an attempt to solution heat treat the weld prior to post-weld aging of welded structures. Slow arc travel speeds were employed to attain 850 to 900 F solution heat treating temperatures for 7075 and 7178. In spite of local re-melting in the weld bead faces and wide heat affected zones, ductility measured by both tensile elongation and bulge height was improved. Controlled flame and electrical resistance heating for locally heat treating welds were evaluated during this third and final phase of the research investigation.

A second area of study during the third phase was investigation of factors affecting weld bead contour in direct current reverse polarity inert-gas metal-arc welds in high-strength aluminum alloy sheet. Schillinger et al reported and later published(4) properties of DCRP-GMA welds in .090-in. 2014-T6 sheet that averaged 10 per cent

---

3. Brown, P.C. and Adams, C.M. Jr., "Fusion Zone Structures and Properties in Aluminum Alloys," Welding Journal 39, (12) Research Supplement, 520-s to 524-s (1960)

4. Schillinger, D.E. Et al, "Improved Weld Strength in 2000 Series Aluminum Alloys," Welding Journal 42, (6) Research Supplement, 269-s to 275-s (1963)

higher tensile strengths than published typical values. One distinguishing feature of Frankford Arsenal's high-strength welds was pronounced nipple-shaped weld beads. Previous welds had bulbous-shaped beads. Factors that control bead shape and weld penetration in DCRP-GMA welded sheet were investigated.

A separate Alcoa-funded investigation showed that 7075-type alloys with low copper and with manganese substituted for chromium gave improved reheat-treated weld strengths. In Alcoa's armor plate program, the beneficial effects of zirconium in reducing weld cracking were established. Several copper-free Al-Zn-Mg base metals and filler metals with and without zirconium were included in this investigation to establish weldability, mechanical properties, and corrosion resistance of promising high-strength base-filler combinations.

This report describes the investigations on local heat treating of welds, bead contour studies, and weldability of controlled composition Al-Zn-Mg alloys.

MATERIALS AND EQUIPMENT

Materials used in this investigation were predominantly 7178 and 2014 base metals, X5080, X5180, and 716 filler metals, and experimental Al-Zn-Mg base and filler metals. Nominal and chemical compositions of these and other alloys mentioned later in this report are listed in Tables 1 and 2. The bulk of the welding studies was conducted on .090-in. or 1/8-in. thick sheet panels of the various base metals using .035 or 3/64 and 1/8-in. filler wire for inert gas metal-arc (GMA) and inert gas tungsten-arc (GTA) welding respectively.

Welding equipment consisted of the following:

DCSP-GTA Automatic

Welder: Airco Heliarc automatic head, Model HMH-E, with 1/8-in. diameter, 2 per cent thoriated tungsten electrode.

Power Supply: Airco 300 amp AC-DC Heliwelder, Model 3 ADB-245CHABP, 60 per cent duty cycle.

Carriage: Oxweld type CM-37.

Table: 36-in. welding table with grooved copper plate backing and water pressure hold-down fixturing.

DCRP-GMA Automatic

Welder: General Electric Model 36761 automatic head with Model 6WGF 201A2 wire feed and Model 6WGF80A1 welding torch.

Power Supply: Linde Model SVI-500 amp, variable slope and inductance DC welder.

Table: 36-in. welding table with grooved copper plate or hollow bar backing and air pressure hold-down fixturing.

The GMA welding equipment is pictured in Figures 1 and 2.

AC-GTA Manual

Power Supply: Airco 300 amp AC-DC Heliwelder, Model No. 3ADB-245CHABP.

Torch: Linde Model HW 12 Heliarc welding torch with 1/4-in. diameter tungsten electrode.

Auxiliary Equipment

Esterline-Angus Model AW automatic chart recorders were used to record volts and amps at the welding head.

Shielding gases were welding grade Linde argon and Airco helium.

WELDING PROCEDURE

14 x 16-in. welded specimens for tensile and bulge testing were prepared from pairs of 7 x 16-in. panels sheared from .090 or 1/8-in. sheet stock. Sheared panels were degreased and caustic-nitric etched. Immediately prior to welding, the edges were draw filed and the adjacent surfaces hand wire brushed. Panels were positioned and clamped in the hold-down fixtures and square-butt welded automatically by direct current, straight polarity inert-gas tungsten-arc (DCSP-GTA) or direct current, reverse polarity inert-gas metal-arc (DCRP-GMA) welding methods with the following procedures:

	DCSP-GTA	DCRP-GMA	AC-GTA*
Welding position	flat	flat	flat
Preheat	none	none	300 F
Filler metal dia. - in.	3/64	.035	1/8
Shielding gas	He	Ar-He	Ar
Shielding gas flow - cfh	80	15-75	50
Arc voltage - volts	12-13	21-29.5	-
Current - amps	200-250	140-255	300
Joint type	square butt	square butt	inverted tee
Wire feed rate - ipm	50	450-550	80-84 in./spec.
Travel speed - ipm	20	55-110	-
Starting tab	yes	yes	-
Welding direction	parallel to rolling direction	parallel to rolling direction	-

*For cracking tests, 1/2 and 1-in. plate was sawed to size, degreased, and caustic-nitric etched prior to welding.

TESTING

Non-Destructive Tests

Welds were inspected visually for smooth flow and complete and uniform penetration. Each weld was radiographed using a suitable penetrameter. Welds that did not exhibit soundness at least as good as Class 2 ABMA-PD-R-27 were not further tested.

Tensile Tests

Two standard ASTM tensile specimens were machined from a 2-in. wide strip sawed from each of the 14 x 16-in. welded panels (Figure 3). One specimen was tensile tested to failure with the bead reinforcement removed ("bead off"); the second had bead reinforcement intact ("bead on"). Two-inch gage marks centered across the weld were used in determining per cent elongation. Results were reported as averages of duplicate or triplicate tests for each welding condition. Types of tensile failures are shown in Figure 4. Symbols A, B, or C denoting type of failure are used later in the tables.

Bulge Tests

The remaining 14 x 14-in. panel from the original 14 x 16-in. specimen was biaxially stressed in a hydraulic bulge tester.[5] Prior to testing, the bead reinforcement was removed approximately 2-1/2 in. from each end with a

---

5. Robinson, I.B., Collins, F.R., and Dowd, J.D., "The Hydraulic Bulge Test for Welded Aluminum Sheet," Welding Journal 39, (12), Research Supplement (1961) 540-s to 545-s

Zephyr weld shaver. Flush beads on the ends were needed to permit clamping of the panel between the 8-in. nominal diameter bulge testing dies. Duplicate or triplicate welded panels were tested for each welding condition. Figure 5 shows diagramatically the types of failures incurred in sheet specimens in the biaxial test. Symbols 1 to 7 are used in the tables of strength data to denote the different types of bulge failures.

Cracking Tests

Alcoa's cracking test consists of manual GTA welding both fillets of an inverted T specimen using base and filler metal combinations to be evaluated. A cracking specimen, shown in Figure 6a, consists of a 1/2-in. thick 4 x 10-in. vertical plate and a 1-in. thick, 4 x 10-in. base plate of the same alloy. The two plates are tack welded together, preheated with an oxyacetylene torch to 300 F, then fillet welded using continuous or discontinuous welding (Figure 6b) according to the procedure in the last column, Page 7.

The discontinuous weld is a series of overlapping welds. The welder melts a small puddle at the fillet with his torch held stationary, adds filler metal, moves his arc ahead to allow the pool to solidify and returns the arc to make another pool which overlaps the previous one. In this manner, the maximum thermal stress on the weld is induced and cracking will occur to various extents depending upon the hot-short crack sensitivity of the base-metal-filler metal combination.[6] Continuous rather than intermittent fillet welds are made in the continuous test. Duplicate tests generally agree within ± 1 inch. Crack lengths are measured for both tests and cracking rated on an established comparative basis. Cracking tests were conducted on several experimental high-strength Al-Zn-Mg alloys.

Corrosion Tests

Stress corrosion of the Al-Zn-Mg alloys was evaluated on duplicate assemblies of two weld strip specimens stressed against each other over an "H" beam to an outer fibre stress of 30 ksi, approximately 50 per cent the yield strength. One assembly had the weld faces stressed in tension; the other had the roots in tension. Stressed and unstressed pairs were exposed to 3-1/2 per cent NaCl solution by alternate immersion (10 minutes in, 50 minutes out) and to the industrial atmosphere at New Kensington, Pennsylvania.

---

6. For a more detailed description of the cracking test see Dowd, J.D., "Weld Cracking of Aluminum Alloys," Welding Journal 31, (10), Research Supplement, 448-s to 456-s (1952)

DISCUSSION

Local Heat Treatment

Oxyacetylene and quartz infrared lamp heating were evaluated for controlled temperature local heat treating of welded 7178-T6 panels. The preliminary work and equipment revisions that led to a successful heating procedure are described in the Appendix.

Early in the resistance heating work, radiant heating both sides of a panel simultaneously was found necessary to eliminate warping due to thermal stresses. Also, double-side heating panels in a vertical position produced temperature gradients from top-to-bottom. A horizontal heating apparatus was constructed to overcome this "chimney effect" that produced low strength areas. Infrared lamps were hinged to allow heating in a horizontal position with provision for upending to drop the unclamped heated panel into the water quench (Figures 7 and 8).

A series of panels of DCSP-GTA welded 1/8-in. 7178-T6 sheet was heated in the horizontal position. Temperatures were fairly uniform along the length of the weld. Tensile and bulge properties for these welds locally heated to 885 F and 925 F, held at temperature for up to 20 minutes, then cold water quenched and step aged 8 hrs at 212 F + 3 hrs at 325 F, are listed in Table 3. Reference values are provided for comparison in Table 20.

Tensile and bulge properties generally increased with heating time and with local heat-treating temperature. In general, properties were best with 10 minutes heating at both the 885 and 925 F temperatures. Both tensile and bulge properties of the 925 F heated welds are higher than the welds heated vertically 10 minutes at 870 F (refer to Tables 20 & 21) and are quite close to the optimum properties attained with post-weld solution heat treatment and artificial aging to the -T6 type temper.

A significant improvement of mechanical properties of welded, high-strength aluminum alloys with local heat treatment is demonstrated. A useable procedure of two-side heating of the welds in a horizontal position has evolved from this work. Electrical radiant tube heating, which provides good temperature control, could be adapted for local heat treating of welds in structures too large for full solution heat treatment after welding. Highest recovery in strength is achieved by water quenching following local heat treating. If water quenching is too severe for large structures where warping might be a problem, less drastic quenching could be employed. Additional work with oxyacetylene flame heating would probably lead to a second useable technique for local heat treatment of welds.

Weld Bead Contour

Producing Nipple-Shaped Weld Beads

Frankford Arsenal DCRP-GMA welds in .090-in. 2014-T6 and 2024-T86 (716 filler) exhibited consistently high bulge strengths in Alcoa tests. Frankford requested Alcoa weld similar alloy panels duplicating as nearly as possible their welding conditions. These welds averaged 19-22 per cent lower bulge strengths than previously tested Frankford welds (Table 4). Metallographic examination showed they had bulbous beads characteristic of DCSP-GTA welds in sheet (Figure 28) whereas the Frankford-made welds had pronounced nipple-shaped beads (Figure 9). Frankford reported their welding schedules were established by exploratory welding at different travel speeds until the desired penetration and bead contour were achieved. Power input, heat flow, backing bar materials, and shielding gases were reviewed to establish their effect on bead shape

Preliminary investigations on welding parameters and procedures that led to a successful method of obtaining high-strength, nipple-shaped weld beads are discussed in the Appendix.

Studies of changing bead contour with parameter changes established 140 amps, 26 volts, 65 ipm travel speed, 75 cfh gas flow, and close clamping on a copper backing bar as conditions that achieved most pronounced nipple-shaped welds in DCRP-GMA welded .090-in. 2014-T6 sheet. Tensile and bulge properties of welds made with these conditions are listed in Item 1 of Table 5.

Dowd[7] found that argon-helium shielding gas mixtures containing 50-65 per cent helium were superior to argon, helium, or other mixtures for consumable-electrode welding of aluminum. His findings were based on occurence of porosity, hot-short cracking, deposition rate, and ease of welding 5052 base metal with 5154 filler Strength of these

---

7. Dowd, J D., "Inert Shielding Gases for Welding Aluminum," <u>Welding Journal 35</u>, (4), Research Supplement, 207-s to 210-s (1956)

is affected little by bead contour. To establish what effect argon additions to helium shielding have on mechanical properties and weld shape, DCRP-GMA welds in .090-in. 2014-T6 sheet were made with different argon-helium mixtures. Also, it was hoped that an optimum shielding gas mixture matched with heat input could be found to achieve consistently highest strength welds.

The first weld series was made with 75 cfh He, 10Ar-65He, 25Ar-50He, 40Ar-35He, and 65Ar. Cross-weld tensile and bulge properties are listed in Table 5. Reference values are listed for comparison in Table 26.

The 10 cfh argon addition to the helium gas shield improved tensile and bulge strengths and elongations. Additions of argon above 25 cfh in the mixture had little effect on properties. To check the validity of these findings, additional welds with 5, 10, 15, and 20 cfh argon additions were made. The 10Ar-65He test was intended as a check on the earlier 10Ar-65He welds made. Properties of these welds are also listed in Table 5. In Figure 11a and 11b, the data are plotted as strength vs argon flow and per cent argon in the shielding mixture. The second set of welds made with 5 to 20 cfh argon confirmed the earlier findings that properties for welds in .090-in. sheet are highest with Ar-He mixtures that contain low proportions of argon. The ideal range of argon was established at 5-25 per cent, balance helium at 75 cfh gas flow.

Russian workers[8] concluded that high proportions of He in Ar-He mixtures make the consumable electrode welding process more stable and increases the depth of penetration by 50-100 per cent. The ideal helium content for Ar-He mixtures, they found, was 75-85 per cent. Our few tests suggested 75-95 per cent.

Figures 12-19 show the weld cross section of mounted broken tensile specimens from the series with Ar-He mixtures. All of the welds exhibit a pronounced smooth reverse ogee contour. The welds are similar in appearance with only small differences in shape and contour to account for the difference in mechanical properties. Some pertinent observations can be drawn from the weld bead dimensions listed in Table 6.

Width and thickness of the bead face and root were measured from the 10X photomicrographs. Values of root angle ϕ were computed, assuming the root bead as a circular segment, and using the root height (y) and width (x) values in the mensuration formula for circular segments[9]. Computed values were considered to be more accurate than optically determined values even though the root beads were not always true circular segments. In general, agreement between computed and optically determined angles was reasonable.

---

8. Rabkin, D.M., Ryabov, V.R., and Dovbishchenko, I.V., "Helium and Helium-Argon Mixtures Used for Welding Aluminum Alloys," Automatic Welding, (9) pp 1-5 (1963)

9. Machinery's Handbook, 14th Edition, Industrial Press, New York, p 152 (1949)

The face width decreased and the bead thickness increased generally with increasing argon content in the gas mixture. As the proportion of argon is increased, it becomes necessary to increase the electrode wire feed rate to stabilize the arc and minimize weld spatter and inconsistent penetration. With the increase in wire feed, more filler is deposited, which makes the beads thicker. Arc current also increases. A drop in arc voltage occurred which in turn caused a decrease in the electrode-to-work distance. The arc cone impinging on the sheet became smaller and caused a gradual narrowing of the weld faces. The net result is that less base metal was melted by the arc and more filler was deposited in the weld.

In the pure helium weld (Figure 12) the bead consists of a higher percentage of fused base metal and less filler than do the other welds. The lowest strength material is in the partially-melted zone where failure occurred.

The 10Ar-65He weld (Figure 14) contains more of the lower strength filler metal and the zone of failure has now been shifted slightly from the weld edge into the weld metal. Failures initiated at the root notch and continued through the weld bead, not through the cast-wrought interface. This cannot account for the 5-8 ksi increase in tensile strength. The high increase likely is due to the larger root angle which decreases the stress-raiser effect of the notch. This seems to be characteristic of low-argon welds and becomes apparent when root bead angle is plotted against increasing argon. Angle values, when plotted against per cent argon in the 75 cfh Ar-He shielding mixture (Table 6), followed a trend similar to the curves of tensile and bulge strength vs per cent argon illustrated in Figure 11b.

Argon ionizes more readily than helium, and being a denser gas, conducts heat more efficiently into the weld. At the same time, with argon added, current is higher and arc voltage lower which provides more efficient heat transfer for the same heat input. These factors increase penetration and bead formation and can result in less drop-through on the root side.

The welds made with greater than 25 per cent argon (Figures 18 and 19) contain predominantly 716 filler in the bead. Failures occur through the weld in each case and the mechanical properties are nearly the same for argon concentrations above 25 per cent (Figure 11b).

Figure 20 shows the fusion zones of the straight He and 10Ar-65He welds at high magnification. No important differences were found between microstructures of the two welds.

Cross-weld tensile properties of welds made with low proportions of argon exceed tensile properties of welds made by Frankford. Bulge strengths are not quite as high although biaxial ductility is slightly higher. There is strong evidence to suggest that the 68 ksi bulge strength value for the Frankford welds (Table 4) is in error. This value is an average of four bulge tests on panels welded at Frankford and tested by Alcoa. The letter report on these tests[10] cites that a damaged bulge height follower was discovered after the tests were conducted. A correction was added to the observed bulge heights. Tensile values were not available though, at the time, to verify the correction factor. In comparing tensile and bulge strength now, there is no valid reason why bulge strength should be significantly higher than tensile strength.

Higher mechanical properties in single pass inert-gas metal-arc welds can be obtained by employing close clamp-down fixtures and proper weld settings that achieve pronounced nipple-shaped beads. Still higher properties are then possible by using gas mixtures containing small amounts of argon. Significantly, nipple-shaped welds and associated high strengths are possible without resorting to brine or liquid nitrogen cooling.

Nipple Beads in 1/8-in. Sheet

A few panels of 1/8-in. 7178-T6 sheet were DCRP-GMA welded to determine if weld properties could be markedly improved with nipple-shaped bead contours. Cross-weld tensile and bulge properties are listed in Table 7 with references provided for comparison. Higher strength welds were produced with a 25Ar-50He mixture than with 15Ar-60He shielding which was so effective for welding .090-in. 2014-T6 sheet. Strengths seemed to increase with increasing argon.

---

10. Collins, F.R. to Frankford Arsenal, Att: Mr. D.E. Schillinger ORDBA-1323, August 2, 1962

It may be that the "ideal range of argon" for 1/8-in. sheet is increased over that for .090-in. sheet. Also, 7178 may not respond to slight changes in heat input brought about by changing the proportions of argon in the shielding mixture as did 2014. Or, as the listed heat inputs indicate, higher strengths might have been achieved by welding faster to lower the energy input. Additional tests could establish a heat input—heat dissipation balance with a set of welding conditions to achieve pronounced papillary depression in the bead and probably attain the higher strengths.

Properties of 1/8-in. 2014-T6 sheet and other high-strength, heat-treatable alloys DCRP-GMA welded with ·ked nipple-shaped beads were also evaluated. Sheet panels of 8 different alloys were welded with 716 and X5180 fillers using conditions that produced desired bead contours. Cross-weld tensile and bulge properties are listed in Table 8a; welding conditions are listed in Table 8b.

As-welded properties were higher with X5180 filler than with lower-strength 716 filler. No comparative values for welds in 2014, 7075, and 7178 base metal made with X5180 filler are listed. These combinations were too crack sensitive to be GMA welded at high speed in our tests. The base metals had lower solidus temperatures than the fillers and solidification stresses caused severe cracking in the base metal at the edge of the weld.

Post-weld aging did not improve 7075 and 7178 welded with 716. Aging lowered the ductility and bulge failures shifted from longitudinal to transverse. Some increase in properties occurred in 2014 welds with aging. Figure 21 shows the microstructure and bead contour in as-welded and post-weld aged 2014 welds.

Al-Zn-Mg alloys inert-gas metal-arc welded with X5180 filler developed quite high properties and responded well to artificial aging. Highest properties were attained in M791 and copper-free Al-6Zn-2Mg (285568) base metals. Actual composition of these Al-Zn-Mg alloys are listed in Table 2. Figure 21 shows cross sections through 1/8-in. X7106 and M791 sheet DCRP-GMA welded with X5180 filler. Bead contours are of the desirable shape.

Copper-Free Al-Zn-Mg Alloys

In the Phase II Report[2], it was recommended that the weldability of new Al-Zn-Mg alloys of lower copper than 7178 and 7075 be investigated and filler metals of 6-8 Zn, 2-4 Mg be developed to reduce weld cracking and improve longitudinal weld elongation. These promising areas were explored in Phase III.

Three experimental copper-free Al-Zn-Mg base metals were chosen for evaluation because in both the Phase II work and concurrent Alcoa-funded investigations, crack sensitivity was found to increase as copper content increased. Standard cracking tests were performed to determine the susceptibility of hot-short cracking on the copper-free Al-Zn-Mg alloys. Inches of cracking and relative ratings are listed in Tables 9 and 10.

All of the combinations cracked less than 7075 welded with base metal. These alloys are less susceptible to grain-boundary melting because they contain no copper. For the alloys welded with base metal, cracking decreased as the magnesium content in the filler increased. The 6Zn-3Mg alloy (285427) would be expected to crack very little in sheet butt-welds in which the weld is composed predominantly of base metal.

The 6Zn, 2-3Mg base metals welded with M743 filler are "Commercially Weldable" combinations, Table 9. Base metals welded with the other fillers evaluated could be "Welded With Care." The titanium in M743 accounts for the lower cracking than occurred with the 6Zn-3Mg-OTi filler.

While these tests were underway, an Alcoa in-house research program on armor plate revealed that a minor addition of zirconium, acting as a grain refiner, reduced hot-short cracking in GTA welding Al-Zn-Mg alloys. Figure 22, showing cross sections through fillets of cracking tests, illustrates the beneficial effect of zirconium. In the case of X7006 welded with X5080 filler, neither of which contains zirconium, large columnar grains formed in the weld and cracking was frequent. In the X7106/X5180 combination, both the base metal and filler contain zirconium. Zirconium promoted formation of fine, equiaxed grains, shown in the inset in Figure 22, to reduce hot-short cracking.

In light of the promising results with zirconium, further work on the Al-Zn-Mg alloys without zirconium was halted pending fabrication of new alloys. In the interim, weldability studies were started on two available Alcoa-developed Al-Zn-Mg alloys containing zirconium. These alloys, M791 and M793, which attain high naturally-aged properties (see Table 11), were welded with filler metals containing 6-9 Zn and 2-3 Mg. Standard cracking tests to establish which base metal-filler metal combination had the lowest sensitivity to hot-short cracking are reported in Table 12. The 6Zn-3Mg-.2Zr filler gave the least amount of cracking, but each of the combinations could be considered "Easy to Weld" in the comparative rating. M791 welded with filler 285431 (Al-9Zn-3Mg), which does not contain zirconium, cracked 17 inches. This combination would be rated barely "Commercially Weldable." With 285404, a similar filler containing zirconium, only 8 inches of cracking occurred in the discontinuous test. Cross-weld tensile and bulge properties for these alloys welded with Al - 6 and 9 Zn - 2 and 3 Mg filler metals are listed in Table 13.

M793 welded with either 6Zn-2Mg or 9Zn-2Mg filler developed higher as-welded properties than did M791 welded with the 6-9Zn, 2-3Mg fillers. Surprisingly, tensile and bulge failures occurred in the parent sheet, in the zone 1/8 to 1/4 inch from the weld that became partially annealed from the heat of welding. Weld efficiency, based on tensile strength, was 78 per cent.

Artificially-aged welds in both M791 and M793 had good longitudinal ductility, indicated from bulge heights that ranged from 0.90 to 1.10 inch. Highest post-weld aged properties were achieved in M791 welded with the 9Zn-3Mg filler. Weld efficiency was 86 per cent. In bulge and tensile testing, most failures occurred in the base metal away from the weld. Several of these outstanding examples were photographed to show location of failure and typical weld microstructures with and without post-weld aging (Figures 23-25).

Strip specimens, prepared from DCSP-GTA welded panels of 1/8-in. M791 and M793, were tested as described on Page 10, to establish their stress corrosion behavior. Test results are summarized in Table 14.

Post-weld artificially aged M791-T6 sheet welded with 6-9Zn, 2-3Mg fillers was highly susceptible to stress corrosion cracking and failures occurred in both alternate immersion in salt solution and industrial atmosphere exposures. Failures occurred in post-weld aged M793-T6 sheet in alternate immersion, but no failures occurred in the industrial atmosphere exposure after 73 days exposure. Failures could be expected with longer exposure times, however. Metallographic examination showed that the items failed as a result of stress corrosion cracking in the partially-melted weld metal-base metal transition zone.

Alcoa-funded investigations indicate post-weld solution-heat treatment before artificial aging improves the stress corrosion performance of welded Al-Zn-Mg alloys.

Post-weld artificially-aged M791 and M793-T6 joints using the 6-9 Zn, 2-3 Mg filler metals do not have sufficient stress corrosion resistance to be recommended for many service environments. More compatible fillers and better post-weld aging are needed for these high-strength alloys.

Three new Cu-free Al-Zn-Mg alloys, nominally 6Zn-2Mg, 6Zn-3Mg, and 6.5Zn-2.5Mg, each containing .15 Zr, were welded with the 6-9Zn, 2-3Mg fillers previously used with M791 and M793. Results of weld cracking tests are listed in Table 15.

These base metal-filler metal combinations cracked from 9-15 inches, in the severe discontinuous test. The higher Mg fillers, 6Zn-3Mg and 9Zn-3Mg, produced less cracking than did the lower Mg fillers; but all of these combinations could be considered "Easy to Weld" in a comparative rating. On an overall basis, the 6Zn-3Mg and the 9Zn-3Mg fillers gave the same amount of cracking.

Panels of 1/8-in. thick sheet of the three Cu-free Al-Zn-Mg alloys containing zirconium were DCSP-GTA welded with zirconium-containing 6-9Zn, 2-3Mg fillers. Post-weld artificially-aged cross-weld tensile and bulge properties are listed in Table 16.

The 6Zn-2Mg alloy (285568) welds developed remarkably high bulge heights (from 1 to 1-1/4 inches), which denotes excellent longitudinal ductility. Bulge and tensile strengths were equivalent. With the bead reinforcement intact, tensile failures for all base-filler combinations occurred in the base metal 1/4 to 1/2 inch away from the weld.

Welds in the 6Zn-3Mg base metal developed slightly higher tensile and yield strengths than did the 6Zn-2Mg welds made with the same filler metal. Cross-weld and longitudinal ductility, though, were lower.

The 6.5Zn-2.5Mg base metal welds developed the highest tensile and bulge strengths and retained high ductility. The best combination, based on both strength and ductility, is 6.5Zn-2.5Mg base metal welded with 9Zn-2Mg filler. This last group of alloys was not corrosion tested.

Properties of DCSP-GTA and DCRP-GMA welded 1/8-in. sheet of the Al-Zn-Mg alloys containing zirconium are compared in Table 17. With bead reinforcement intact, GMA properties approached or, as for M791, equaled the high properties developed in DCSP-GTA welds.

The Al-Zn-Mg alloys hold great promise as high-strength, easily-weldable alloys. More work is needed to establish compatible fillers and thermal treatments to overcome the problem of stress corrosion cracking.

CONCLUSIONS

Mechanical properties of welded 7178-T6 sheet were markedly improved by locally heat treating the weld with quartz infrared lamps. Ultimate tensile and bulge strengths of local heat-treated and aged welds were 87 and 115 per cent of welds reheat-treated to the -T6 temper. Best properties were obtained by heating the welds horizontally 10 minutes at 885 F with quartz infrared lamps spaced 2 inches apart followed by cold water quenching and artificial aging.

High gains in strength and ductility of DCRP-GMA welds in 2014-T6 sheet were achieved by producing weld beads having pronounced papillary depressions. Weld contour could be controlled by proper balance of energy input, heat extraction, and shielding gas flow during welding. Narrow heat-affected zones that followed bead contour were obtained by positioning hold-down plates close to the sheet edges being welded. A 5-20 per cent argon, balance helium shielding gas mixture flowing at 75 cfh produced shallower root bead angles that increased tensile strengths 2-4 ksi. Welds up to 10 ksi stronger than those normally obtained prior to this investigation were achieved.

Copper-free Al - 6 to 6.5 Zn - 1.5 to 3 Mg alloys DCSP-GTA welded with Al-Zn-Mg fillers of 6-9Zn, 2-3Mg and post-weld artificially aged developed remarkably high strengths with excellent cross-weld and longitudinal ductility. With bead reinforcement intact, tensile and bulge failures occurred in the base metal. The best combination, based on strength and ductility, was Al-6.5Zn-2.5Mg alloy welded with Al-9Zn-2Mg filler. Alternate immersion corrosion tests of welded M791 and M793 in 3-1/2 per cent NaCl solution showed that these alloys, when post-weld artificially aged, are highly susceptible to stress corrosion cracking. Post-weld heat-treated and aged Al-Zn-Mg weldments are less susceptible to stress corrosion cracking. With more compatible fillers, high-strength Al-Zn-Mg alloys can be useful engineering alloys for many applications.

In the course of this work:

1. A procedure was developed to locally heat treat welds in structures too large to be furnace heated.

2. DCRP-GMA welding procedures were improved so that higher strength welds in 2014-T6 alloy sheet can be obtained.

3. A better understanding of the factors controlling weld bead shape, which markedly influences weld properties, was established.

4. Experimental high-strength Al-Zn-Mg alloys proved easy to weld and yielded high weld efficiency.

These were essentially the objectives of the program.

APPENDIX

The Appendix describes the preliminary tests and results that led to the successful procedures developed for local heat treating welds and producing high-strength, nipple-shaped welds reported in the Discussion.

Local Heat Treatment of Welds

A flame heating apparatus was constructed to further explore local heat treatment of welds begun during Phase II of this investigation. In the first experimental set-up, an oxyacetylene torch and water spray quenching device were mounted on a controlled speed motor-driven carriage. DCSP-GTA welded panels of 1/8-in. 7178-T6 sheet were laid horizontally on firebrick supports in an otherwise empty container. The weld bead and heat affected zones were locally heated by traversing the torch along the horizontally positioned panel. The flame jets impinged on the face side of the weld bead; water spray was directed onto the heated panel immediately behind the torch flame. Warpage of the unrestricted panel was severe. Also, stray splash and steam often extinguished the oxyacetylene flame. These difficulties led to revision of the apparatus.

In the second set-up, the torch was held stationary and the panel, in its clamping fixture, was lowered vertically past the torch and into a water quench tank. Speed of the descending panel was regulated by a Variac-controlled motor and gear reducer (Figures 26 and 27).

Travel speeds were found, for different flame lengths, to achieve heat treating temperature within the 870-925 F range recommended for 7178 alloy. Temperatures were determined both with temperature-sensitive lacquers and with percussion-welded thermocouples connected to a high-speed recorder.

Some of the early panels warped badly and failed in bulge tests at sub-normal bulge pressures. With an improved welded steel angle clamping fixture, bowing was greatly reduced--but not sufficiently to permit meaningful bulge testing. Mechanical testing was confined to cross-weld tensile specimens to establish improvement gained in weld properties. Tensile properties of these welds, which were not aged after flame heating, are listed in Table 18.

Welds quenched rapidly after heating showed increased tensile elongations but lower tensile strengths than unheated welds. Those quenched directly behind the oxyacetylene flame (1-1/2 i .) showed the least drop in yield strength for the accompanying gain in elongation. Low strengths were probably due to the slight bow in the specimens that introduced a bending stress during testing. Metallographic comparison of microstructures did not show any significant changes in the structure of the weld or heat-affected zones brought about by flame heating. Yet mechanical properties showed some benefits achieved with the local heat treatment. The critical zones were apparently not at heat-treating temperature long enough to attain maximum benefit. Figure 28 shows the microstructure of reheated and unheated welds in 1/8-in. 7178-T6 sheet

(X5080 filler). No melting occurred in welds reheated with an oxyacetylene flame.

Heating from both sides was considered to minimize thermal stresses causing warpage. Resistance heated quartz infrared lamps were used in the double-side heating apparatus. Variac control regulated the heat-treating temperatures to permit the beneficial metallurgical changes to occur in the weld bead and heat-affected zones. Some slight bowing might be expected and could be tolerated. For normal slight bowing, clamping stresses could be computed from strain gage measurements and be accounted for in determining true bulge stress. While the heating apparatus was being revamped, some panels were heated with a low-current arc to provide a comparison for flame-heated welds.

Panels were clamped in the original hold-down fixture on the welding table. Thermocouples were percussion welded to the root side of the weld bead for temperature measurement. The welds were insulated from the copper backing bar with sheet insulation. Welds were reheated with AC-GTA, DCSP-GTA, and DCRP-GTA arcs at different currents and travel speeds to vary the heat input. Reverse polarity gas tungsten-arc heating was evaluated because it might provide a softer arc for reheating than did the alternating current, argon shielded, gas tungsten arc used in the Phase II investigation. Cross-weld tensile properties for "bead on" and "bead off" specimens are listed in Table 19.

Some improvement in tensile elongation was gained with each of the arc heating methods. This gain, though, was accompanied by a decrease in yield strength. Small longitudinal cracks in each of the welds reheated with the argon-shielded DCRP-GTA arc account for the low strengths even though the root bead reached only 800 F. Tensile properties with helium-shielded DCSP-GTA or argon-shielded AC-GTA arc reheating may have been higher if the welds were quenched rapidly from the heat-treating temperature. Air-blast or water-spray quenching was considered, but work was postponed pending the promising results with double-side heating. Figure 28c shows the microstructure of a weld reheated with a low current DCSP-GTA arc. The bead face was partially re-fused during local heating.

The third experimental setup for local heat treating of welds involved double-side heating using quartz infrared lamps. The apparatus consisted of six resistance-heated infrared elements vertically mounted in two hinged fixtures positioned above a water quench tank (Figures 29 and 30). The three elements in each hinged fixture could be spaced 1 or 2 inches apart to locally heat a 1 or 2-inch band on either side of the weld. Panels to be heated were suspended unclamped between the two hinged fixtures, heated to temperature, then quenched by snipping the wire supporting the panel and letting the panel drop into the cold water quench tank.

Temperatures were measured with a high-speed recorder using percussion welded thermocouples on the root bead. Good temperature control was maintained by adjusting Variacs that controlled power to the quartz infrared lamps.

DCSP-GTA welded (X5080 filler) 1/8-in. 7178-T6 panels were heated to 870 F and held from a few seconds to 20 minutes, and cold water quenched. Two-side heating of unclamped panels followed by very rapid quenching virtually eliminated warpage. Tensile specimens were removed from both the top and bottom of each panel because the top and bottom experienced different temperatures during heating. Tensile and bulge properties are listed in Table 20. The data are plotted in Figure 31.

Tensile and bulge strength and elongation generally increased with heat treating time. In comparing these properties with the listed reference typical properties for as-welded or post-weld aged 7178-T6, the improvement in strength and ductility gained through local heat treatment becomes obvious. For instance, after 10 minutes heating with a 2-in. element spacing, tensile and bulge strengths are equivalent to those obtained when welded 7178-T6 is given an optimum post-weld aging treatment of 8 hrs at 212 F + 3 hrs at 325 F. Tensile elongation and bulge height though were markedly higher.

"Bead-off" tensile strength and elongation were, in many cases, higher than the corresponding "bead-on" values. Normally, the reverse is true. The weld face or root bead may have acted as a notch or stress concentrator to give lower values. Yet strengths were surprisingly high, approaching the maximum -T6 properties achieved by a full post-weld solution-heat treatment and aging treatment.

Although bulge strength and maximum bulge height values were gratifyingly high, these values must be viewed with some reservation. The values, calculated from the membrane formula, do not necessarily represent the true biaxial stress imposed on the weld. The reason for this is that with the vertical heating setup a chimney effect produces a higher temperature at the top of the panel than at the bottom. For instance, when the top of the panel was at 870 F, the measured temperature at the bottom was approximately 790 F. Figure 32 shows a temperature profile of a typical heated panel. Thus, the weld and heat-affected zones at the bottom of the panel did not experience the same degree of metallurgical change as occurred at the top at 870 F.

Certain areas of the panel reached 600 F temperature, a temperature that has previously been shown to produce the lowest properties in 7178-T6 sheet.[(2)]. In such areas a greater amount of local yielding tended to mask the true yielding that took place in the weld. The spherical geometry of the panel in test was changed slightly because of this yielding some distance away from the weld. The local heat treatment, never-the-less, did improve bulge properties.

Another set of vertically heated panels was artificially aged after infrared heating. Tensile and bulge properties for these welds, step-aged 8 hrs at 212 F + 3 hrs at 325 F, are listed in Table 21. Typical properties of as-welded, post-weld aged, and post-weld solution heat-treated and aged 7178-T6 are listed for reference. The mechanical properties of as-quenched and quenched and artificially aged welds that were infrared heated for 10 and 20 minutes are listed in Table 22 for comparison.

As expected, tensile and bulge properties after aging are higher than as-quenched properties. In some instances tensile and yield strengths decreased with time at heat-treating temperature, whereas previously reported as-quenched values generally increased with heat-treating time. Still the properties approach the optimum properties attained with full solution heat treatment to -T6 temper. For instance, after 10 minutes heating with a 2-in. element spacing, tensile and yield strengths are 94 and 91 per cent of those when welded 7178-T6 is reheat-treated to -T6. Bulge strength and bulge height are equivalent or higher. A revised apparatus that overcame the chimney effect is described in the Discussion.

ely

Weld Bead Contour

Panels of .090-in. 2014-T6 were DCRP-GMA square-butt welded (716 filler) on a steel backing bar and a copper backing bar to try to produce nipple-shaped weld beads. Voltage, current, and gas flow were held constant and travel speed increased from 60 ipm in 5 or 10 ipm increments until the weld no longer penetrated the root side. With the steel bar, which contained a 1/4-in. wide x 1/32-in. deep rectangular groove, 80 ipm was the limit in travel speed for full penetration welds. With the copper backing bar having a 1/8-in. radius x 1/32-in. deep groove, full penetration welds could be made up to 105 ipm with the same parameters used in welding on the steel backing bar. Cross-weld tensile and bulge properties of these welds are listed in Tables 23 and 24. Macrographs of welds made at 60, 80, and 105 ipm are shown in Figure 10.

No pronounced deep central core of penetration resembling a nipple shape was obtained. Bead contours of the 105 ipm weld approached the ogee curve contour of the Frankford welds (Figure 9). The width and shape of the overaged band revealed by etching that the Alcoa and Frankford-made welds were different. In the Frankford welds, the backing bar was in intimate contact with the bottom surface of the sheet next to the bead root and dissipated heat rapidly from the weld during early solidification. Our copper backing bar was bowed slightly and prevented intimate contact.

A new backing bar was constructed and the welding fixture was revised to increase clamping pressure. DCRP-GMA welds were made in .090-in. 2014-T6 sheet using different arc currents at constant travel speed. Mechanical properties of these welds, post-weld aged 10 hrs at 340 F, are listed in Table 25. Macrographs of welds made at 160, 140 and 130 amps are shown in Figure 33.

The desired central deep core of penetration was obtained with 140 amps. Penetration was marginal with 130 amps and somewhat excessive in the off-centered 160-amp weld. This series established a heat input condition to achieve marked papillary depression, but nipple-shaped beads were not produced repetitively. The heat-affected bands were just commencing to follow the nipple shape of the weld beads. These welds were made with the hold-down plates 1/2 to 3/4 in. from the abutted sheet edges, which is a normal distance in conventional semi-automatic welding. Very close clamping, perhaps 1/4-in., was indicated to obtain a more pronounced contour. On this premise, the hold-down fixturing was revised for clamping very close to the abutted edges.

Using the established travel speed - arc current values as a starting point, shielding gases in DCRP-GMA welding of .090-in. 2014-T6 sheet were investigated to study their role in affecting bead shape. A series of welds was made at fairly constant energy input (140 amps, 26 volts, 65 ipm travel speed) but with increased flow rate of helium shielding gas. Quarter-size panels were welded and immediately sectioned, filed, and etched to provide a quick answer to how a change in any parameter affected bead contour. Figure 34 shows the gradual change from a narrow root bead and sharply defined papillary depression to a wide root bead and bulbous weld by decreasing helium flow. Welding was most consistent in the 60-75 cfh range of helium flow. Undercutting, at the edge of the bead face commenced at about 60 cfh flow and increased as helium flow decreased. Narrow heat affected zones that follow the bead contour as a result of very close clamping are readily evident. Figure 35 shows the change in bead shape of welds made at fairly constant volts x amps and 75 cfh helium flow and increased travel speed. Papillary depression in the bead was achieved at each travel speed, but penetration and bead size diminished with increasing travel speed, as would be expected.

Welds made with 100 per cent argon at decreasing travel speeds are shown in Figure 36. Because of argon's different ionization characteristics, higher current and lower arc voltage were required. The higher heat input generally produced a wider heat affected zone. Weld beads were generally quite porous with 100 per cent argon shielding.

These studies established 140 amps, 26 volts, 65 ipm travel speed, 75 cfh gas flow, and close clamping on a copper backing bar as conditions that achieved most pronounced papillary depression and best heat-affected zone contour in the .090-in. sheet welds. Investigation of various argon-helium mixtures in the 75 cfh gas flow established ideal gas mixtures for producing highest strength welds. These results appear in the Discussion.

Nitrogen-Cooled Weld

To establish whether rapid heat extraction would produce a more pronounced bead contour or other change that would influence mechanical properties, .090-in. 2014-T6 sheet was square-butt, DCRP-GMA welded with low proportions of argon on a liquid nitrogen-cooled backing bar. In the set-up, the entire welding table was enclosed in a plastic bag. After clamping the panels in place, the bag was sealed and purged for a short time with nitrogen and helium. Liquid nitrogen was passed through a hollow copper backing bar and exhausted inside the bag below the welding table. In this way, any moisture present condensed on the lower walls and permitted welding with no visible frost on the panel or backing bar. Mechanical properties of a limited number of welds made with liquid nitrogen cooling and the welding conditions used are listed in Table 26. Properties of room-temperature welds and of Frankford-made welds are provided for reference comparison.

The Alcoa-made welds on a refrigerated backing bar developed lower properties than those made at room temperature. In comparing Alcoa and Frankford-made welds, Alcoa's liquid nitrogen-cooled welds have properties equivalent to Frankford's room-temperature welds, and their welds made on a chilled backing bar have strengths equal to our room-temperature welds. These observations are made on the results of only a few tests on a nitrogen-cooled bar. With additional work, it is probable that weld conditions could be found to increase the properties of chilled welds to equal or to exceed the high properties achieved at room temperature. Figure 37 shows cross sections through welds made on a liquid nitrogen-cooled and room-temperature backing bar. Bead dimensions are listed in Table 6.

During a visit to Frankford, samples were removed from earlier bulge-tested panels of Frankford-made welds for metallographic comparison. The panels were .090-in. 2024-T86 or 2014-T6 sheet welded on a liquid nitrogen-cooled or room temperature backing bar, then either naturally or artificially aged. Figures 38-41 show the welds at low and high magnification.

The welds made on a nitrogen-cooled backing bar (Frankford Nos. 93B, 95B, and 100A) have a narrower heat-affected zone than do those made on a room-temperature backing bar (Nos. 121B, 118A, and 109A).

The differences in width of the heat-affected zones are obvious in Figures 38 and 39. In addition, the welds made on a room-temperature backing bar exhibited a denser general precipitate in the overaged region in the parent sheet than did welds made using a nitrogen-cooled backing bar. No significant differences, however, were evident in grain-boundary precipitation.

The most pronounced microstructural differences between the two weld types, besides the width of the heat-affected zones, were in cell size at the edge of the weld nugget and width of the partially melted zone. These are shown in Figures 40 and 41. The nitrogen-cooled welds have a smaller cell size and narrower partially melted zone.

These findings agree with earlier reported work by Frankford.

REFERENCES

1. Collins, F.R., "Investigation Toward Obtaining Significantly Higher Mechanical Properties of As-Welded Joints in High-Strength, Heat-Treatable Aluminum Alloys," DA Project 593-32-005, Sept. 6, 1961

2. Collins, Fred R., "Investigation Toward Obtaining Significantly Higher Mechanical Properties of As-Welded Joints in High-Strength, Heat-Treatable Aluminum Alloys," DA Project No. 1-H-0-24401-A-111-01 Sept. 20, 1963

3. Brown, P.C. and Adams, C.M. Jr., "Fusion Zone Structures and Properties in Aluminum Alloys," Welding Journal 39, (12), Research Supplement, 520-s to 524-s (1960)

4. Schillinger, D.E. et al, "Improved Weld Strength in 2000 Series Aluminum Alloys," Welding Journal 42 (6), Research Supplement, 269-s to 275-s (1963)

5. Robinson, I.B., Collins, F.R., and Dowd, J.D., "The Hydraulic Bulge Test for Welded Aluminum Sheet," Welding Journal 39 (12), Research Supplement 540-s to 545-s (1961)

6. Dowd, J.D., "Weld Cracking of Aluminum Alloys," Welding Journal 31 (10), Research Supplement, 448-s to 456-s (1952)

7. Dowd, J.D., "Inert Shielding Gases for Welding Aluminum," Welding Journal 35, (4), Research Supplement, 207-s to 210-s (1956)

8. Rabkin, D.M., Ryabov, V.R., and Dovbishchenko, I.V., "Helium and Helium-Argon Mixtures Used for Welding Aluminum Alloys," Automatic Welding (9), pp 1-5 (1963)

9. Machinery's Handbook, 14th Edition, Industrial Press, New York, p 152 (1949)

10. Collins, F.R. to Frankford Arsenal, Att: Mr. D.E. Schillinger ORDBA-1323, August 2, 1962

TABLE 1

NOMINAL COMPOSITION OF ALUMINUM BASE AND FILLER METALS

Element	Si	Fe	Cu	Mn	Mg	Cr	Zr	Zr	Ti
Base Metals									
2014	.8	-	4.4	.8	.4	-	-	-	-
7075	-	-	1.6	-	2.5	.3	5.6	-	-
X7106	-	-	-	.2	2.25	.1	4.25	.15	-
7178	-	-	2.0	-	2.7	.3	6.8	-	-
M791	-	-	-	.2	2.3	.2	6.5	.12	-
M793	-	-	-	.2	1.5	.2	6.5	.12	-
Filler Metals									
716 (4145)	10	-	4	-	-	-	-	-	-
X5080	-	-	-	.5	-	-	2	-	.1
X5180	-	-	-	.5	4	-	2	.15	.1
M577	-	-	-	.1	4	.1	4	-	.1
M743	-	-	-	-	3	-	6	-	.2

TABLE 2

ACTUAL COMPOSITION OF BASE AND FILLER METALS

Element	Si	Fe	Cu	Mn	Mg	Cr	Ni	Zn	Ti	Zr
Base Metal										
M791	.09	.16	.12	.21	2.22	.13	.00	6.20	.01	.10
M793	.09	.18	.12	.20	1.64	.13	.00	6.54	.01	.10
285428	.06	.19	.01	.11	2.06	.11	.00	5.91	.04	.00
27	.06	.19	.01	.11	3.10	.11	.00	5.92	.03	.00
29	.06	.20	.00	.11	2.54	.11	.00	6.51	.04	.00
285568	.05	.17	.02	.11	1.98	.09	.02	5.84	.06	.18
69	.06	.18	.01	.09	3.00	.08	.02	5.92	.06	.15
70	.05	.18	.01	.11	2.52	.10	.02	6.45	.06	.17
Filler Metals										
M577	.07	.09	.03	.10	3.75	.09	-	3.98	.03	-
M743	.08	.15	.01	.01	3.01	.00	-	5.93	.17	-
285431	.07	.00	.00	.00	2.99	.00	.00	8.94	.13	.00
266060	.10	.14	.06	.55	1.99	.00	.01	5.95	.11	.21
62	.10	.13	.07	.01	3.03	.00	.01	5.92	.10	.20
63	.10	.13	.07	.01	2.04	.00	.01	8.86	.10	.23
285404	.06	.19	.05	.01	3.00	.00	.00	8.81	.09	.22

TABLE 3

MECHANICAL PROPERTIES OF DCSP-GTA WELDS IN 1/8-IN. 7178-T6 SHEET (X5180 FILLER) LOCALLY HEAT TREATED IN HORIZONTAL POSITION WITH INFRARED HEATING LAMPS

Time at Temp			Top of Panel			Bottom of Panel			Bulge		
Min.	°F	Bead	TS ksi	YS ksi	% El 2 in.	TS ksi	YS ksi	% El 2 in.	BS (1) ksi	Hgt. in.	Failure Type (2)
.1	925	on	25.5	*	0	75.3	71.5	1.5	33.5	.35	1
		off	77.8	71.6	2.0	71.6	65.1	1.5			
1	925	on	31.5	*	0	72.3	71.6	1.0	43.5	.41	1
		off	76.3	70.3	2.5	74.0	67.1	2.5			
10	925	on	85.3	77.6	3.0	83.3	76.3	3.0	73.1	.58	1
		off	21.5	*	0	82.0	73.4	4.0			
20	925	on	77.3	74.6	2.0	82.8	76.3	2.0	73.7	.67	1
		off	80.7	72.7	3.0	81.5	73.7	2.5			
5	885	on	71.1	*	1.5	80.4	73.2	2.5	68.8	.55	1
		off	75.4	70.1	2.0	76.2	68.3	2.5			
10	885	on	76.3	72.0	2.0	75.8	69.6	2.0	78.2	.77	1
		off	74.3	69.5	3.0	75.8	68.3	2.5			
20	885	on	79.5	73.1	3.0	77.8	69.4	3.0	72.4	.70	1
		off	77.5	69.2	3.5	74.6	67.2	3.0			

* Failed before reaching 0.2% offset (1) Bulge Strength (2) See Figure 5

All panels cold water quenched and aged 8 hrs at 212 F + 3 hrs at 325 F after heating with 2-in. element spacing.

TABLE 4

PROPERTIES OF FRANKFORD AND EARLY ALCOA-MADE DCRP-GMA WELDS IN .090-IN. SHEET

			Tensile			Bulge	
Base Metal	Welded By	Bead	TS	YS	% El	BS	Hgt.
2014-T6	Frankford	on	60	56	.8	68	.49
	Alcoa	on	55	51	1.5	53	.49
	Unwelded	-	70	60	10	73	1.9
2024-T86	Frankford	on	-	-	-	65	.4
	Alcoa	on	-	-	-	53	.4
	Unwelded	-	-	-	-	77	1.7

2014-T6 panels post-weld aged 10 hrs at 340 F

2024-T86 panels post-weld aged 8 hrs at 375 F

Filler metal- .035-in. 716 (4145)

TABLE 5

MECHANICAL PROPERTIES OF .090 IN. 2014-T6 SHEET DCRP-GMA WELDED (716 FILLER) WITH VARIOUS Ar-He MIXTURES

Shielding Gas		Arc	Arc	Heat		Tensile Test				Bulge Test		
Ar cfh	He cfh	Current amps	Voltage volts	Input Joules/in	Bead	TS ksi	YS ksi	% El 2 in.	Failure Location	BS ksi	Hgt in.	Failure Type
0	75	141	26	3380	on	58.4	56.7	1.0	A	51.7	.46	2
					off	53.7	48.8	1.5	A			
5*	70	145	26	3480	on	62.8	59.0	1.3	A	60.2	.53	2
					off	57.0	52.2	1.5	A			
10	65	150	26	3600	on	63.7	58.0	1.5	A	57.8	.55	3
					off	55.0	51.6	1.5	A			
10*	65	150	26	3600	on	65.4	59.8	1.8	A	58.5	.52	3
					off	54.3	52.7	1.5	A			
15*	60	155	25.5	3650	on	65.6	60.3	1.5	A	56.4	.52	2
					off	58.2	54.6	1.5	A			
20*	55	160	25	3690	on	63.5	59.9	1.2	A	58.2	.53	2
					off	56.6	52.7	1.7	A			
25	50	162	24.5	3660	on	61.6	57.2	1.3	A	48.6	.47	2
					off	54.5	51.9	1.3	A			
40	35	170	22.5	3530	on	60.7	57.9	1.0	A	49.7	.47	2
					off	54.6	50.4	1.5	A			
65	0	175	21.0	3390	on	61.4	57.5	1.0	A	51.2	.48	2
					off	54.8	52.2	1.5	A			

All panels welded at 65 ipm travel speed and post-weld aged 10 hrs at 340 F.
Values are averages of triplicate tests
* Denotes second series of tests

TABLE 6

WELD BEAD DIMENSIONS OF DCRP-GMA WELDS IN .090-IN. 2014-T6 SHEET

Shielding Gas Ar cfh	Shielding Gas He cfh	Heat Input joules/in	W mm	t mm	x mm	y mm	ϕ avg.
0	75	3380	84	38	34	9	124°
5	70	3480	82	36	33	7.5	133
10	65	3610	84	38	35	7	137
15	60	3650	78	37	31	7.5	126
20	55	3690	77	38	31	8.5	123
25	50	3660	77	39	37	10	123
40	35	3530	79	40	39	10	126
65	0	3390	73	41	28	7	127
Liquid nitrogen-cooled weld - See figure 38							
10	65	3740	86	42	35	6	126

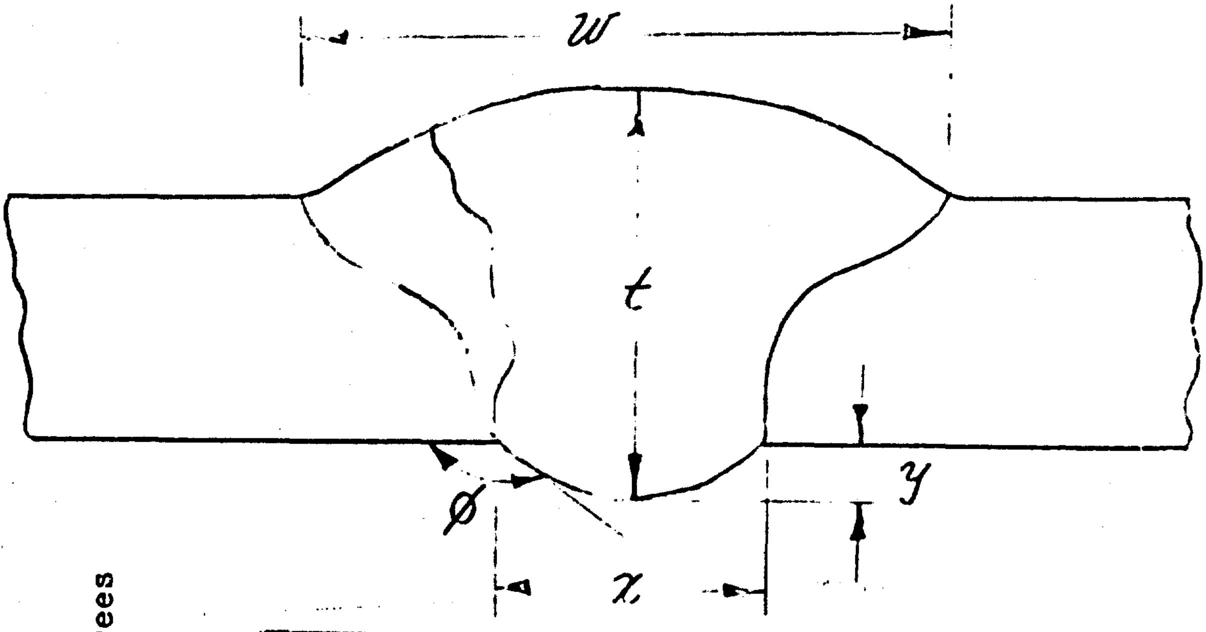

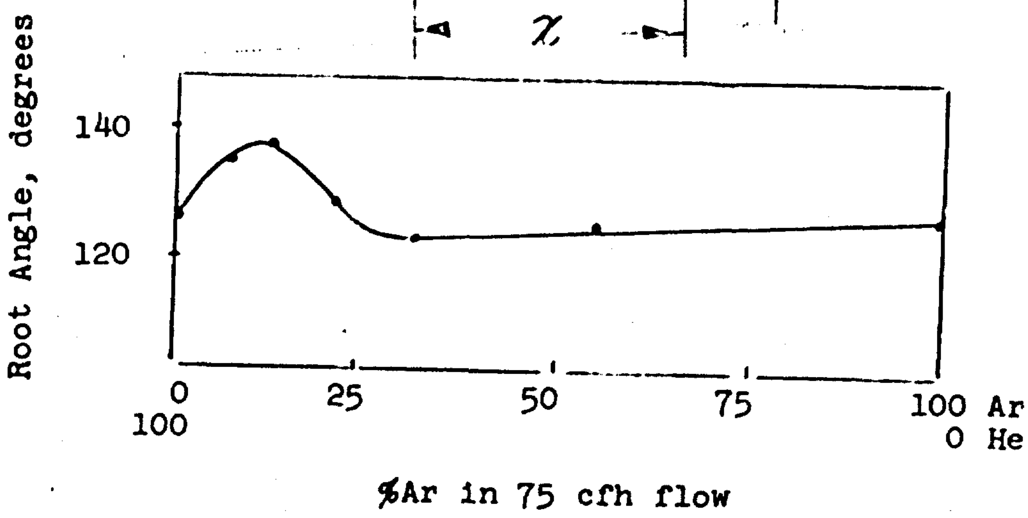

TABLE 7

MECHANICAL PROPERTIES OF 1/8-IN. 7178-T6 SHEET (716 FILLER) DCRP-GMA WELDED WITH DIFFERENT Ar-He SHIELDING GAS MIXTURES

Ar cfh	He cfh	Post Weld Treat*	Bead	Tensile Test TS ksi	YS ksi	% El 2 in	Failure Location	Bulge Test BS ksi	Hgt in.	Failure Type
15	60	A	on	48.0	PF**	0.5	A	47.7	.40	2
			off	47.1	45.4	1.0	A			
25	50	A	on	53.3	PF	0.8	A	49.9	.44	2
			off	46.3	PF	1.0	A			
50	25	B	on	54.6	PF	1.0	A	40.3	.41	4
			off	52.9	PF	0.5	A			
Reference - .090-in. GMA***										
17	33	C	on	60.1	PF	0.5	B	45.7	.41	4
			off	53.6	52.3	0.5	A	40.6	.37	3

Welding Conditions

Ar cfh	He cfh	amps	volts	Travel Speed ipm	Heat Input joules/in.
15	60	200	29.5	40	8850
25	50	195	25.8	40	7550
50	25	220	23.0	55	5520
17	33	200	25	80	3750

* A - Aged 24 hrs at 250 F
B - Aged 8 hrs at 225 F + 16 hrs at 300 F
C - Aged 8 hrs at 212 F + 3 hrs at 325 F

** Premature Failure - specimens failed before reaching .2% offset

*** Data taken from "Phase Report No. 2", Table III, p 32, Reference 2

TABLE 8a

MECHANICAL PROPERTIES OF 1/8-IN. HIGH-STRENGTH ALLOY SHEET DCRP-GMA WELDED WITH CONDITIONS THAT PRODUCED PRONOUNCED NIPPLE-SHAPED BEADS

				Tensile Test				Bulge Test		
Base Metal	Filler Metal	Thermal Condition	Bead	TS ksi	YS ksi	% El 2 in.	Fail. Loc.	BS ksi	Hgt in.	Fail. Type
2014-T6	716	As-welded	on	52.5	41.9	1.5	A	54.4	.51	2
			off	42.9	34.3	1.5	A			
		Aged	on	54.7	48.9	1.5	A	56.0	.52	4
			off	45.0	41.1	1.2	A			
7075-T6	716	As-welded	on	53.0	*	1.0	A	53.8	.49	2
			off	47.3	44.4	1.0	A			
		Aged	on	54.3	*	0.5	A	51.7	.49	4
			off	54.3	*	0.5	A			
7178-T6	716	As-welded	on	55.7	55.0	1.0	A	52.4	.50	2
			off	49.1	46.2	1.0	A			
		Aged	on	54.6	*	1.0	A	40.3	.41	4
			off	52.9	*	0.5	A			
X7106-T6	716	As-welded	on	48.1	42.0	1.8	A	50.1	.51	2
			off	42.9	36.0	1.5	A			
		Aged	on	53.0	51.0	2.8	A	47.5	.46	2
			off	48.0	47.5	0.8	A			
X7106-T6	X5180	As-welded	on	55.2	40.0	5.0	B	52.6	.80	1 & 7
			off	43.4	33.5	3.7	A			
		Aged	on	54.7	44.9	6.0	C	55.3	.88	1 & 7
			off	45.8	39.1	3.3	A			
285568-T6	716	As-welded	on	52.7	48.5	0.8	A	55.6	.53	2
			off	48.6	40.7	1.2	A			
		Aged	on	58.5	*	0.5	A	54.2	.49	3
			off	50.5	*	1.0	A			
285568-T6	X5180	As-welded	on	61.9	48.4	3.2	A	60.1	.61	3
			off	45.9	37.3	2.5	A			
		Aged	on	66.8	58.0	5.2	A	63.2	.92	3
			off	47.8	45.6	1.5	A			
285569-T6	716	As-welded	on	48.1	*	0.8	A	49.3	.45	2
			off	43.6	41.9	0.8	A			
		Aged	on	53.3	*	0.7	A	43.6	.40	4
			off	49.1	*	0.5	A			
285569-T6	X5180	As-welded	on	55.0	48.9	1.2	A	54.9	.52	3
			off	48.8	37.5	3.0	A			
		Aged	on	63.5	60.5	1.3	A	63.5	.61	3
			off	50.0	47.0	1.8	A			

continued

TABLE 8a CONTINUED

Base Metal	Filler Metal	Thermal Condition	Bead	Tensile Test TS ksi	YS ksi	% El 2 in.	Fail. Loc.	Bulge Test BS ksi	Hgt. in.	Fail. Type
285570-T6	716	As-welded	on	52.8	51.7	1.0	A	50.2	.44	2
			off	47.2	42.7	0.8	A			
		Aged	on	50.4	*	0.8	A	48.5	.46	4
			off	49.9	*	0.7	A			
285570-T6	X5180	As-welded	on	62.1	51.9	2.2	A	59.9	.58	2
			off	47.3	38.3	2.5	A			
		Aged	on	65.8	63.2	1.5	A	62.8	.57	3
			off	53.4	49.7	1.8	A			
M791-T6	716	As-welded	on	51.0	*	1.0	A	49.7	.43	2
			off	44.0	39.9	1.0	A			
		Aged	on	58.3	*	1.0	A	46.3	.42	3
			off	47.7	*	0.5	A			
M791-T6	X5180	As-welded	on	61.2	50.6	2.3	B	54.7	.67	1
			off	48.1	39.7	2.2	A			
		Aged	on	67.4	58.4	5.5	B	64.6	.78	3
			off	54.0	49.1	1.8	A			

* Specimens broke before reaching 0.2% offset

Values listed are average of triplicate tests except for a few cases where one out of 3 failed before reaching 0.2% offset.

Aged specimens were held 4 days at R.T. after welding then aged 8 hrs at 225°F + 16 hrs at 300 F

TABLE 8b

WELDING CONDITIONS USED IN DCRP-GMA WELDING 1/8-IN. SHEET TO ACHIEVE PRONOUNCED BEAD CONTOUR

Base Metal	Filler* Metal	Amps	Volts	Heat Input Joules/in.
2014-T6	716	220	23.5	5640
7075-T6	"	220	23.0	5520
7178-T6	"	220	23.0	5520
X7106-T6	"	210	23.0	5270
285568-T6	"	220	23.0	5520
285569-T6	"	220	23.0	5520
285570-T6	"	220	23.0	5520
M791-T6	"	220	23.0	5520
X7106-T6	X5180	250	24.0	6540
285568-T6	"	255	23.5	6540
285569-T6	"	255	23.0	6400
285570-T6	"	250	23.0	6270
M791-T6	"	255	24	6680

* 3/64-in. diameter

Travel speed - 55 ipm
Shielding gas mixture - 25Ar-50He (cfh)

TABLE 9

CRACKING TESTS OF EXPERIMENTAL
COPPER-FREE Al-Zn-Mg ALLOYS

Base Metal	Filler Metal	Inches of Cracking Continuous	Inches of Cracking Discontinuous
285428	285428	10	18
	M577	3	18
	M743	0	17
	285431	1	17
285427	285427	1	17
	M577	2	17
	M743	1	15
	285431	1	16
285429	285429	7	18
	M577	1	18
	M743	1	16
	285431	1	17
7075	7075	13	20
	M743	0	17

Values are averages of duplicate tests that varied within ±1 in. except for 285429 welded with base metal, which cracked 3-3/4 and 11 inches in the two tests.

Base Metal

285428 - 6Zn-2Mg-0Cu
27 - 6Zn-3Mg-0Cu
29 - 6.5Zn-2.5Mg-0Cu

Filler Metal

M577 - 4Zn-4Mg
M743 - 6Zn-3Mg + .2Ti
285431 - 9Zn-3Mg

TABLE 10

GENERAL CORRELATION OF WELD CRACKING RESULTS WITH ANTICIPATED DIFFICULTY IN WELDING

Crack Sensitivity Rating	In. Weld Cracking		Welding Characteristics	Typical Examples
	Cont. Test	Disc. Test		
A	0	0-6	Very easy to weld with automatic or manual methods, even when the joint is under restraint.	5456/5556 2219/2319 6061/4043
B	0	6-12	Easily welded with automatic or manual methods but joint restraint should be minimized.	5154/5154
C	0-2	12-17	Commercially weldable, but requires close control of fitup, preheat, and travel speed. May crack in highly restrained repair welds.	5454/5554
D	2-8	17-20	Weld with care. Requires precise control of welding parameters.	2014/2014 5052/5052
E	8-20	17-20	Weld with extreme care. Normally not recommended	7075/7075 2024/2024

TABLE 11

BASE METAL MECHANICAL PROPERTIES
FOR M791 AND M793 (.128") SHEET

Alloy	Thermal Treatment*	Specimen Direction**	TS ksi	YS ksi	% El 2 in.
M791	Art. Aged	Long.	69.6	62.6	10.2
		Trans.	70.4	63.2	11.0
	Nat. Aged	Trans.	75.8	54.4	16.8
M793	Art. Aged	Long.	66.9	60.6	11.5
		Trans.	65.9	59.3	11.5
	Nat. Aged	Trans.	73.8	54.7	16.0

* Artificially aged -- solution heat treated at 860 F, stretched, aged 8 hrs at 225 F + 16 hours at 300 F four days after quenching.

Naturally aged -- solution heat treated at 860 F, aged 3 months at room temperature after quenching.

** Longitudinal or transverse with respect to rolling direction.

TABLE 12

WELD CRACKING TESTS ON M791 AND M793 ALLOYS

Base Metal	Filler	Inches Cracking Continuous	Inches Cracking Discontinuous
M791	266060	-	9
	266062	-	5
	266063	-	8
	285404	-	8
	285431	0	17
M793	266060	-	8
	266062	-	8
	266063	-	9
	285404	-	7

Nominal Compositions

	Zn	Mg	Zr	Other
M791	6.5	2.5	.12	
M793	6.5	1.5	.12	
266060	6	2	.20	.5 Mn
266062	6	3	.20	
266063	9	2	.20	
285404	9	3	.20	
285431	9	3		.10Mn-.15Ti

Values are averages of duplicate tests that varied within ±1 inch.

TABLE 13

MECHANICAL PROPERTIES OF DCSP-GTA WELDED 1/8-IN. M791 AND M793 SHEET

Base Metal	Filler Metal	Aging Treat	Bead	Cross-Weld Tensile TS ksi	YS ksi	% El 2 in	Fail. Loc.*	Bulge Test BS ksi	Hgt. in.	Fail. Type*
M791-T6	266060	R.T.	on	56.2	44.3	2.8	B	54.1	.52	1
			off	50.0	36.0	3.8	A			
	266062	R.T.	on	56.9	43.6	3.0	B	55.3	.56	1
			off	49.5	34.9	4.0	B			
	285404	R.T.	on	58.6	41.8	4.2	B	56.9	.57	1
			off	44.4	30.3	4.5	B			
M793-T6	266060	R.T.	on	56.5	40.2	4.0	C	59.8	.75	1&7
			off	40.6	28.1	4.0	B			
	266063	R.T.	on	56.9	42.4	5.0	C	59.8	.76	7
			off	46.0	32.4	4.5	B			
M791-T6	266060	Aged	on	69.1	62.0	5.5	C	68.2	.84	1
			off	65.0	59.7	3.5	A			
	266062	Aged	on	68.0	60.3	4.8	C	70.1	.90	1&7
			off	65.3	59.1	2.7	B			
	285404	Aged	on	67.2	60.2	5.2	C	70.0	1.09	5&7
			off	66.4	59.5	4.8	C			
M793-T6	266060	Aged	on	63.3	56.8	6.5	C	65.1	1.00	5&7
			off	61.3	55.9	4.3	B			
	266063	Aged	on	62.3	56.0	5.8	C	65.1	.93	5&7
			off	61.7	55.7	5.7	C			

* See Figures 6 and 7 for illustration of failure types.
R.T. - Aged 4 days at room temperature before testing
Aged - Aged 4 days at room temperature, then artificially aged 8 hrs. at 225°F + 16 hrs at 300°F.

Nominal Compositions

	Zn	Mg	Zr	Mn	Ti
M791	6.5	2.3	.12	.2	
M793	6.5	1.5	.12	.2	
266060	6	2	.20	.5	.12
266062	6	3	.20		.12
266063	9	2	.20		.12
285404	9	3	.20		.10

TABLE 14

STRESS CORROSION RESULTS ON POST-WELD AGED* M791 AND M793-T6 SHEET

Base Metal	Filler Metal	3-1/2% NaCl - AI: Face in Tension (Days to Failure)	3-1/2% NaCl - AI: Root in Tension (Days to Failure)	N.K. Atmosphere: Face in Tension (Days to Failure)	N.K. Atmosphere: Root in Tension (Days to Failure)
M791-T6	266060	3	DNF	63	45
	62	3	DNF	55	66
	285404	1	32	42	38
M793-T6	266060	6	DNF	DNF	DNF
	63	1	DNF	DNF	DNF

DNF - did not fail after 73 days exposure.
* 8 hrs at 225 F + 16 hrs at 300 F

TABLE 15

WELD CRACKING TESTS OF Cu-FREE Al-Zn-Mg ALLOYS CONTAINING ZIRCONIUM

Base Metal	Filler Metal	Inches of Cracking** Discontinuous Test
285568	266060	11
	62	9
	63	14
	285404	10
285569	266060	14
	62	12
	63	15
	285404	9
285570	266060	12
	62	10
	63	15
	285404	11

Nominal Compositions

	Zn	Mg	Zr	Others
285568	6	2	.15	.2 Fe
69	6	3	.15	.2 Fe
70	6.5	2.5	.15	.2 Fe
266060	6	2	.20	.5 Mn
62	6	3	.20	-
63	9	2	.20	-
285404	9	3	.20	-

** Values are averages of 3 tests which varied within ±2 inches.

TABLE 16

MECHANICAL PROPERTIES OF DCSP-GTA WELDED 1/8-IN. SHEET OF Cu-FREE Al-Zn-Mg ALLOYS CONTAINING ZIRCONIUM

Base Metal	Filler Metal	Bead	Tensile Test: TS ksi	Tensile Test: YS ksi	Tensile Test: % El 2 In.	Tensile Test: Fail. Loc.	Bulge Test: BS ksi	Bulge Test: Hgt. in.	Bulge Test: Failure, Predominant Type
285568 (6Zn-2Mg)	266060 (6Zn-2Mg)	on	69.2	63.3	7.5	C	68.3	1.25	5
		off	64.7	60.0	3.7	A			
	266062 (6Zn-3Mg)	on	69.5	63.7	7.0	C	69.3	1.28	4 & 5
		off	64.6	60.1	3.0	A			
	266063 (9Zn-2Mg)	on	69.5	63.5	7.7	C	68.3	1.22	5
		off	65.8	61.3	3.3	A			
	285404 (9Zn-3Mg)	on	69.0	62.8	7.3	C	68.8	1.10	5
		off	65.3	61.2	2.8	A			
285569 (6Zn-3Mg)	266060	on	71.0	68.0	1.2	B	68.4	0.73	3
		off	68.2	63.8	2.7	A			
	62	on	72.2	68.6	1.3	B	69.7	0.73	3
		off	68.6	64.2	2.3	A			
	63	on	73.1	68.2	2.5	B	66.5	0.72	3 & 6
		off	70.3	65.0	2.8	A			
	285404	on	73.8	67.1	3.8	B	66.3	0.75	6
		off	70.2	65.6	2.3	A			
285570 (6.5Zn-2.5Mg)	266060	on	73.0	67.9	3.8	C	70.6	1.02	1 & 4
		off	68.1	64.2	2.7	A			
	62	on	74.2	68.2	5.2	C	70.7	0.92	1
		off	68.1	64.1	2.5	A			
	63	on	74.1	69.0	6.3	C	69.8	0.80	1 & 4
		off	70.5	66.0	2.8	A			
	285404	on	73.8	68.1	5.7	C	71.0	0.87	5
		off	71.4	66.4	3.0	A			

Values are average of 3 tests

All panels welded in -T6 temper and aged 8 hrs at 225 F + 16 hrs at 300 F after welding.

TABLE 17

COMPARISON OF PROPERTIES OF DCSP-GTA AND DCRP-GMA WELDED 1/8-IN. Al-Zn-Mg ALLOY SHEET

Base Metal	Filler Metal	Type	Bead	Tensile Test TS ksi	YS ksi	% El 2 in	Fail. Loc.	Bulge Test BS ksi	Hgt. in.	Failure Type
285568-T6	266063	GTA	on	69.5	63.5	7.7	C	68.3	1.22	5
			off	65.8	61.3	3.3	A			
	X5180	GMA	on	66.8	58.0	5.2	A	63.2	0.92	3
			off	47.8	45.6	1.5	A			
285569-T6	285404	GTA	on	73.8	67.1	3.8	B	66.3	0.75	6
			off	70.2	65.6	2.3	A			
	X5180	GMA	on	63.5	60.5	1.3	A	63.5	0.61	3
			off	50.0	47.0	1.8	A			
285570-T6	266063	GTA	on	74.1	69.0	6.3	C	69.8	0.80	1&4
			off	70.5	66.0	2.8	A			
	X5180	GMA	on	65.8	63.2	1.5	A	62.8	0.57	3
			off	53.4	49.7	1.8	A			
M791-T6	285404	GTA	on	67.2	60.2	5.2	C	70.0	1.09	5&7
			off	66.4	59.5	4.8	C			
	X5180	GMA	on	67.4	58.4	5.5	B	64.6	0.78	3
			off	54.0	49.1	1.8	A			

Values listed are averages of triplicate tests. All weldments post-weld aged 4 days at room temperature, then artificially aged 8 hours at 225 F plus 16 hours at 300 F.

TABLE 18

PROPERTIES OF REHEATED DCSP-GTA WELDS IN 1/8" 7178-T6 SHEET - X5080 FILLER

Torch Travel Speed ipm	Heat Input(1) Joules/in.	Temp(2) °F	Weld Side Heated	Quench(3) Distance	Bead	TS ksi	YS ksi	% El 2 in	No. Tests	Failure Location(5)
-Oxyacetylene Flame Heated - H_2O Quench										
-- As-welded - Not reheated --					on	53.0	51.5	1.0	3	C
16	2100	805	Face	(4)	on	48.8	41.5	1.5	3	B
16	2100	835	Root	(4)	on	51.3	44.7	1.5	3	B
19-1/2	1700	760	Face	7-1/2	on	45.8	36.1	2.0	2	A
17	1950	800	Face	7-1/2	on	51.0	41.8	1.5	2	B
17	1950	800	Face	7-1/2	off	55.2	40.9	3.0	2	B
16	2100	800	Root	7-1/2	on	49.3	40.7	2.0	2	A
16	2100	770	Face	1-1/2	on	52.8	42.8	1.5	2	A
16	2100	760	Root	1-1/2	on	51.0	50.2	1.5	2	B

(1) Approximate values calculated from flow rates of oxygen and acetylene and BTU output for combustion

(2) Temperature measured on root side of weld bead

(3) Distance from heating flame to water. Panel traveled downward past the stationary torch, then into water quench tank

(4) Entire length of weld bead flame heated before quenching

(5) See Figure 6 for explanation of symbols

TABLE 19

PROPERTIES OF REHEATED DCSP-GTA WELDS IN 1/8" 7178-T6 SHEET - X5080 FILLER
(Electric Arc Heated - Air Quench)

Amperes	Travel Speed ipm	Power Input Joules/in.	Temp. °F	Bead	TS ksi	YS ksi	% El 2 in	No. Tests	Failure Location
--As-welded - Not reheated --				on	53.0	51.5	1.0	3	C
AC-GTA									
87	15-1/2	6100	805	on	52.6	48.1	1.5	1	B
87	15-1/2	6100	805	off	44.5	40.7	2.0	1	A
75	10	7700	835	on	53.2	45.2	1.5	1	B
75	10	7700	835	off	50.0	41.6	2.5	1	A
DCSP-GTA									
50	6-1/4	7700	780 start*	on	52.1	45.2	1.5	1	B
50	6-1/4	7700	790 end*	on	54.8	44.5	1.5	1	B
DCRP-GTA									
50	6	10,000	700	on	44.5	43.8	1.5	1	B
50	6	10,000	700	off	51.3	39.0	2.5	1	B
40	4	12,000	805	on	43.6	39.1	1.5	1	B
40	4	12,000	805	off	44.3	39.3	1.5	1	A

All welds reheated on face side of weld bead

* "Start" and "end" are for same panel

TABLE 20

MECHANICAL PROPERTIES OF DCSP GTA WELDS IN
1/8-IN. 7178-T6 SHEET (X5080 FILLER) REHEATED TO 870F
WITH QUARTZ INFRARED LAMPS AND WATER QUENCHED

Time at Temp. Min.	Weld Bead	Cross Weld Tensile: Top of Panel TS ksi	YS ksi	% El 2 in.	Bottom of Panel TS ksi	YS ksi	% El 2 in.	Bulge Stress ksi	Bulge Max. Hgt. in.	Failure Type
Elements spaced 1 in. apart										
.1	on	52.6	44.8	1.5	51.8	37.7	3.0	48.1	.63	1
	off	55.4	42.2	3.0	50.0	37.1	3.0			
1	on	58.5	52.6	2.0	52.3	39.4	2.5	49.9	.66	1
	off	68.4	50.3	5.0	56.9	39.2	4.5			
10	on	65.2	54.2	2.5	49.9	34.2	3.5	54.1	.71	1
	off	69.1	51.7	5.0	54.4	34.7	5.0			
20	on	69.7	53.6	4.0	50.3	38.6	2.5	53.5	.77	1
	off	71.1	51.6	6.5	57.6	39.2	5.5			
Elements spaced 2 in. apart										
.1	on	56.5	52.5	1.0	51.9	42.2	2.0	54.0	.68	1
	off	66.3	49.7	4.0	53.3	40.5	2.5			
1	on	57.0	52.2	1.0	52.9	39.7	2.5	53.8	.67	1
	off	68.5	52.2	5.5	54.8	39.5	3.5			
10	on	66.2	53.8	3.0	52.4	40.2	2.5	59.4	.85	1
	off	71.1	51.8	6.5	56.7	40.1	4.0			
20	on	65.0	53.5	3.0	52.8	39.5	3.0	55.9	.74	6
	off	66.6	49.7	5.0	57.9	38.8	5.5			

"Bead on" failures occurred predominantly in the heat affected zone and "bead off" failures were mostly through the weld.

References for comparison - 1/8-in. 7178-T6 sheet, DCSP welded

	Bead	TS ksi	YS ksi	% El 2 in.	BS ksi	Max. Hgt.	Failure
As welded	on	57	53	1.0	46	.42	-
Art. aged	on	70	68	1.0	58	.42	-
Heat treated and aged to -T6	on	87	82	2.8	68	.47	-
Radiant heated 10 min. at 870°F, air cooled	on	47.2	23.9	7.8	38.8	.98	1

TABLE 21

MECHANICAL PROPERTIES OF DCSP-GTA WELDS IN 1/8-IN. 7178-T6 SHEET (X5080 FILLER) REHEATED WITH QUARTZ INFRARED LAMPS THEN AGED 8 HRS AT 212 F + 3 HRS AT 325 F

Time at Temp. Min.	Weld Bead	Cross-Weld Tensile: Top of Panel TS ksi	YS ksi	% El 2 in.	Bottom of Panel TS ksi	YS ksi	% El 2 in.	Bulge Stress ksi	Hgt. in.	Failure Type
Elements spaced 1 in. apart										
5	on	85.0	*	2.5	55.3	44.5	3.0	47.9	.49	4
	off	73.8	72.8	2.0	61.4	48.8	6.5			
10	on	79.5	75.0	2.0	59.1	45.8	6.5	50.5	.47	4
	off	77.4	73.4	2.5	62.3	49.8	6.0			
15	on	78.8	72.5	2.5	58.6	48.7	3.5	49.4	.54	4
	off	74.1	71.1	2.0	63.8	50.8	5.5			
20	on	77.0	75.9	.5	61.0	50.4	4.0	60.6	.72	1 & 6
	off	79.4	73.9	3.5	64.1	53.0	5.5			
Elements spaced 2 in. apart										
5	on	79.4	74.8	1.5	59.7	51.7	2.0	63.1	.57	6
	off	77.1	70.0	2.5	59.5	52.5	2.0			
10	on	81.4	74.8	2.0	65.8	58.6	2.5	66.8	.55	6
	off	79.1	71.5	2.5	65.5	58.7	2.5			
15	on	77.7	73.1	1.5	64.2	55.9	3.0	59.2	.52	6
	off	77.0	69.3	2.5	63.8	55.7	3.0			
20	on	76.0	70.3	1.5	66.8	61.2	2.0	62.3	.56	1 & 6
	off	76.4	68.8	3.5	68.4	58.1	3.0			

* Failed before reaching 0.2% offset.

"Bead on" failures occurred predominantly in the heat affected zone and "Bead off" failures were mostly through the weld

References for comparison - 1/8-in. 7178-T6 sheet, DCSP-GTA welded

	Bead	TS ksi	YS ksi	% El	BS ksi	Max. Hgt.
As welded	on	57	53	1.0	46	.42
Art. aged	on	70	68	1.0	58	.42
Heat treated and aged to -T6	on	87	82	2.8	68	.47
Radiant heated 10 min, at 870°F, air cooled	on	47.2	23.9	7.8	38.8	.98

TABLE 22

COMPARISON OF MECHANICAL PROPERTIES OF INFRARED LOCALLY HEATED DCSP-GTA WELDS IN 1/8-IN. 7178-T6 SHEET (X5080 FILLER)

Time at Temp Min.	Condition	Weld Bead	Cross Weld Tensile: Top of Panel TS ksi	Top of Panel YS ksi	Top of Panel % El 2 in.	Bottom of Panel TS ksi	Bottom of Panel YS ksi	Bottom of Panel % El 2 in	Bulge Stress ksi	Bulge Max. Hgt. in.	Failure Type
Elements spaced 1 in. apart											
10	nat. aged	on	65.2	54.2	2.5	49.9	34.2	3.5	54.1	.71	1
		off	69.1	51.7	5.0	54.4	34.7	5.0			
	art. aged	on	79.5	75.0	2.0	59.1	45.8	6.5	50.5	.47	4
		off	77.4	73.4	2.5	62.3	49.8	6.0			
20	nat. aged	on	69.7	53.6	4.0	50.3	38.6	2.5	53.5	.77	1
		off	71.1	51.6	6.5	57.6	39.2	5.5			
	art. aged	on	77.0	75.9	0.5	61.0	50.4	4.0	60.6	.72	1 & 6
		off	79.4	73.9	3.5	64.1	53.0	5.5			
Elements spaced 2 in. apart											
10	nat. aged	on	66.2	53.8	3.0	52.4	40.2	2.5	59.4	.85	1
		off	71.1	51.8	6.5	56.7	40.1	4.0			
	art. aged	on	81.4	74.8	2.0	65.8	58.6	2.5	66.8	.55	6
		off	79.1	71.5	2.5	65.5	58.7	2.5			
20	nat aged	on	65.0	53.5	3.0	52.8	39.5	3.0	55.9	.74	6
		off	66.6	49.7	5.0	57.9	38.8	5.5			
	art. aged	on	76.0	70.3	1.5	66.8	61.2	2.0	62.3	.56	1 & 6
		off	76.4	68.8	3.5	68.4	58.1	3.0			

TABLE 23

MECHANICAL PROPERTIES OF DCRP-GMA WELDS IN 0.090-IN. 2014-T6 SHEET MADE AT VARIOUS TRAVEL SPEEDS ON STEEL BACKING BAR

Travel Speed ipm	Tensile Strength Test TS ksi	YS ksi	% El	Fracture Location	Bulge Strength Test BS ksi	Max. Hgt in.	Fracture Type
60	39.5	37.0	1.5	A	49.8	.42	2
65	50.7	40.1	2.0	A	47.0	.46	2
70	49.1	39.4	2.0	A	48.4	.43	2
75	43.8	38,1	1.0	A	40.5	.40	2
80	38.9	-	1.0	A	26.4	.28	2

Panels welded at 170 amps, 26 volts, 17 cfh Ar, 33 cfh He using 0.035-in. 4145 filler,

All tests made with "bead on", as-welded condition

Values are averages of two tensile tests and one bulge test.

TABLE 24

MECHANICAL PROPERTIES OF DCRP-GMA WELDS IN 0.090-IN. 2014-T6 SHEET MADE AT VARIOUS TRAVEL SPEEDS ON COPPER BACKING BAR

Travel Speed ipm	Tensile Strength Test TS ksi	YS ksi	% El	Fracture Location	Bulge Strength Test BS ksi	Max. Hgt. in.	Fracture Type
60	55.1	51.2	1.5	A	58.7	0.46	2
65	54.9	49.7	1.5	A	54.2	0.43	2
70	56.0	51.3	1.5	A	57.2	0.46	2
75	53.3	50.2	1.5	A	58.5	0.48	2
80	56.1	50.9	1.5	A	52.3	0.43	2
90	57.3	52.6	1.4	A	51.8	0,44	2
100	54.6	53.0	1.3	A	57.2	0.46	2
105	57.5	52.1	1.2	A	60.0	0.49	3
110	56.4	52.1	1.0	A	54.7	0.43	3

Panels welded at 170 amps, 26 volts, 17 cfh Ar, 33 cfh He, using 0.035-in. 4145 filler.

All tests made with "bead on" - post weld aged 10 hrs at 340°F.

Values are averages of 4 tensile tests and 2 bulge tests.

TABLE 25

MECHANICAL PROPERTIES OF DCRP-GMA WELDS IN 0.090-IN. 2014-T6 SHEET (716 FILLER) WELDED WITH DECREASING ARC CURRENT AT CONSTANT TRAVEL SPEED

	Tensile Strength					Bulge Strength	
Current	TS ksi	YS ksi	% El 2 in.	Fracture Location	BS ksi	Max. Hgt. in.	Fracture Type
160	51.4	49.3	1.0	A	53.5	.40	2
150	53.5	49.4	1.0	A	54.9	.44	2
140	60.0	52.5	1.5	A	55.4	.45	3
135	58.2	60.5	1.2	A	55.0	.44	1
130	56.6	53.3	1.0	A	58.8	.51	1

All panels post-weld aged 10 hrs at 340 F.
Panels tested "bead on"
Listed values are averages of four tensile and two bulge tests.
Parameters: 55 ipm, 26 volts, 17Ar-33He.

	TS ksi	YS ksi	% El 2 in.	Fracture Location	BS ksi	Max. Hgt. in.	Fracture Type
Reference Frankford-made welds	60	56	.8		67.8	.49	

Frankford-made welds

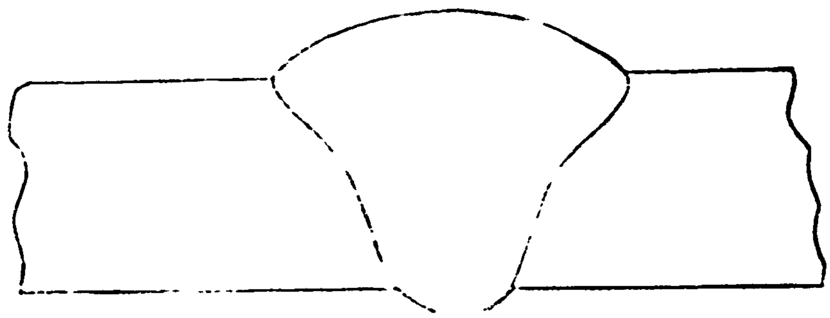

Early Alcoa welds

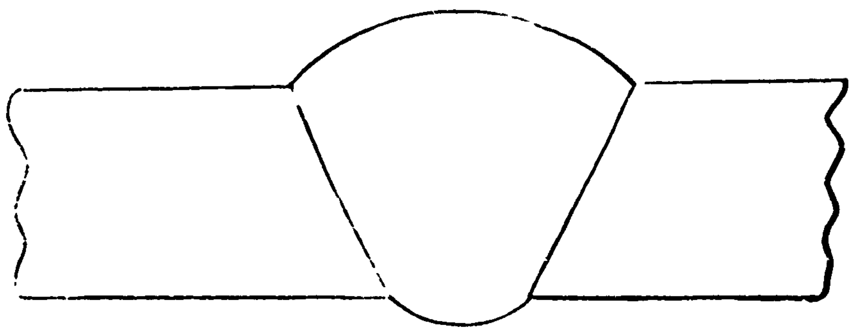

TABLE 26

MECHANICAL PROPERTIES OF .090-IN.
2014-T6 SHEET DCRP-GMA WELDED (716 FILLER)
ON A LIQUID NITROGEN-COOLED BACKING BAR

	Welding Temp. °F	Shielding Gas Ar cfh	He cfh	Bead	Tensile Test TS ksi	YS ksi	% El 2 in.	Failure Location	Bulge Test BS ksi	Hgt in.	Failure Type
1.	-91	25	50	on	61.2	59.2	1.0	A	55.5	.46	3
				off	52.8	47.7	1.5				
2.	-91	10	65	on	59.7	57.3	1.2	A	54.5	.47	3
				off	53.4	48.6	1.3				
3	RT	10	65	on	65.4	59.8	1.8	A	58.5	.52	2
				off	54.3	52.7	1.5				
Frankford-made Welds											
4.	-25	25	47	on	65	59	2.3	-	69*	.47	-
5.	RT	25	47	on	60	57.5	0.8	-	67*	.49	-

Welding Conditions

	Temperature Specimen	Backing Bar	No. of Tests	Current amps.	Voltage volts	Travel Speed ipm	Heat input joules/in.
1.	-91	-134	1	165	24.5	65	3730
2.	-91	-156	4	150	27	65	3740
3.	RT	RT	6	150	26	65	3600
Frankford-made Welds**							
4.	-25	-55	-	150-160	23-25	55	3800-4400
5.	RT	RT	-	170	25	55	4700

* These are suspect values as discussed in the report
**Listed Frankford welding conditions are taken from Reference 4

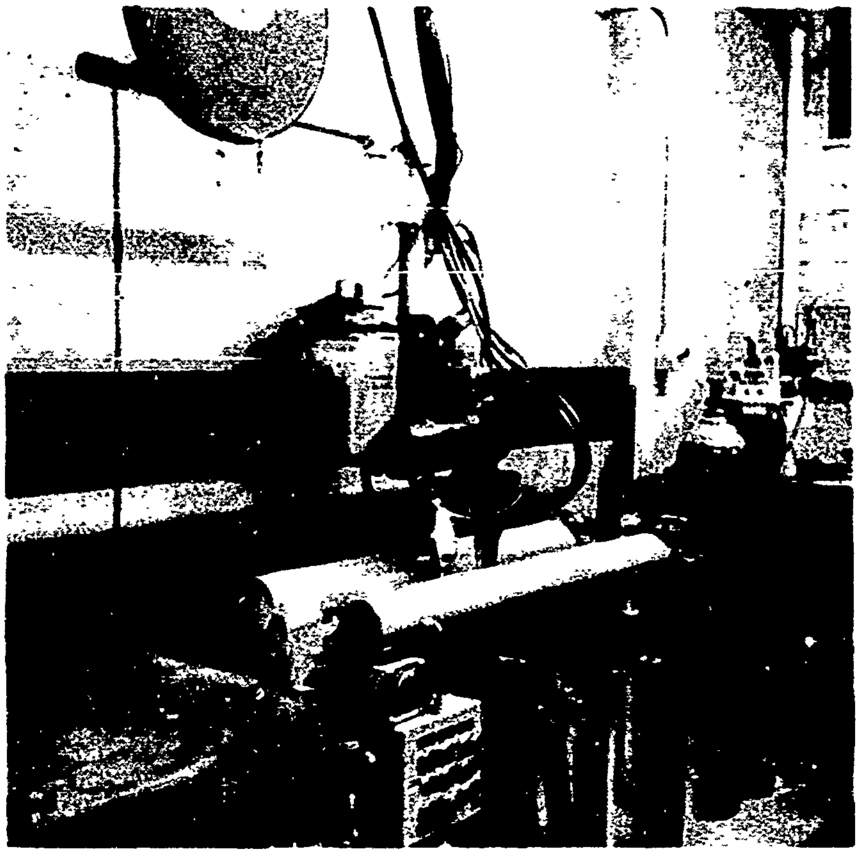

Figure 1 - Equipment for DCRP-GMA welding panels for bead contour studies

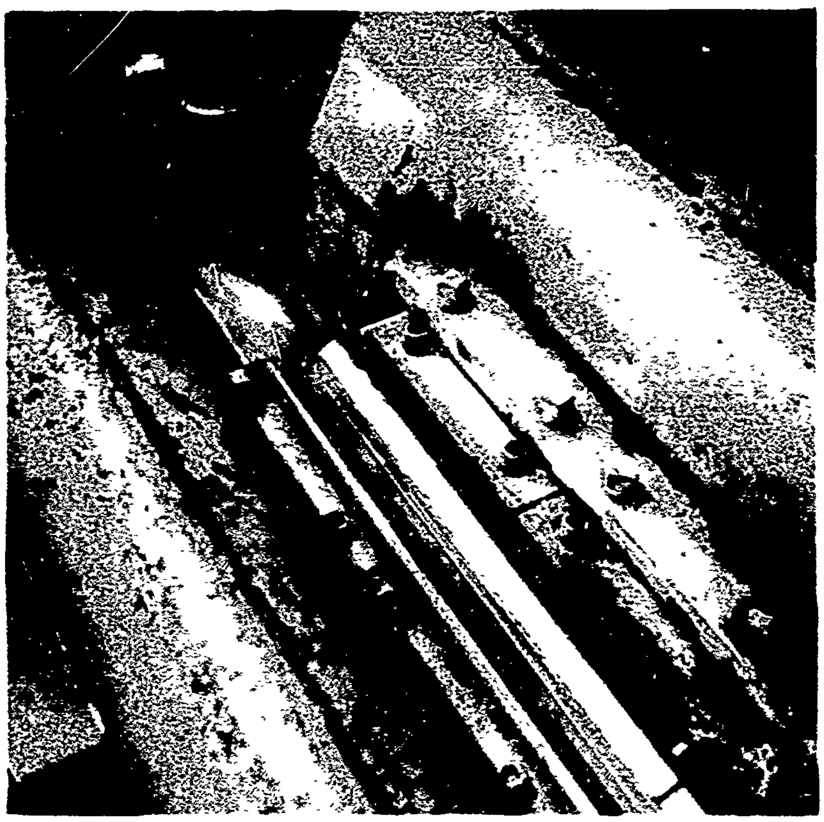

Figure 2 - Close-up of welding table showing close positioning of hold-down plates

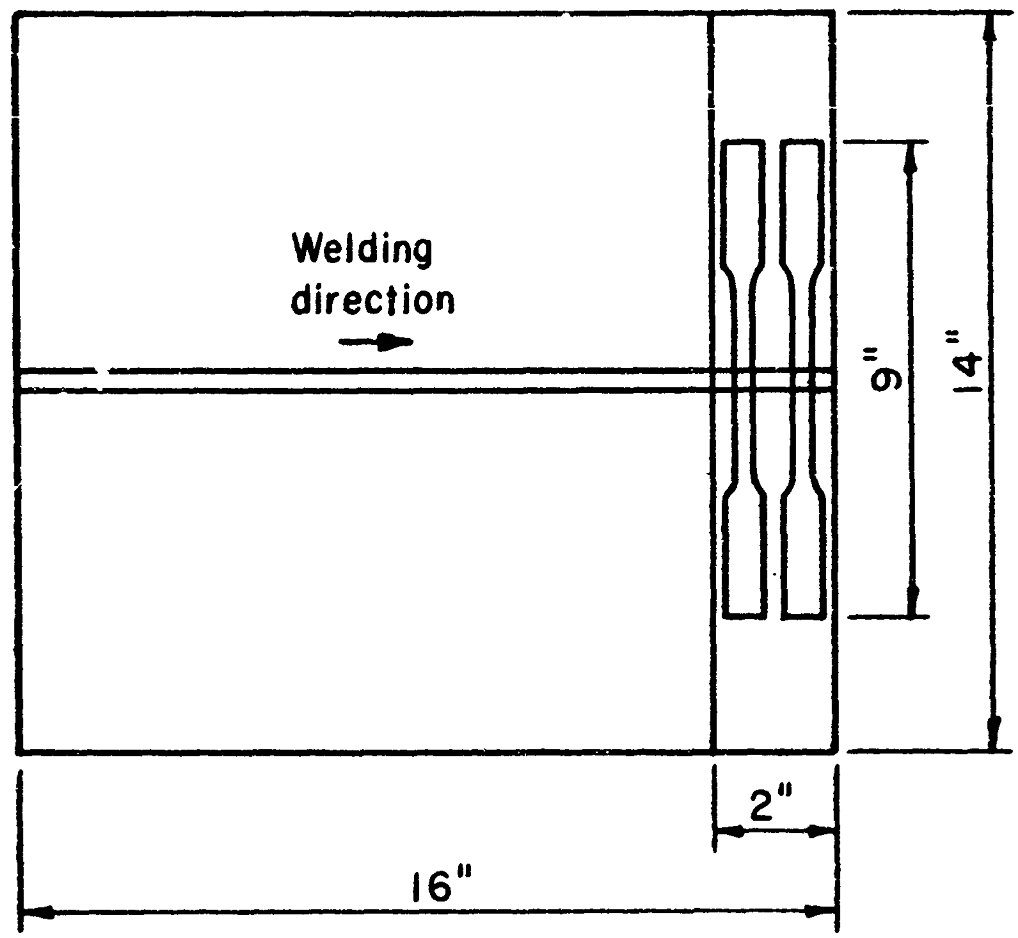

WELDED PANEL FROM WHICH TENSILE AND BULGE TEST SPECIMENS WERE REMOVED

Figure 3

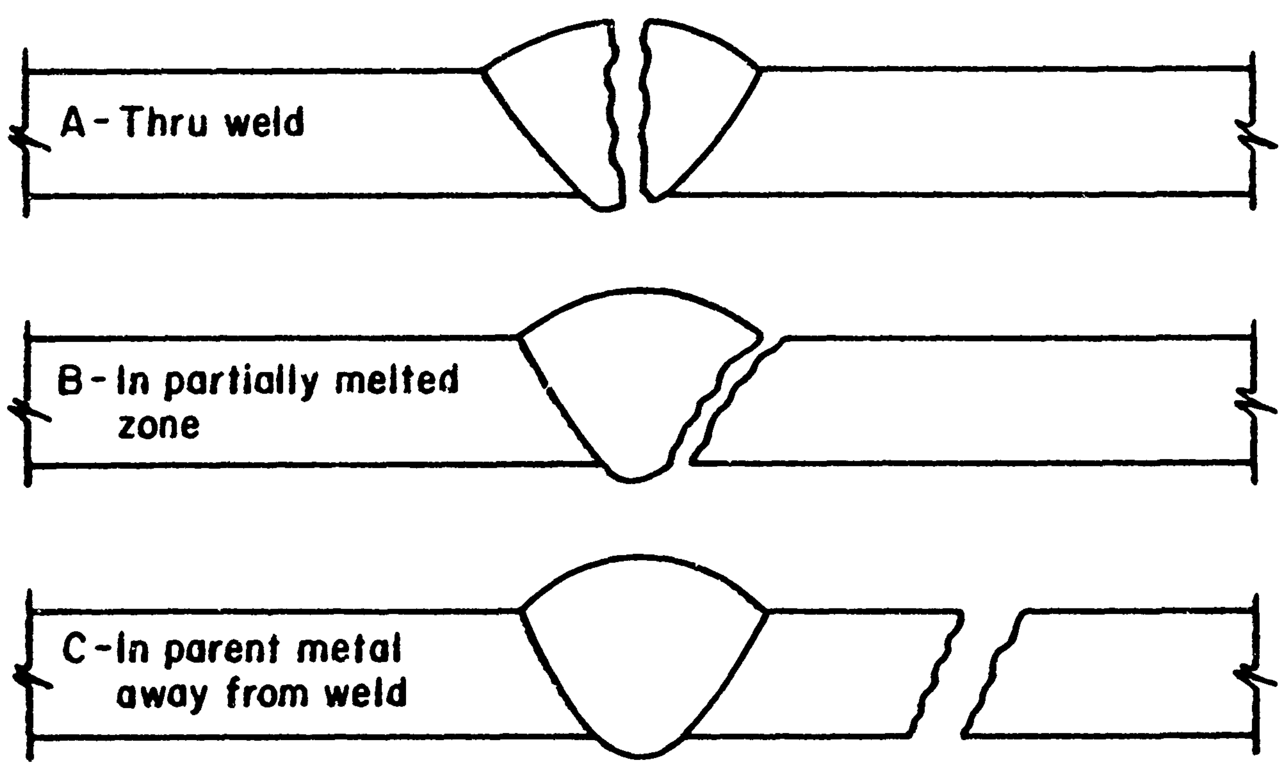

TYPES OF TENSILE FAILURES. SYMBOLS A, B AND C ARE USED IN THE TABLES

Figure 4

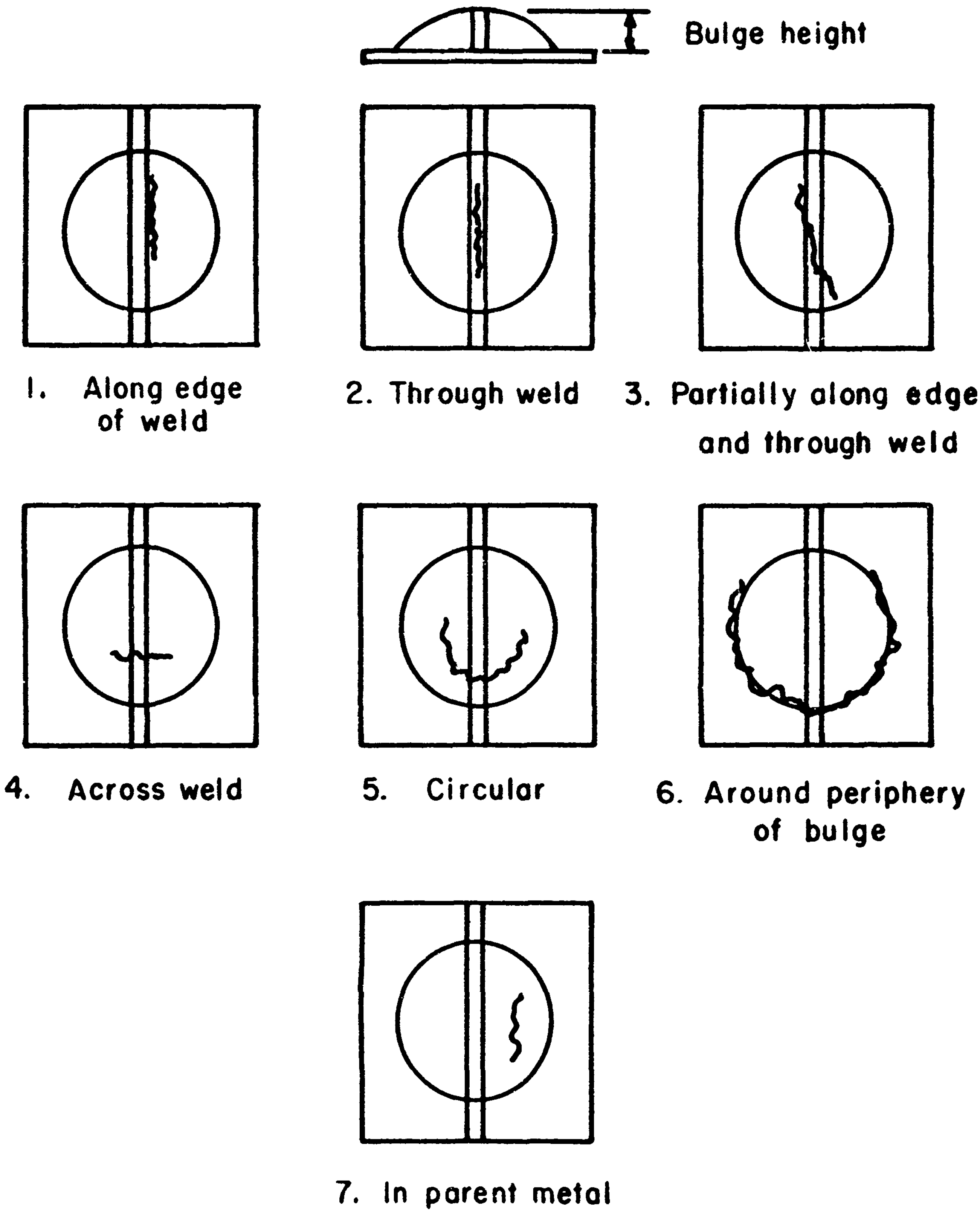

TYPES OF FAILURE OF SHEET SPECIMENS IN BULGE TEST

Figure 5

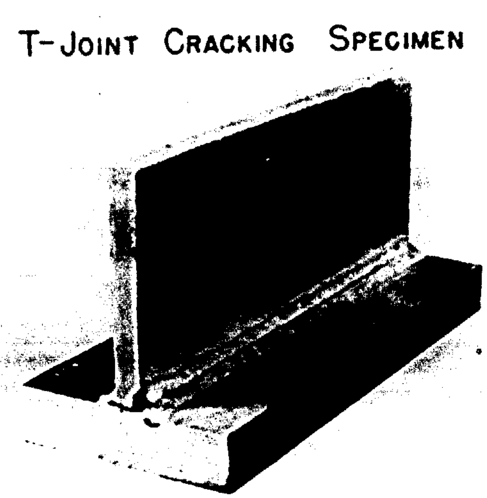

Figure 6a

Weld Cracking Specimen

(Neg. 74971 D)

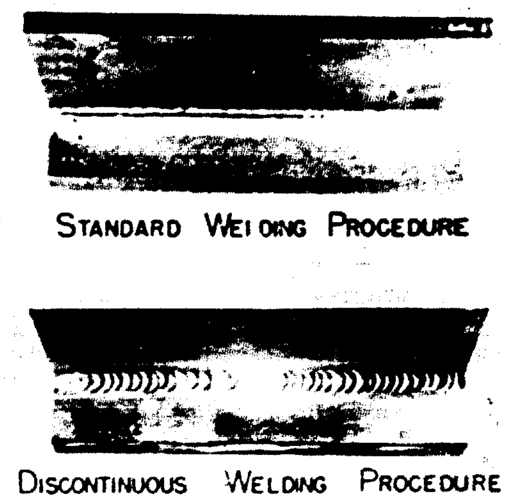

Figure 6b

Welding Procedure for Cracking Test

(Neg. 74972D)

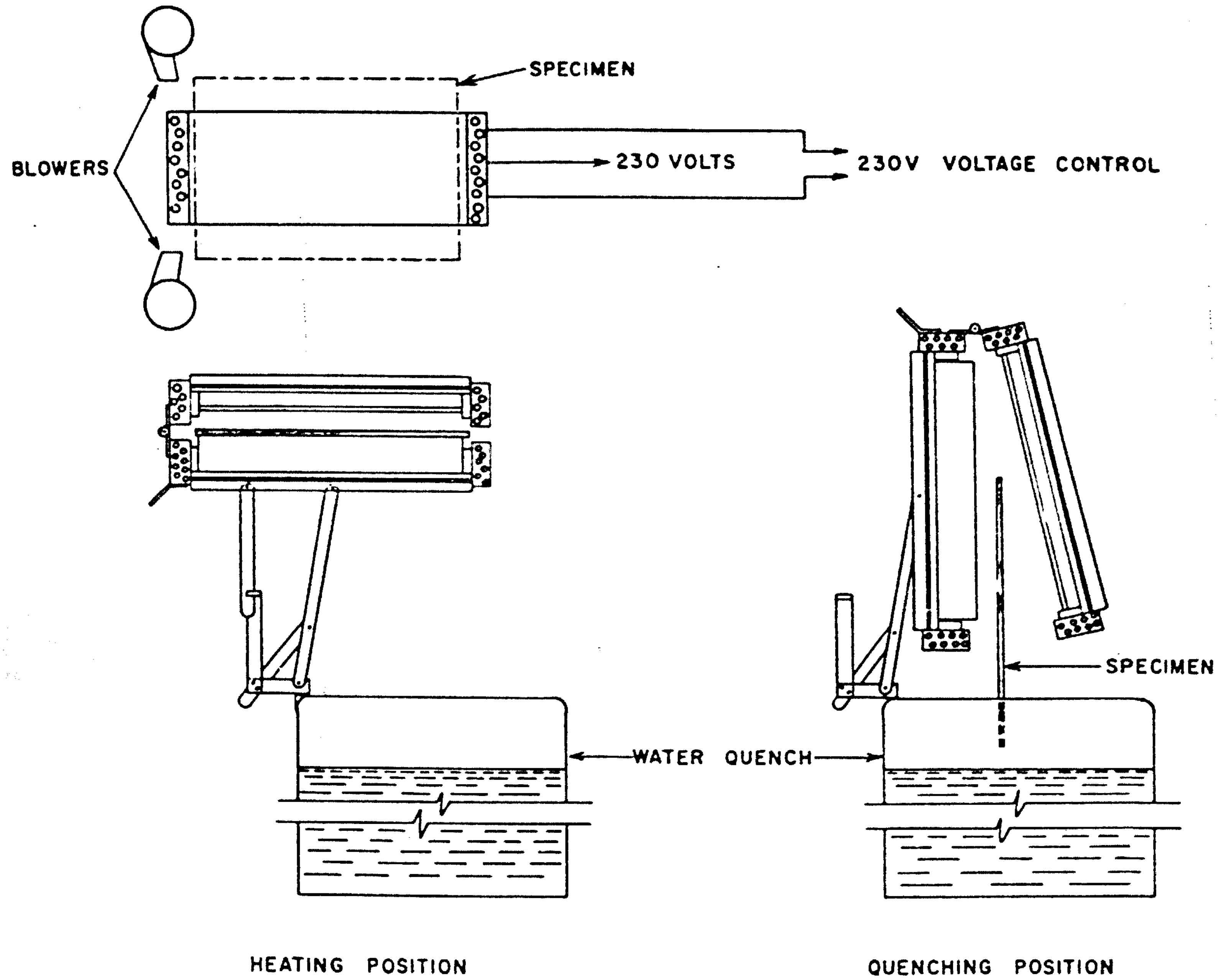

FIG. 7 – SCHEMATIC DIAGRAM OF HORIZONTAL INFRARED LAMP HEATING UNIT

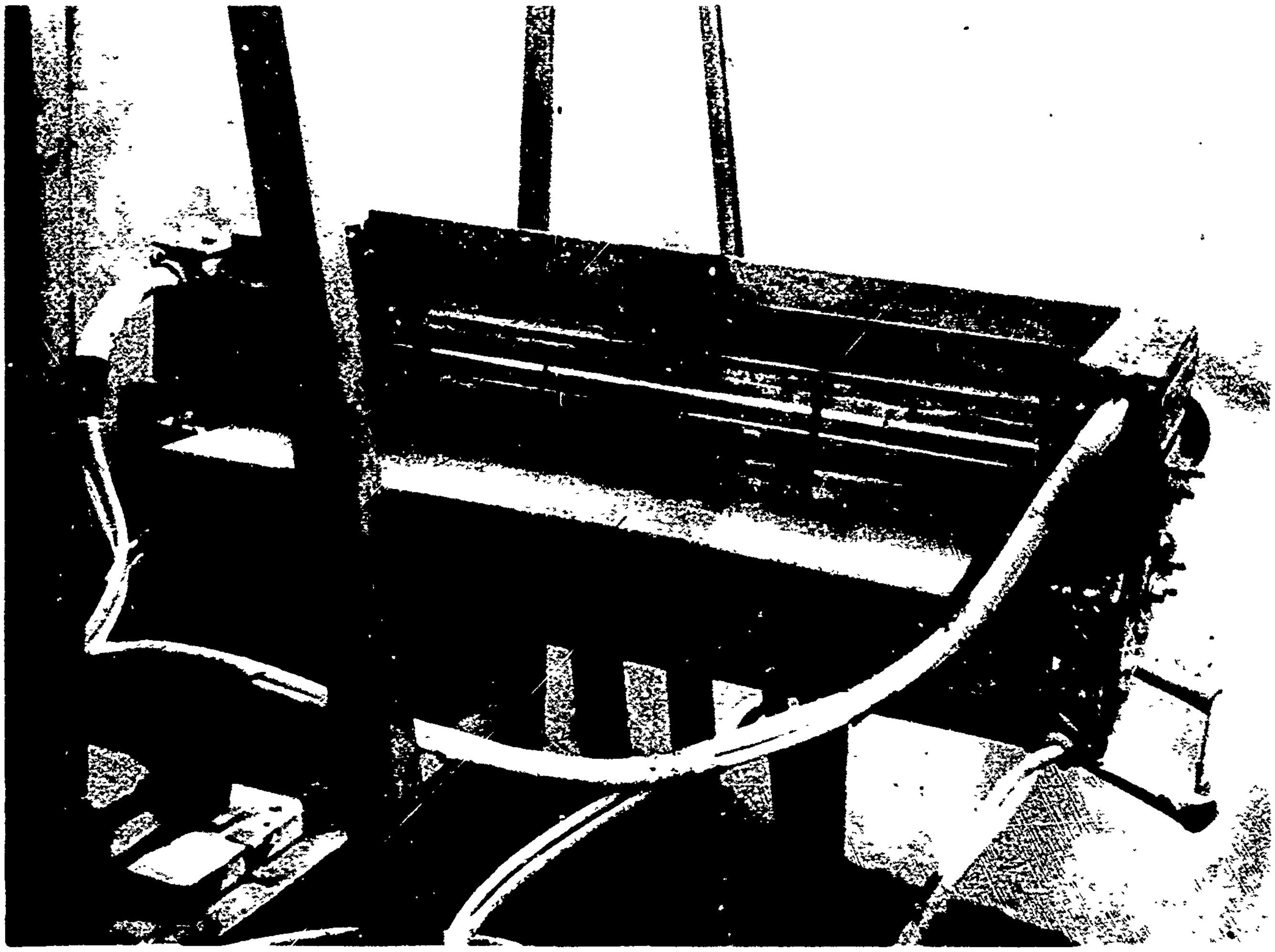

Horizontal infrared heating apparatus with a 14 x 16 welded 1/8-in. 7178-T6 panel in position. (Neg. PBK 068)

Figure 8

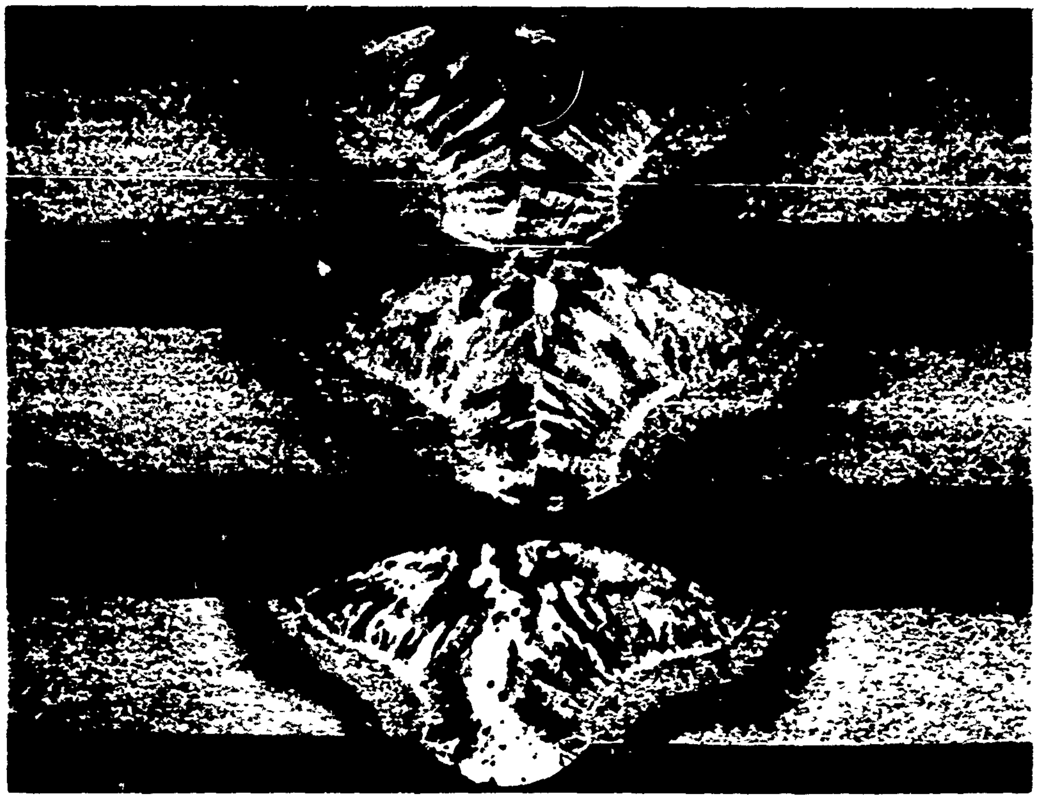

138534A Keller's Etch

Frankford welds made at 55 ipm on a brine-cooled backing bar

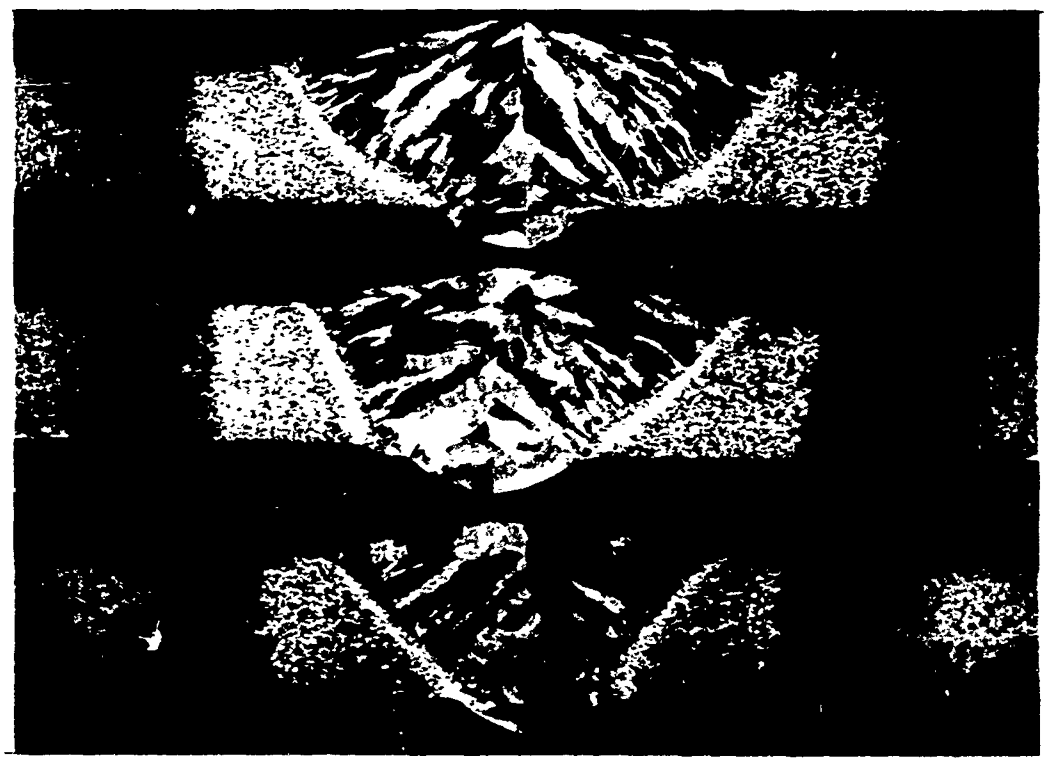

60

80

105

285500 138701A 10X Keller's Etch
04
10 Alcoa welds made at 60, 80, and 105 ipm on a room-temperature backing bar

Figures 9, 10 DCRP-GMA welds in .090-in. 2014-T6 sheet

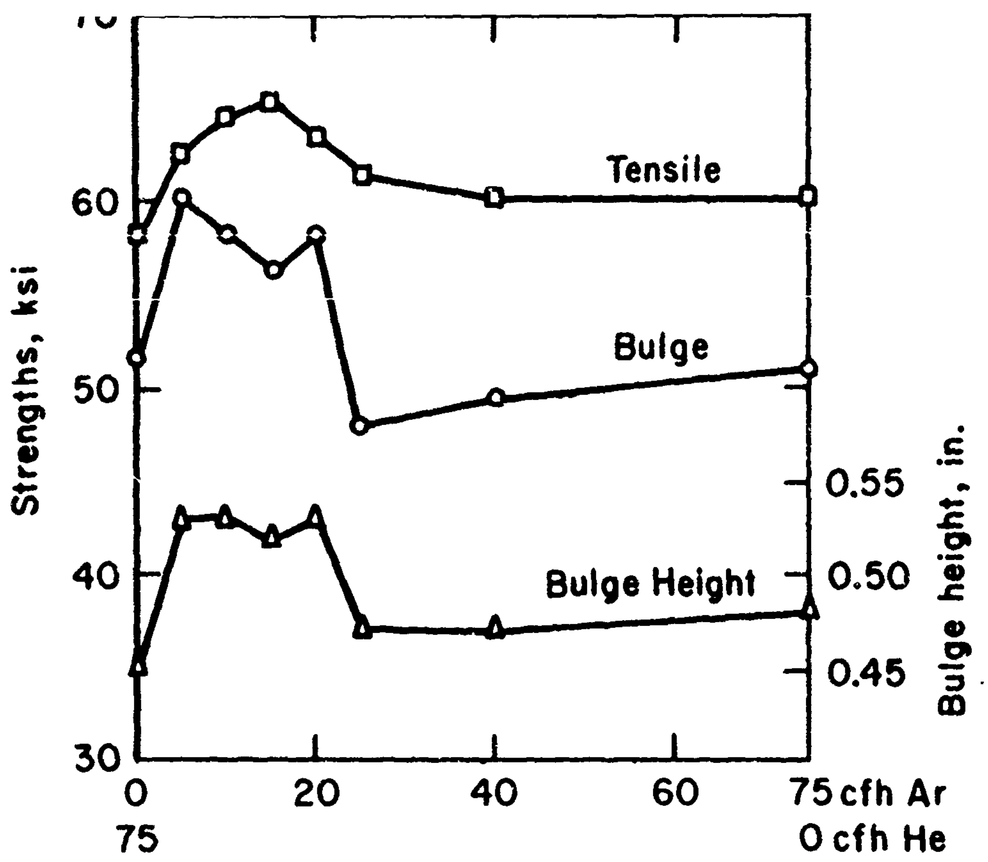

(a) CONSTANT 75 CU. FT. PER HR. GAS FLOW

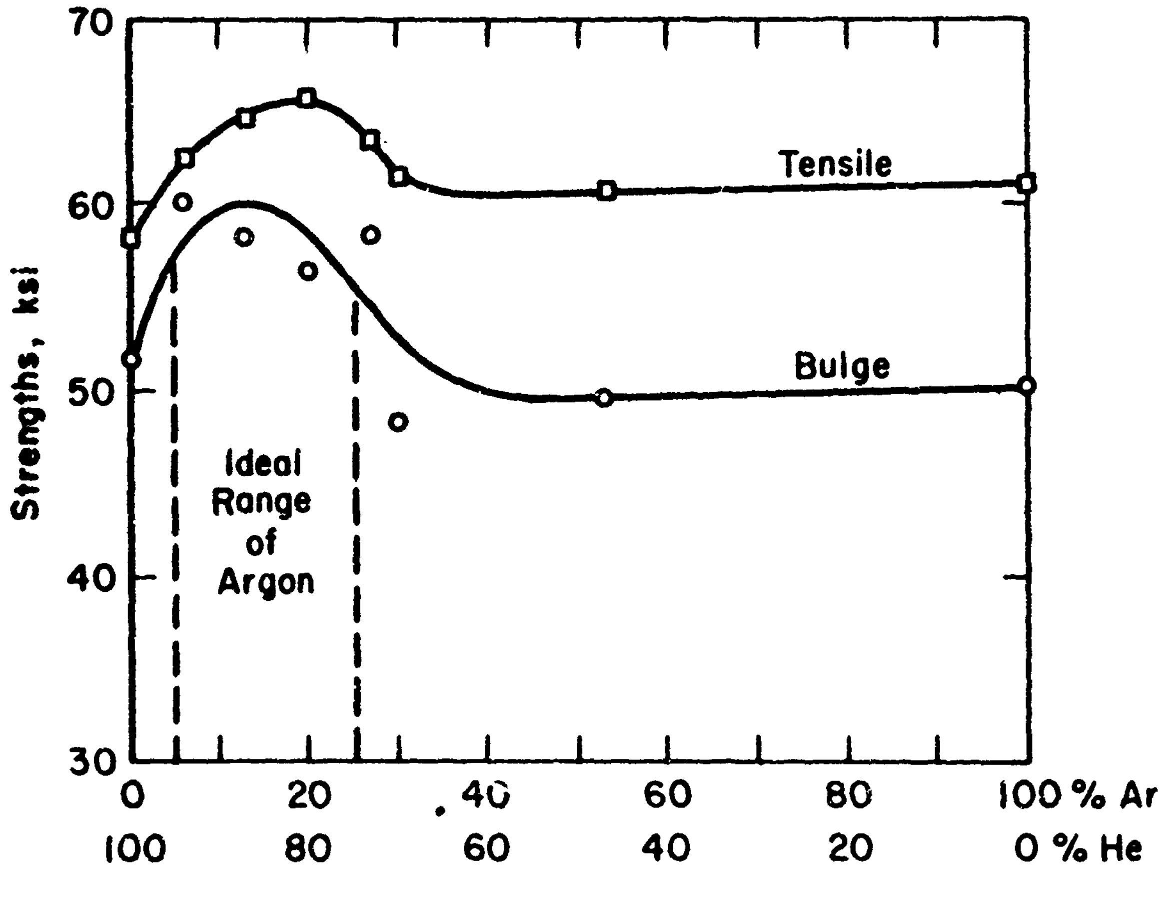

(b) PER CENT ARGON IN 75 CU. FT. PER HR. FLOW

PROPERTIES OF DCRP-GMA WELDS IN .090-IN. 2014-T6 SHEET MADE WITH VARIOUS Ar-He GAS MIXTURES

Figure 11

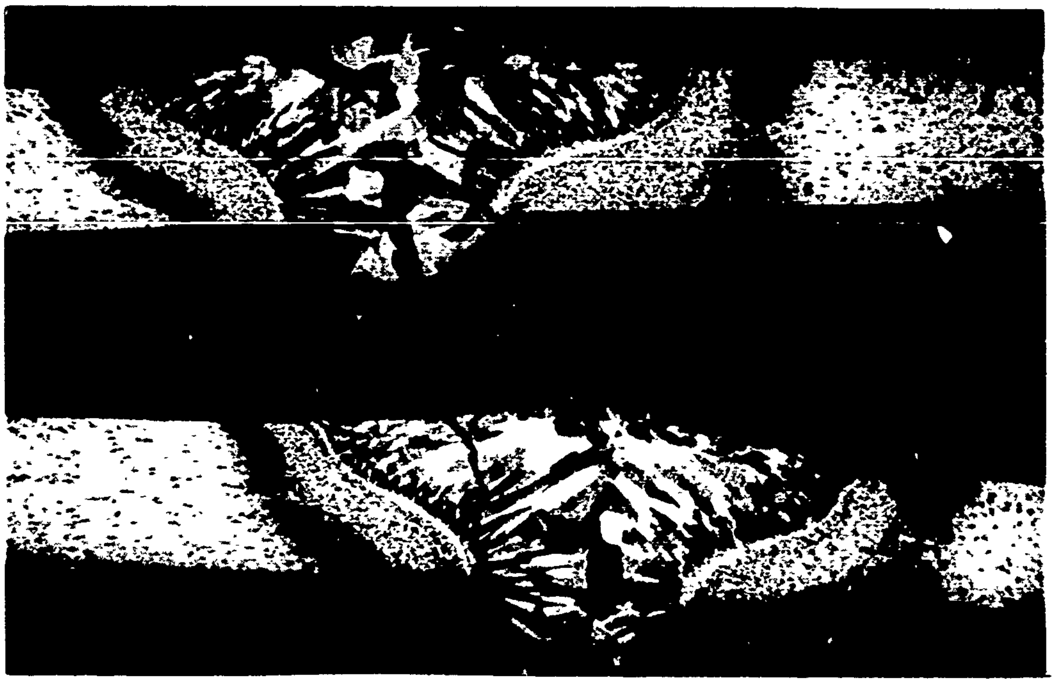

S-285655 140350A 10X Keller's Etch

Made with 75 cfh He shielding gas

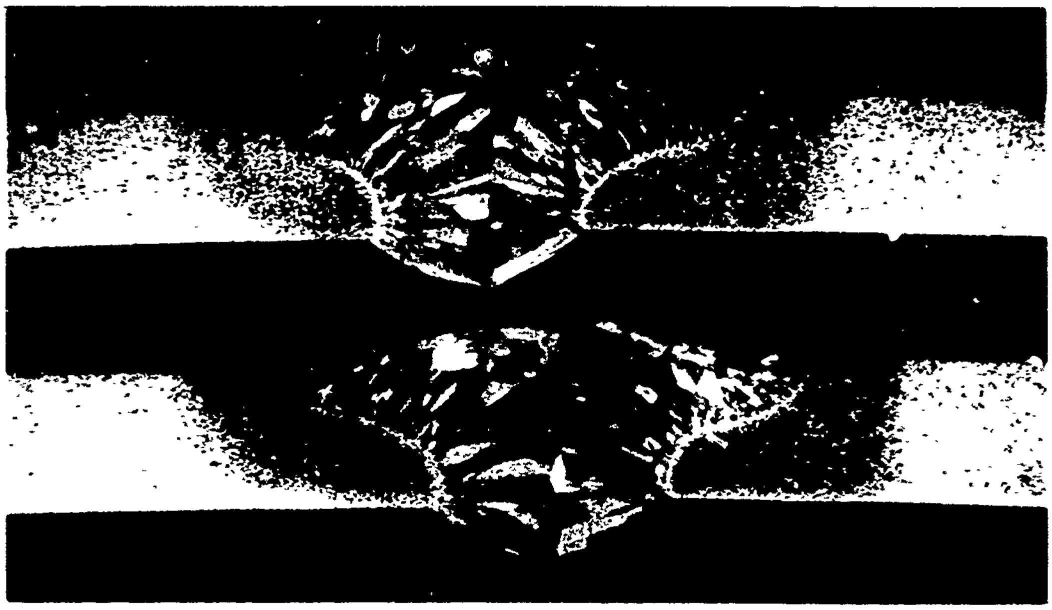

S-285795-2 and -3 140751A Keller's Etch

Made with 5Ar-70He cfh shielding gas

Figures 12, 13 - DCRP-GMA welds in .090-in. 2014-T6 sheet

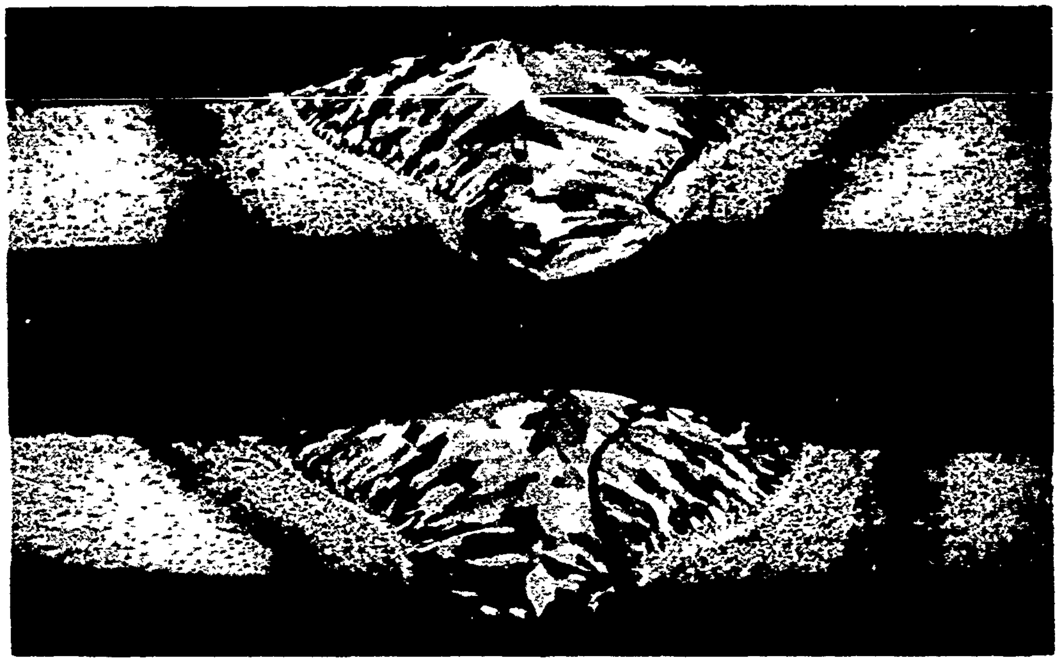

S-285658 140351-A 10X Keller's Etch

Made with 10Ar-65He cfh shielding gas

S-285798-1 140753-A 10X Keller's Etch
-3

Made with 15Ar-60He cfh shielding gas

Figures 14
15 - DCRP-GMA welds in .090-in. 2014-T6 sheet

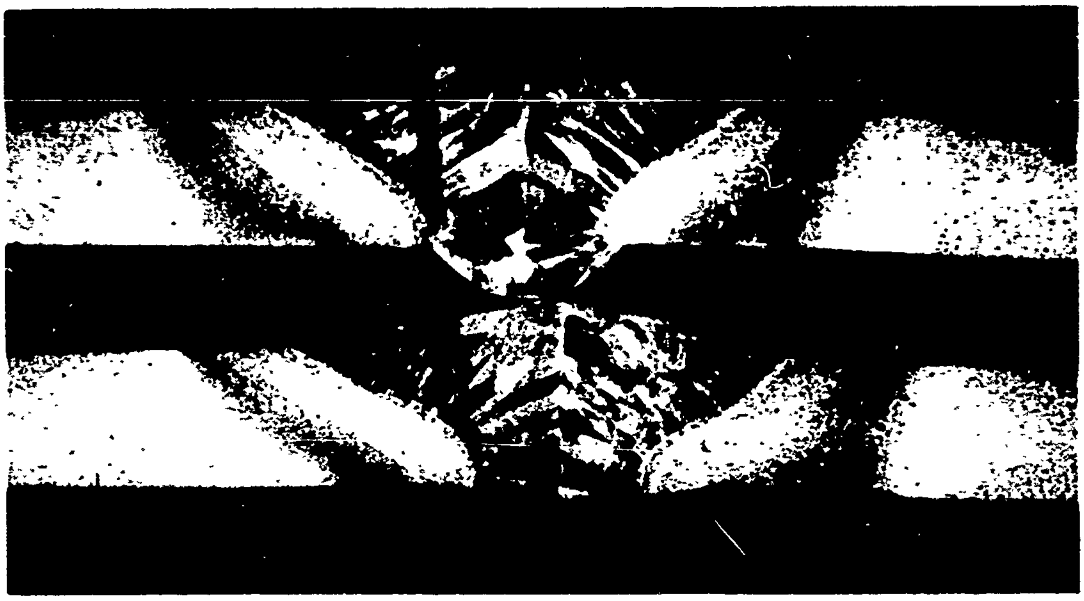

S-285799-1 140754-A 10X Keller's Etch
-2

Made with 20Ar-55He cfh shielding gas

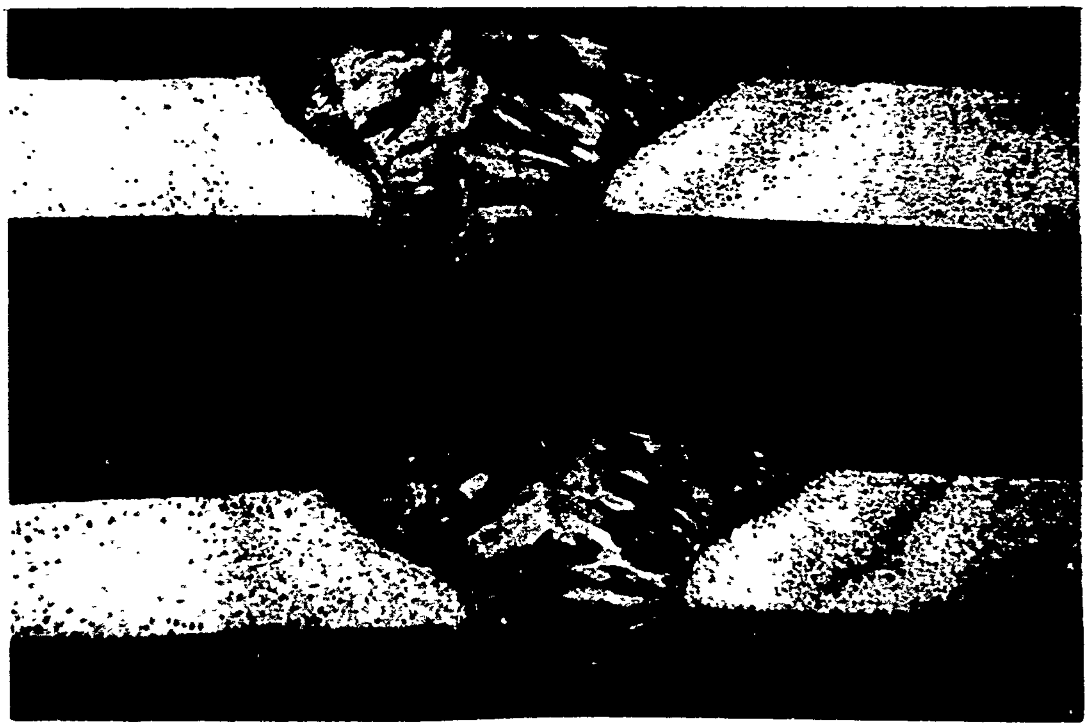

S-285668 140352-A 10X Keller's Etch

Made with 25Ar-50He cfh shielding gas

Figure 16 17 - DCRP-GMA welds in .090-in. 2014-T6

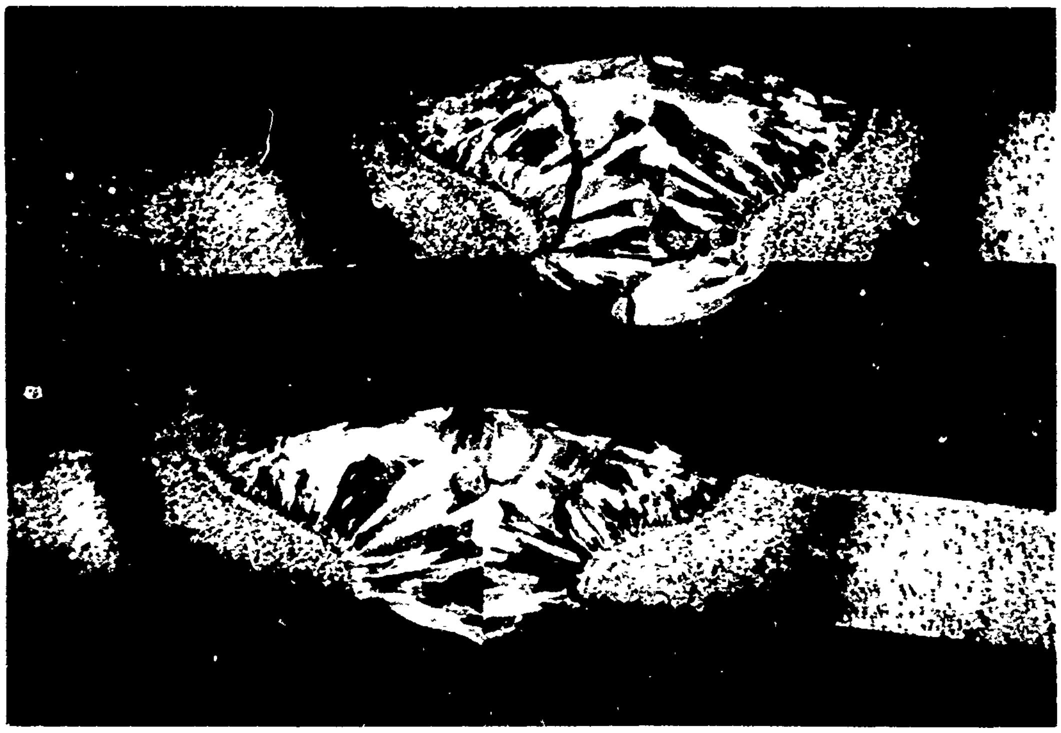

S-285669 140353-A 10X Keller's Etch

Made with 45Ar-35He cfh shielding gas

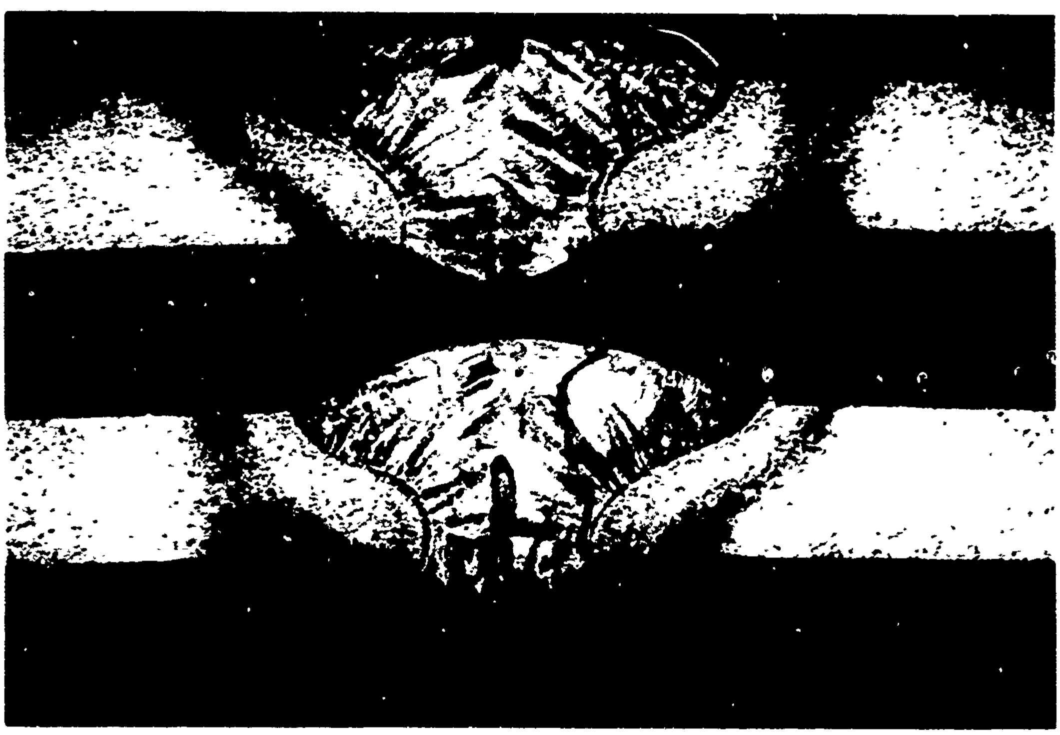

S-285670 140354-A 10X Keller's Etch

Made with 65Ar-0He cfh shielding gas

Figure 18
19 - DCRP-GMA welds in .090-in. 2014-T6

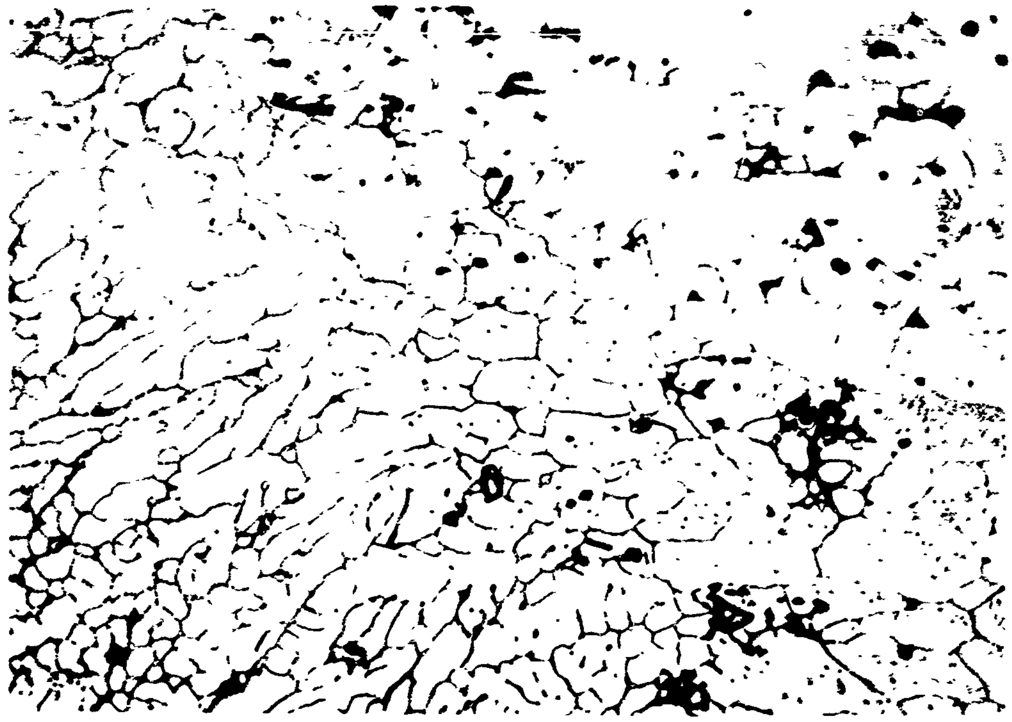

S-285655 140355A 500X Keller's Etch

Made with 0Ar-75He cfh shielding gas

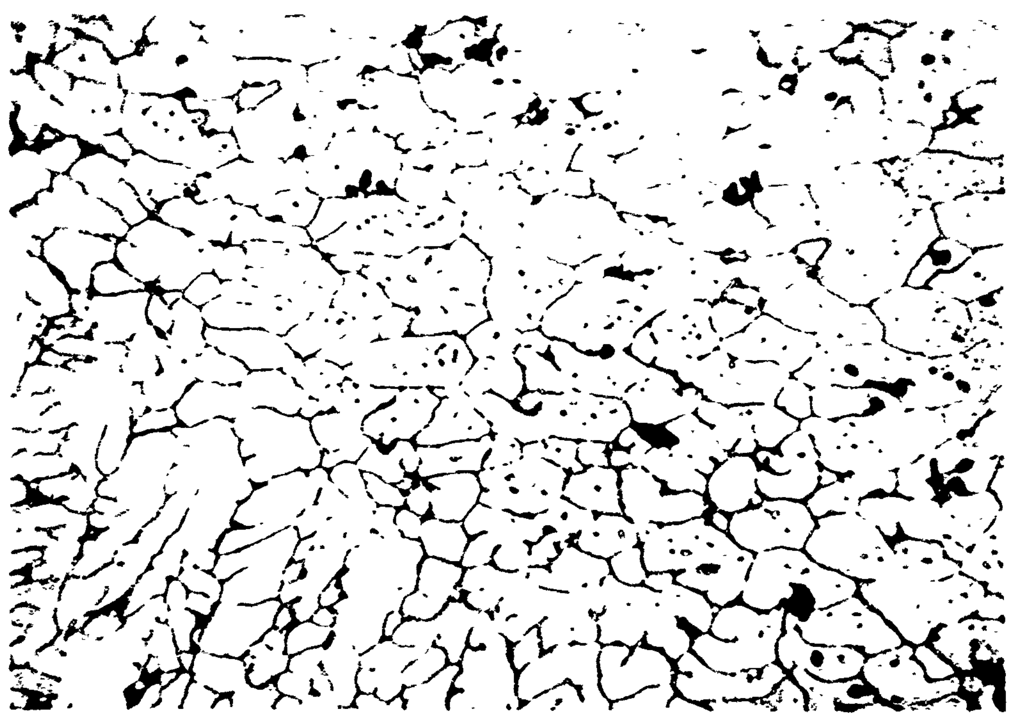

S-285658 140356-A 500X Keller's Etch

Made with 10Ar-65He cfh shielding gas

Figure 20 - Microstructure of the partially melted zone in the DCRP-GMA weld in .090-in. 2014-T6 sheet

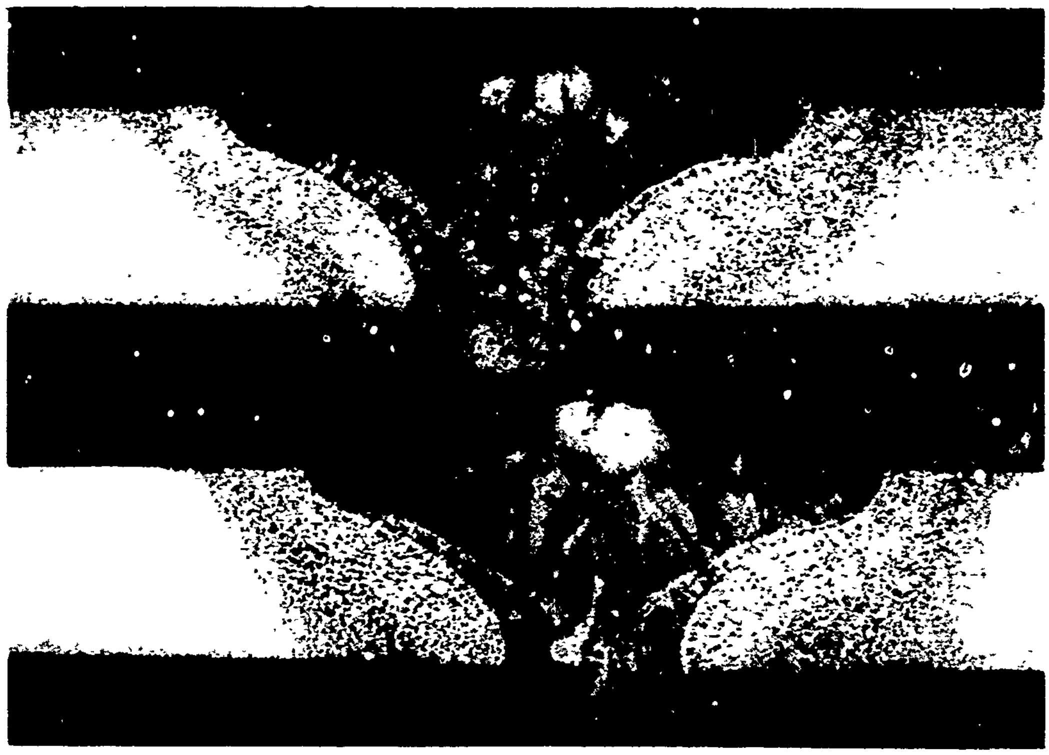

As welded

Post-weld aged

S-285757-3 and -4 140807-A 10X Keller's Etch

1/8-in. 2014-T6 (716 filler)

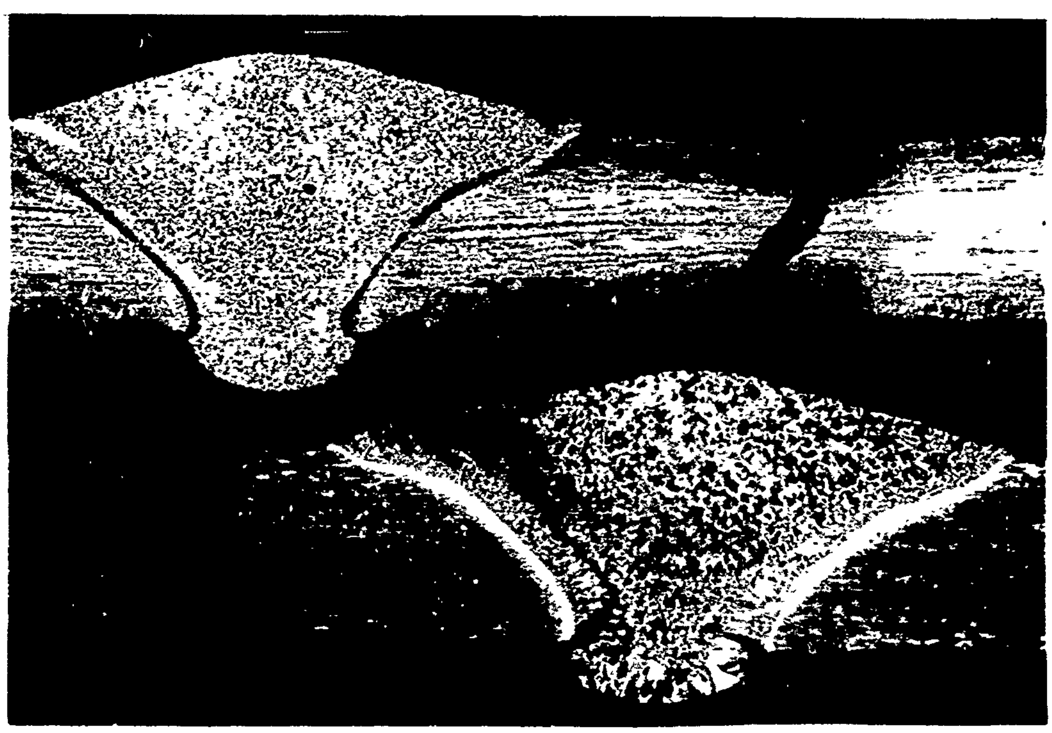

7106-T6

M791-T6

S-285740-4 285737-4 140808-A 10X Keller's Etch

Welded with 5180 filler and post weld aged

Figure 21- DCRP-GMA welds in 1/8-in. sheet made with conditions that produced pronounced nipple-shaped weld beads.

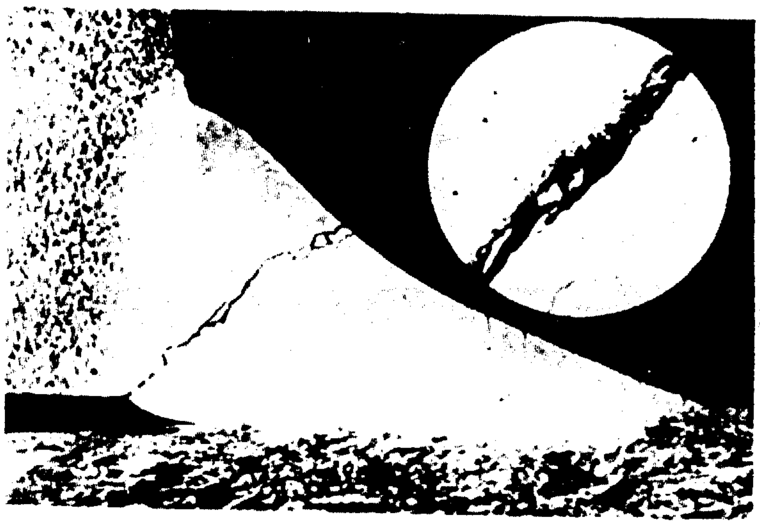

Hot short cracking in X7006/X5080 combination (Neg. PBE 167)

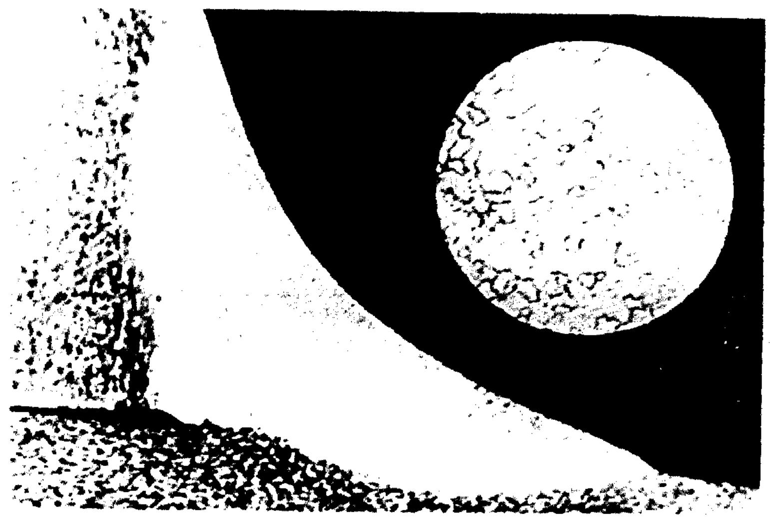

No cracking with X7106/X5180, which contains zirconium. (Neg. PBE 166)

Figure 22

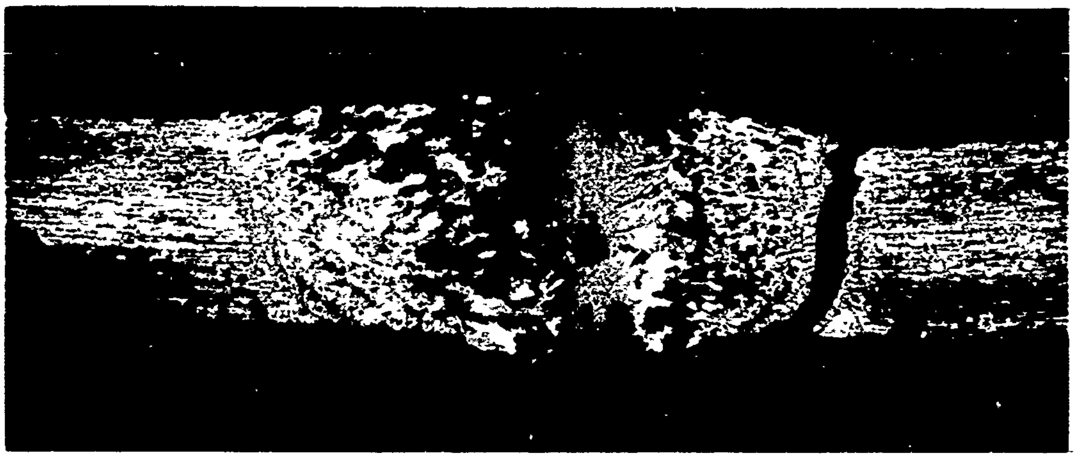

As-welded

S-285608-2 140197-A 10X Keller's Etch

Tensile failures occurred along fusion zone

TS- 58,600 YS-41800 4.2% El; BS - 56,900 Hgt. .57-in.

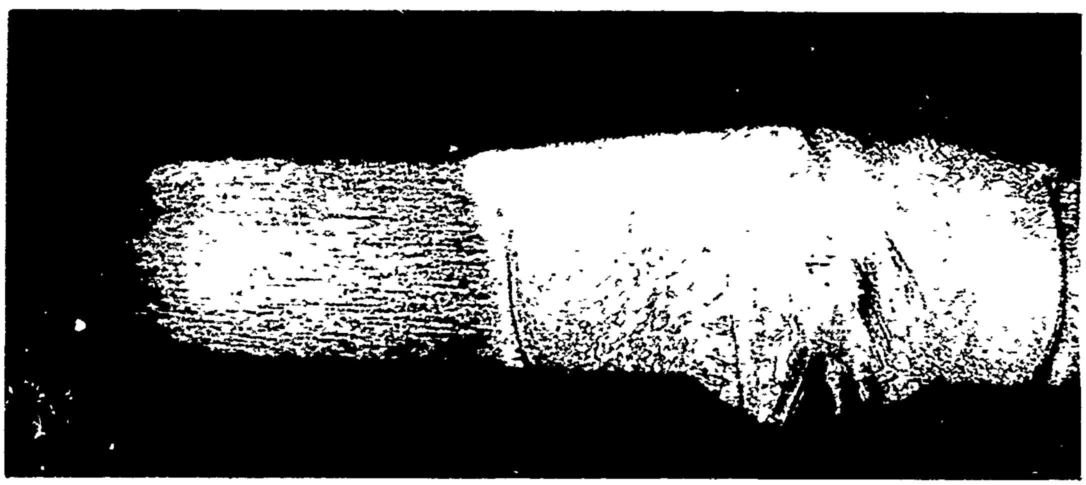

Post-weld aged

S-285609-4 140199-A 10X Keller's Etch

Tensile failures occurred in parent sheet 1/4-in. from weld

TS - 67,200 YS - 60,200 5.2% El BS - 70,000 Hgt. 1.09 [illegible]

Figure 23 - 1/8-in. M791-T6 sheet DCSP-GTA welded with 9Zn-3Mg filler

d

As welded

S-285606-3 140201-A 10X Keller's Etch

Tensile failures occurred in parent sheet 1/4-in. from weld

TS - 56,900 YS - 42,400 5% El; BS - 59,800 Hgt. .76-in.

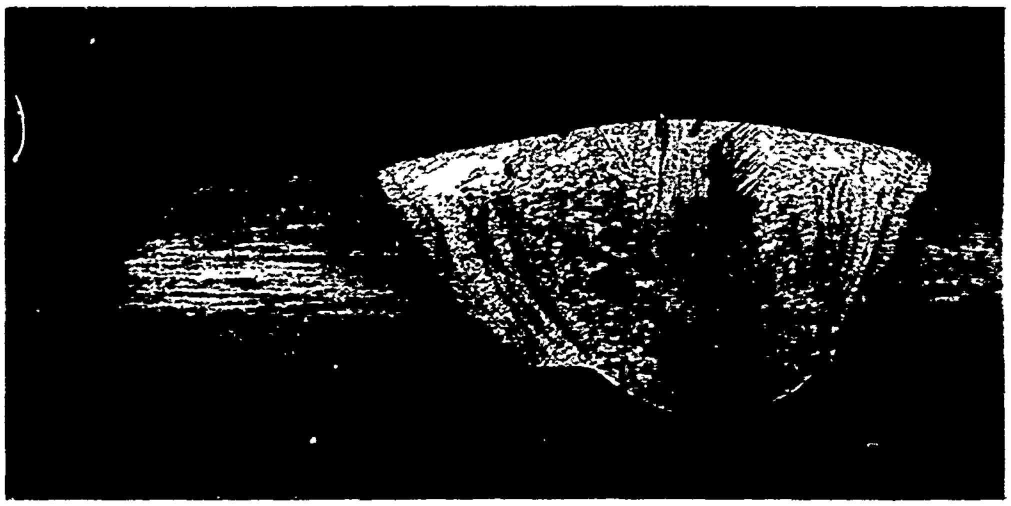

Post-weld aged

S-285607-2 140203-A 10X Keller's Etch

Tensile failures occurred in parent sheet 1/4-in. from weld

TS - 62,300 YS - 56,000 5.8% El; BS - 65,100 Hgt. 1.0 in.

Figure 24 - 1/8-in. M793-T6 sheet DCSP-GTA welded with 9Zn-2Mg filler

As welded

S-285606-2 140202-A 10X Keller's Etch

Tensile failure occurred through weld

TS - 46,000 YS - 32,400 4.5% El

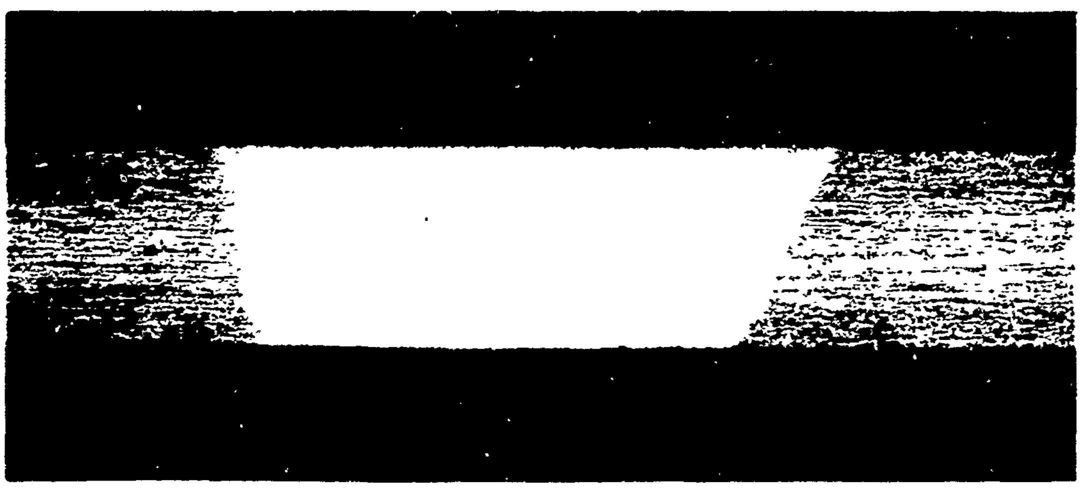

Post-weld aged

S-285607-2 140204-A 10X Keller's etch

Figure 25 - 1/8-in. M793-T6 sheet DCSP-GTA welded with 9Zn-2Mg filler. Weld bead shaved flush.

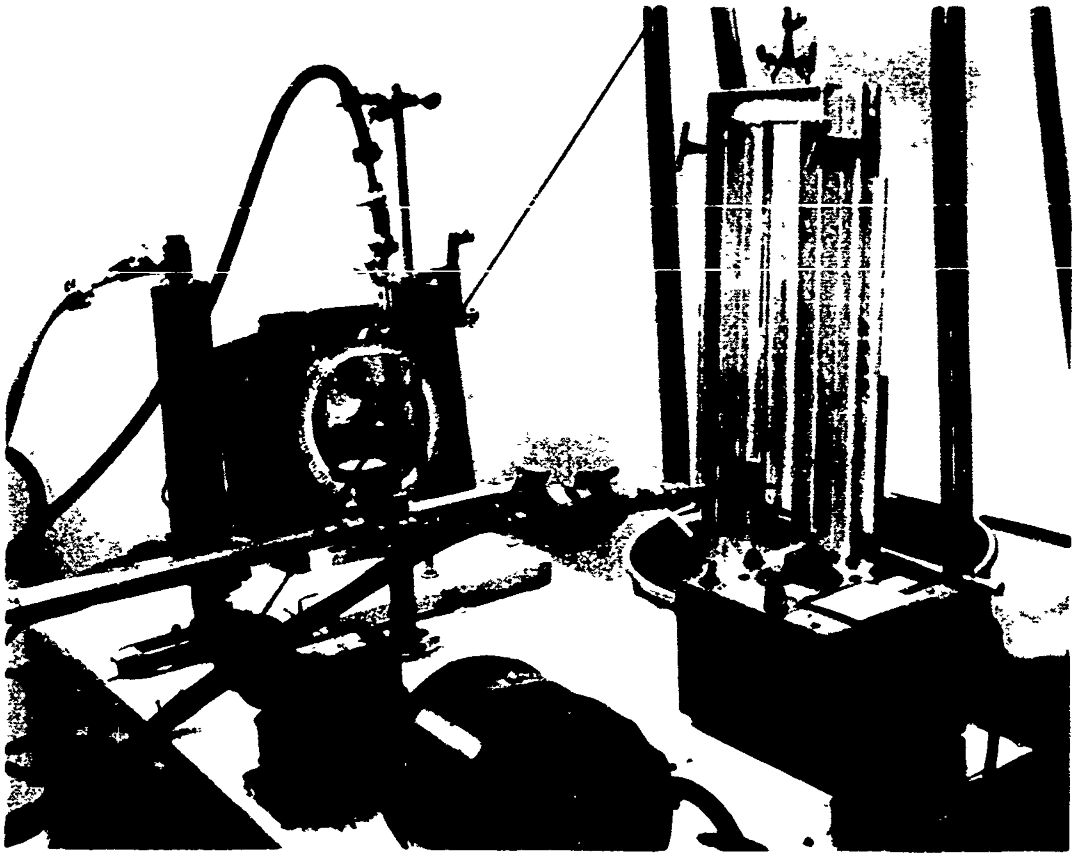

Figure 26 - Oxyacetylene flame heating apparatus for local heat treating of welds (Neg. PBC 240)

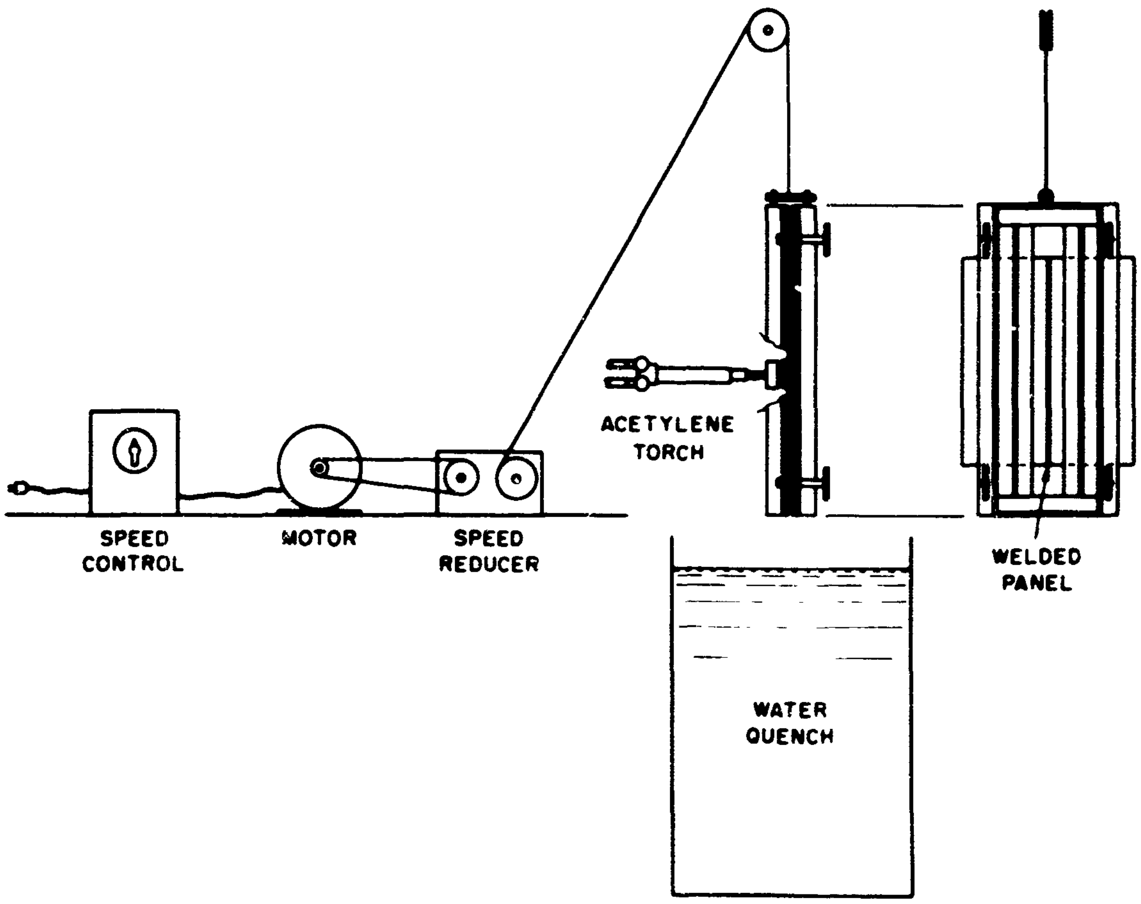

Figure 27 - Schematic illustrating the principal components of the above flame heating apparatus (Neg. PBF 014)

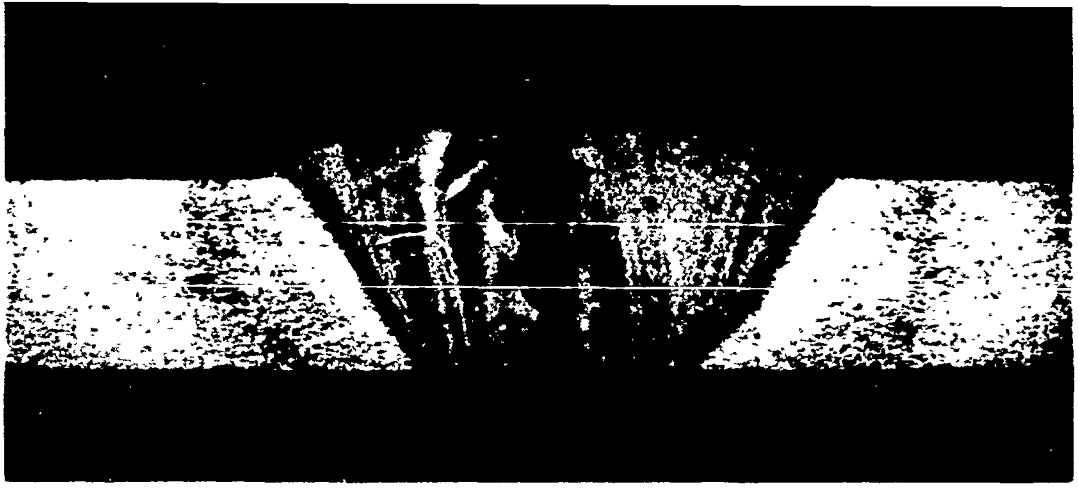

S-285519-1 138702-A 10X Keller's Etch

(a) - Not Reheated -

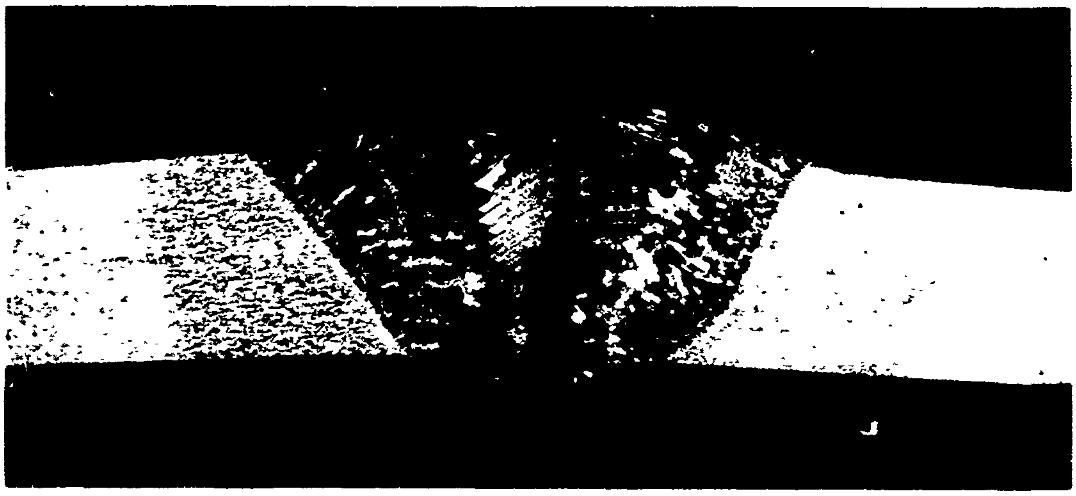

S-285448-8 138703-A 10X Keller's Etch

(b) Reheated with oxyacetylene flame on face side

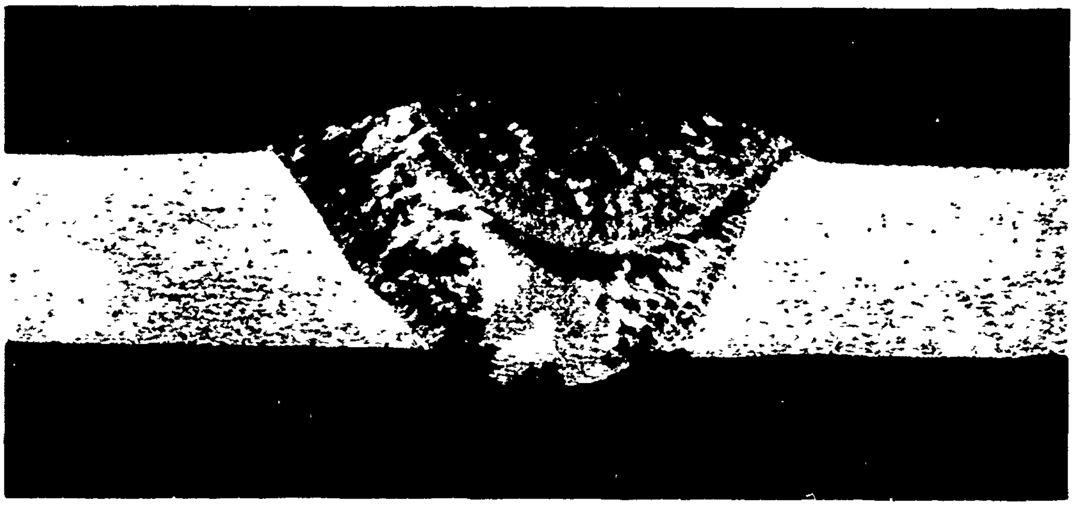

S-285448-12C 138704-A 10X Keller's Etch

(c) Reheated with low power DCSP-GTA arc on face side

Figure 28 - DCSP-GTA welds in 1/8-in. 7178-T6 sheet

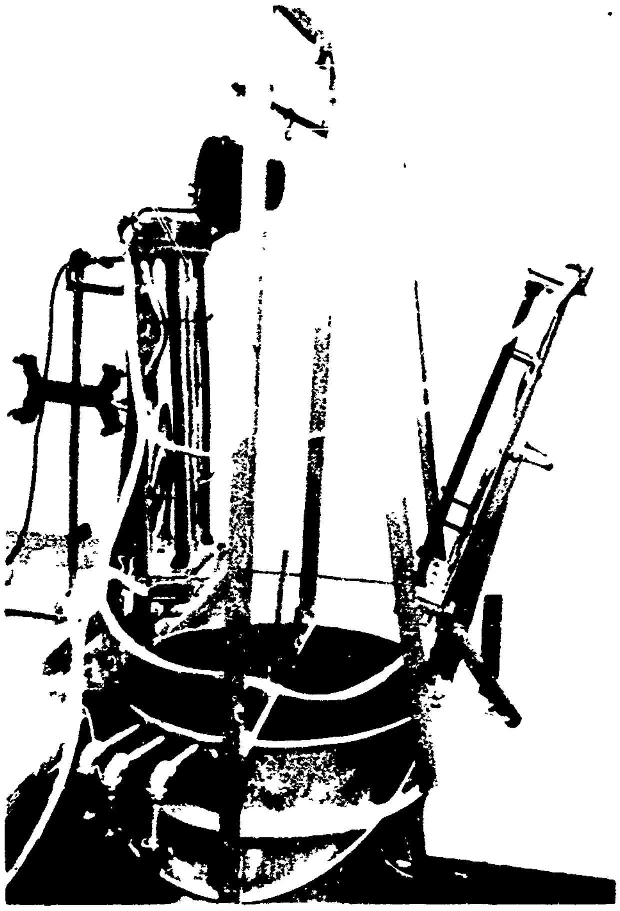

Hinged multiple-element quartz infrared heaters positioned above a water quench tank. (Neg. PBI 090)

Figure 29

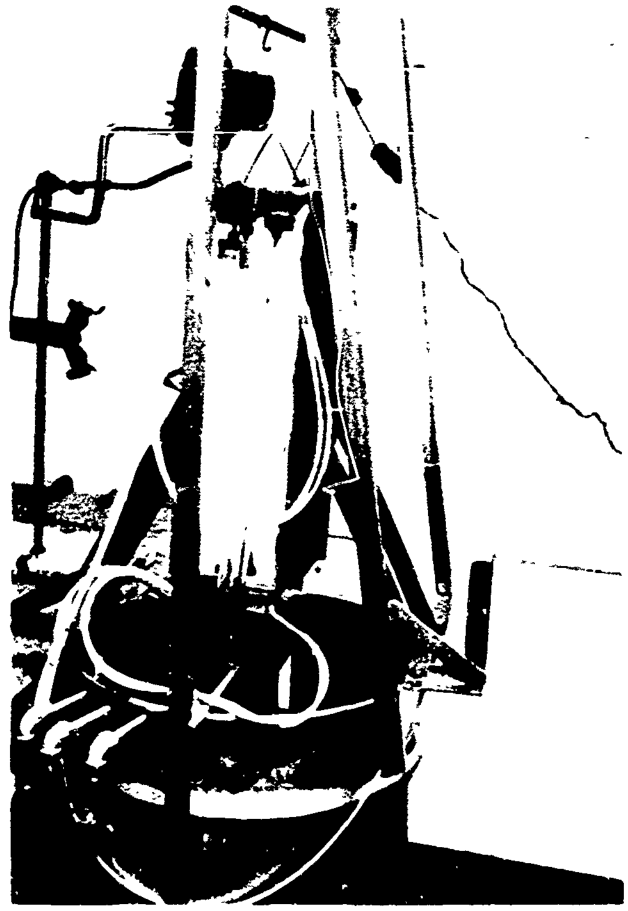

Welded panel being locally heat treated. The supporting wire was snipped to drop the panel into the water. (Neg. PBI 091)

Figure 30

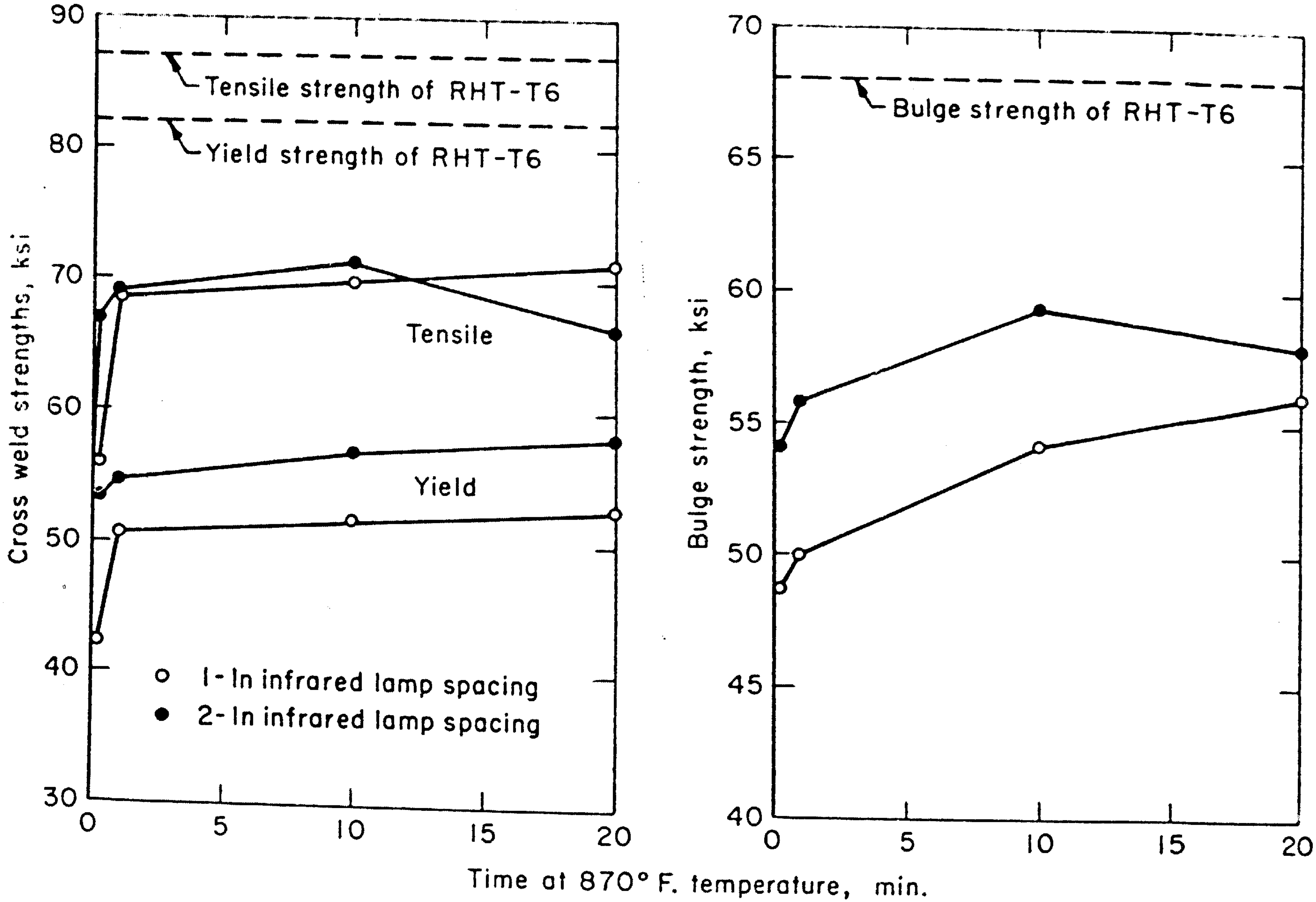

PROPERTIES OF DCSP-GTA WELDED 1/8 IN. 7178-T6 SHEET LOCALLY HEAT TREATED WITH QUARTZ INFRARED HEATERS MOUNTED VERTICALLY

Figure 31

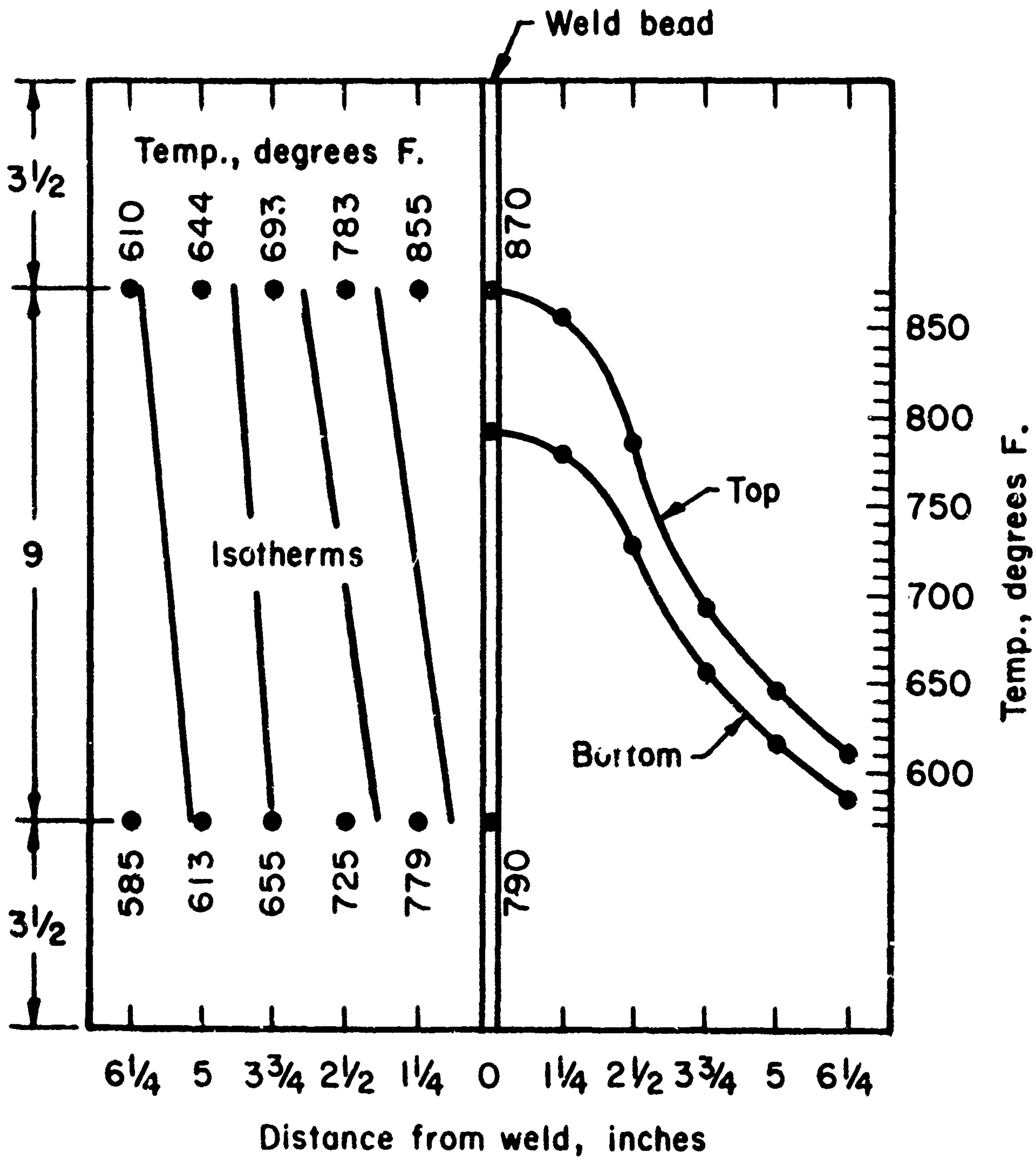

TEMPERATURE PROFILE OF 1/8 x 14 x 16-IN. PANEL LOCALLY HEAT TREATED VERTICALLY BETWEEN TWO BANKS OF INFRARED HEATERS

Figure 32

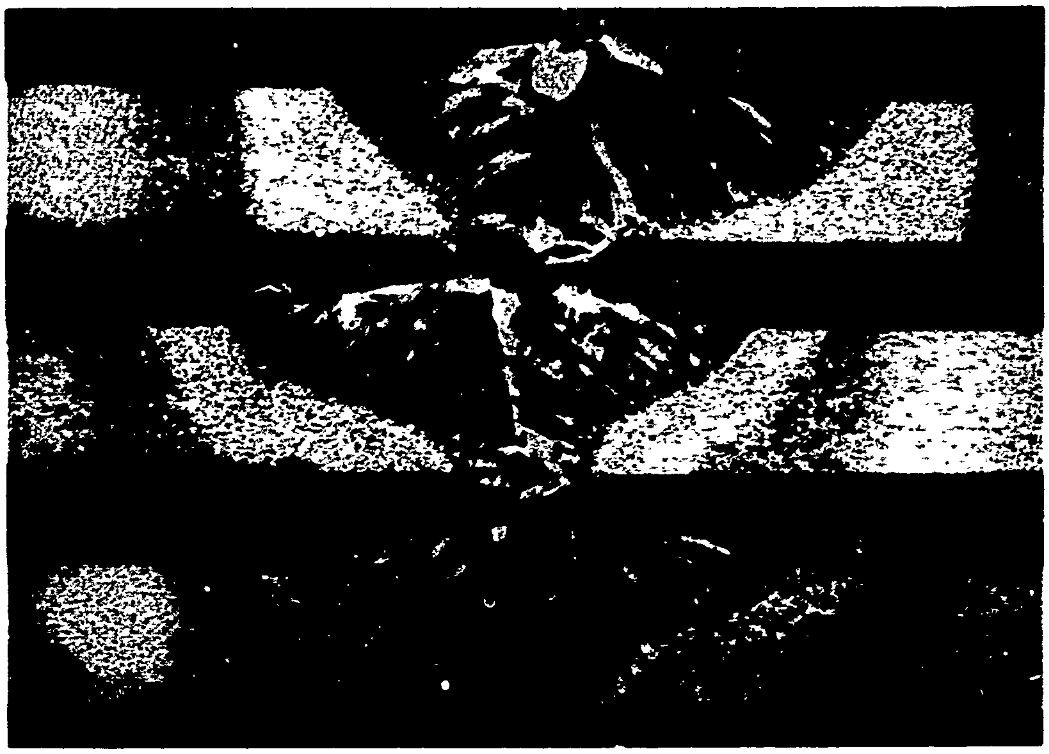

160

140

130

S-285512
22
23 138917A 10X Keller's Etch

Figure 33 - DCRP-GMA welds in .090-in. 2014-T6 made at 160, 140, and 130 amps at 26 volts, 55 ipm, 17Ar-33He

T

ERS

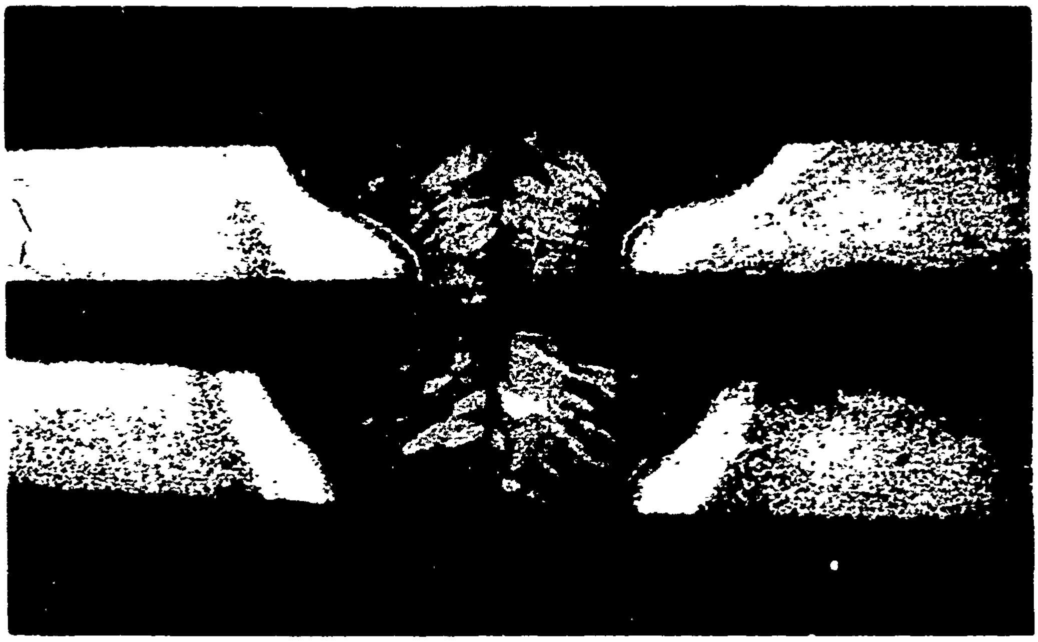

cfh He

75

60

S-285618-23 -25 | 139433A | 10X | Keller's Etch

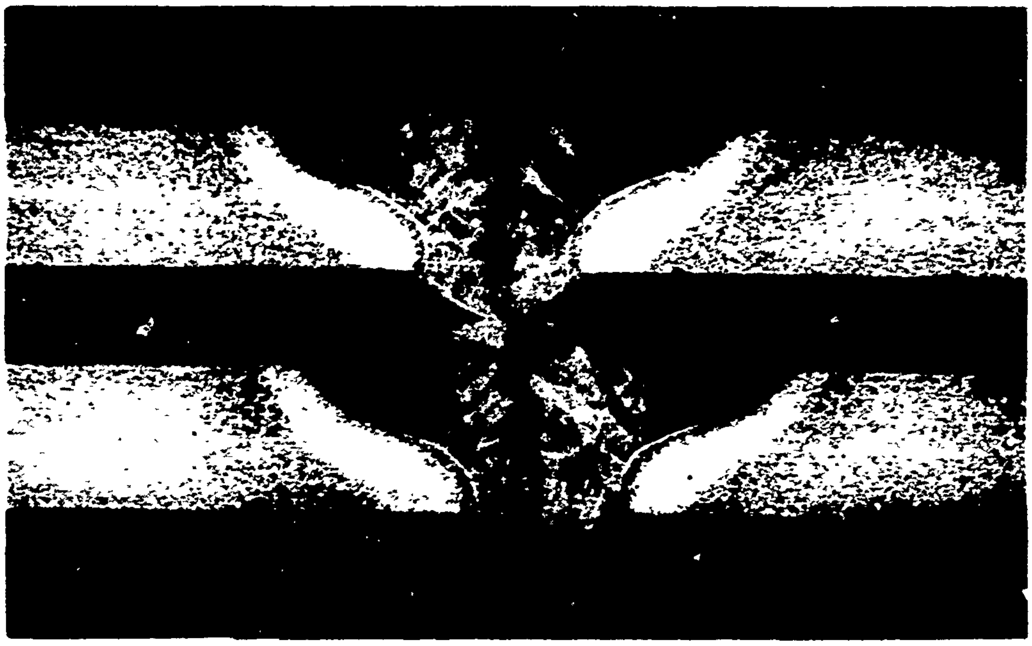

45

30

S-285618-27 -28 | 139433A | 10X | Keller's Etch

Figure 34 - Shows the change in bead shape of DCRP-GMA welds in .090-in. 2014-T6 sheet made with decreasing gas flow

ipm

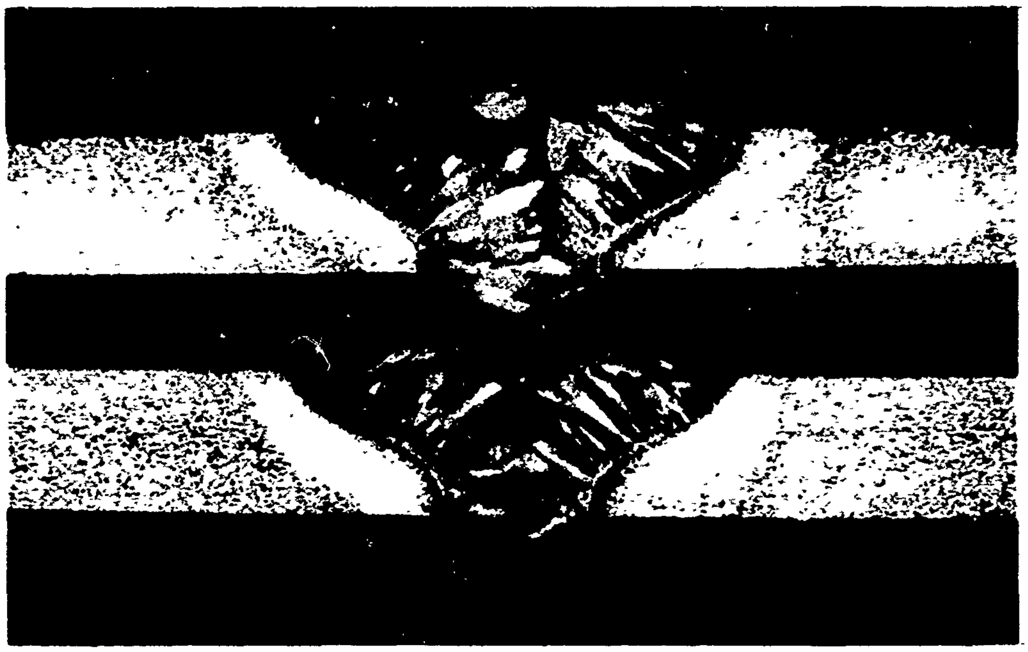

55

65

S-285618-3
-8 139427-A 10X Keller's Etch

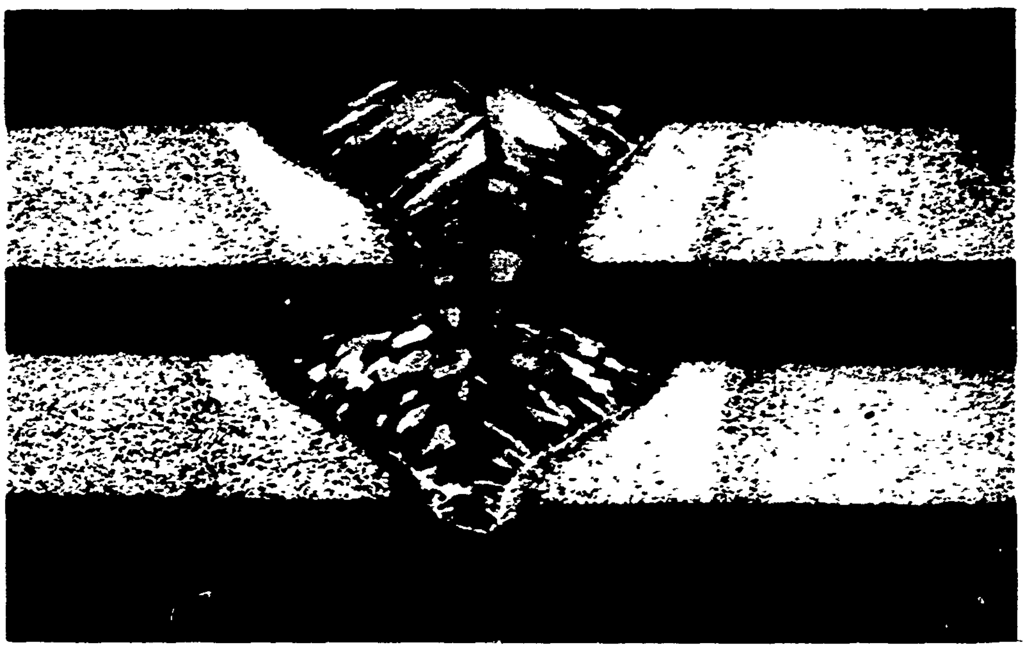

70

80

S-285618-9
-10 139428-A 10X Keller's Etch

Figure 35 - DCRP-GMA welds in .090-in. 2014-T6 sheet showing changes in bead shape with increasing weld travel speed

Travel Speed ipm	Heat Input Joules/sec
50	2930
40	2280

S-285618-35 -38 139434-A 10X Keller's Etch

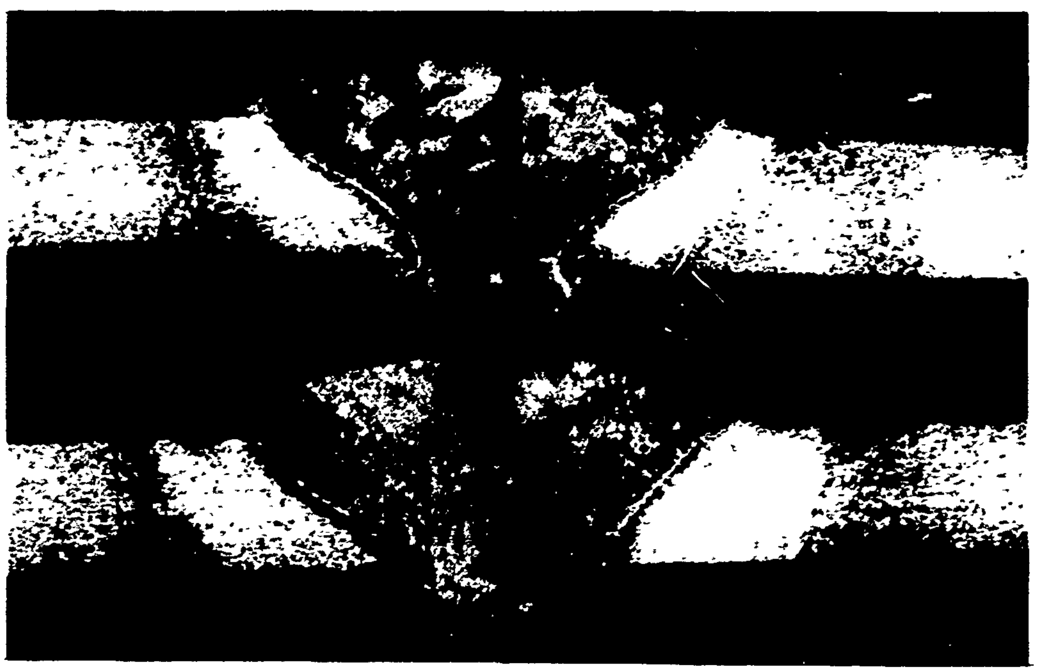

Travel Speed ipm	Heat Input Joules/sec
35	n2040
35	2050

S-285618-40 -41 139435-A 10X Keller's Etch

Figure 36 - DCRP-GMA welds in .090-in. 2014-T6 sheet showing change in bead shape with 100% Ar shielding and decreasing weld travel speed

eat
nput
les/sec

:930

:80

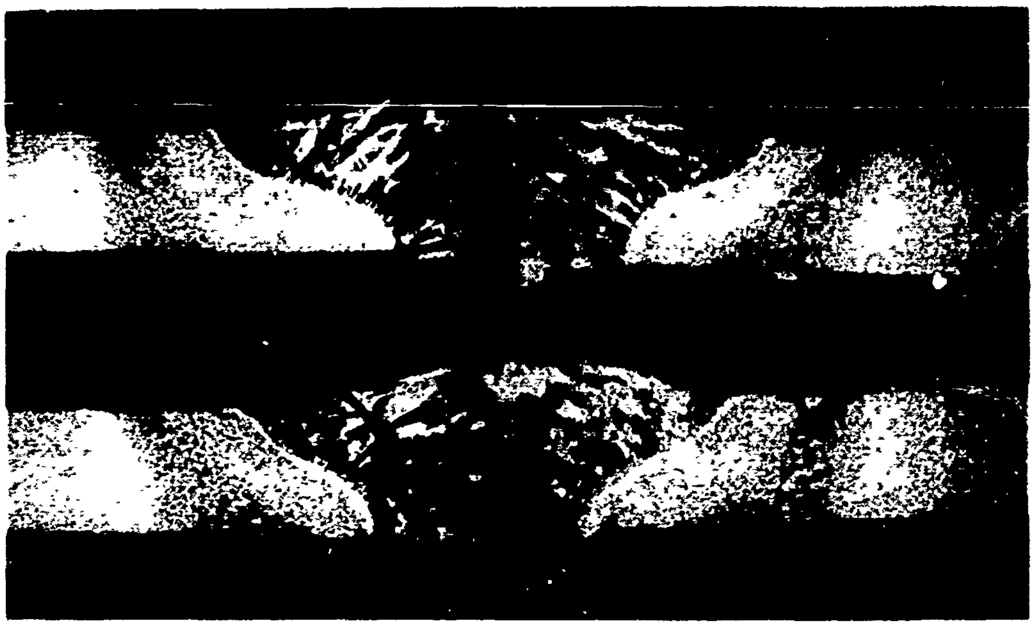

S-285841 140806-A 10X Keller's Etch

Made on a liquid nitrogen cooled copper backing bar

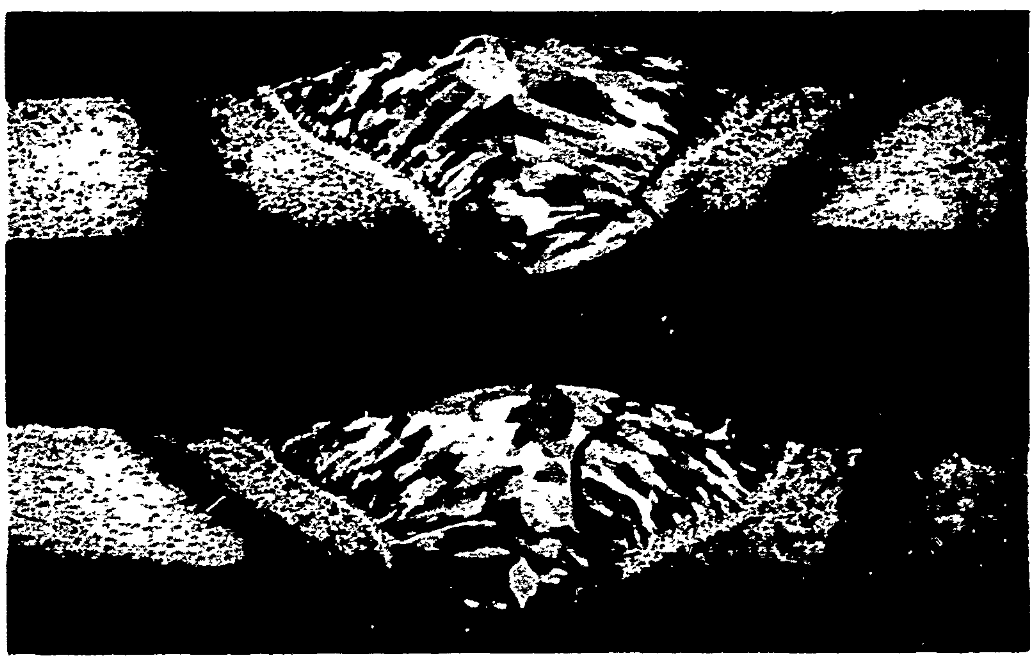

S-285658 140351-A Keller's Etch

Made on a room temperature copper backing bar

Figure 37 - DCRP-GMA welds in .090-in. 2014-T6 sheet made with 10Ar-65He cfh shielding gas mixture

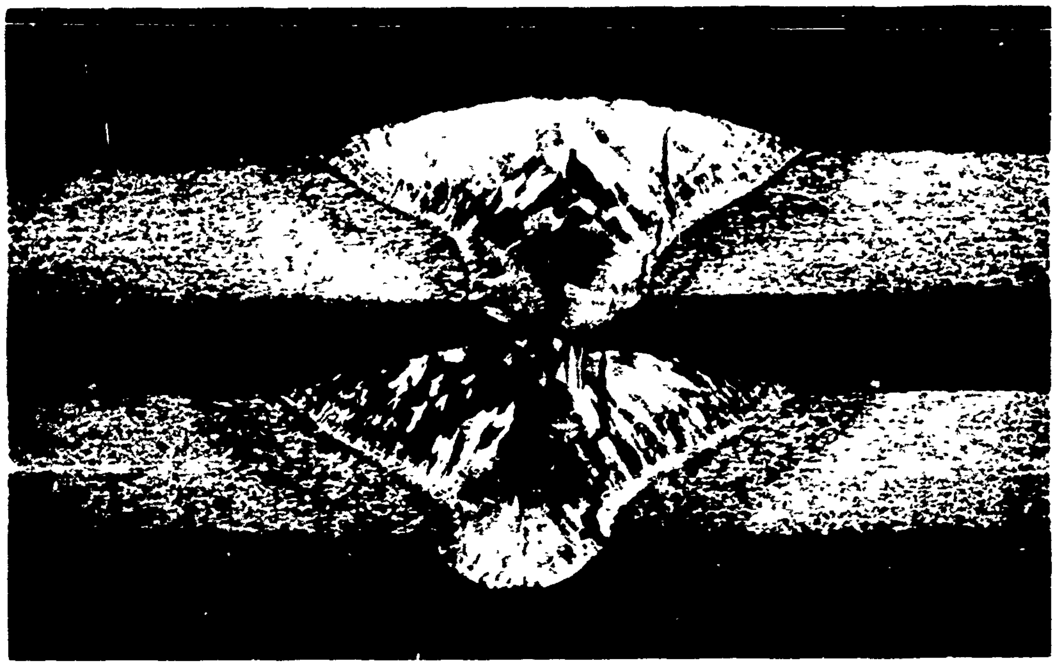

Liq. N_2

R.T.

S-93 B
121 B   139010-A   10X   Keller's Etch

Figure 38 - Frankford DCRP-GMA welds in .090-in. 2024-T86 sheet made on a liquid nitrogen-cooled and room-temperature backing bar. Notice the difference in width of the heat-affected zones.

N_2

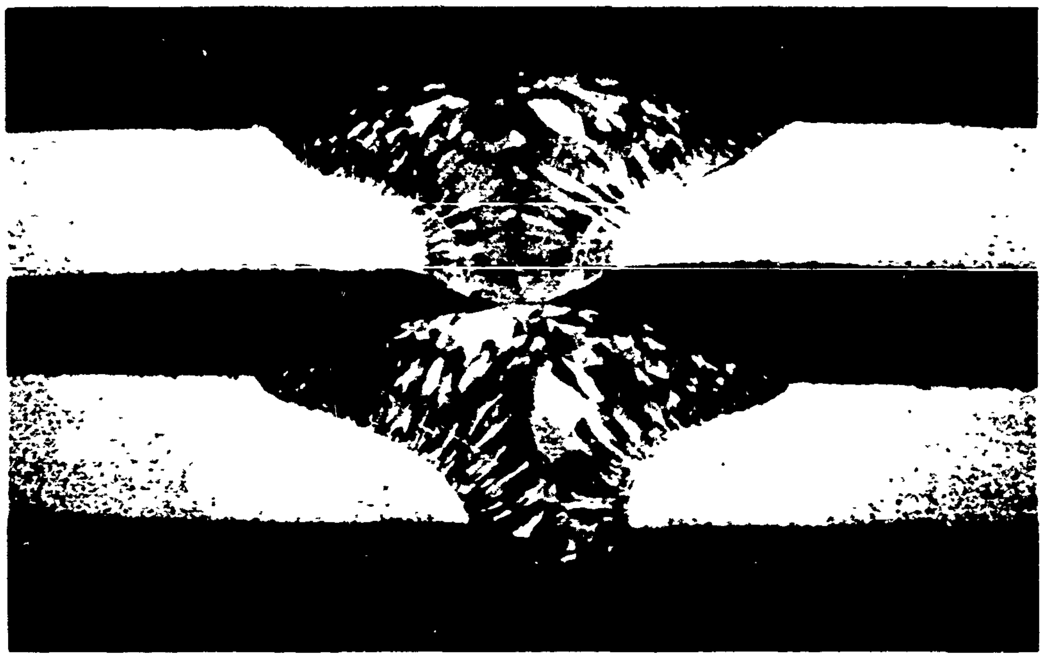

Naturally aged

Artificially aged

S-95B and 100A 139011-A 10X Keller's Etch

Made on liquid nitrogen cooled backing bar

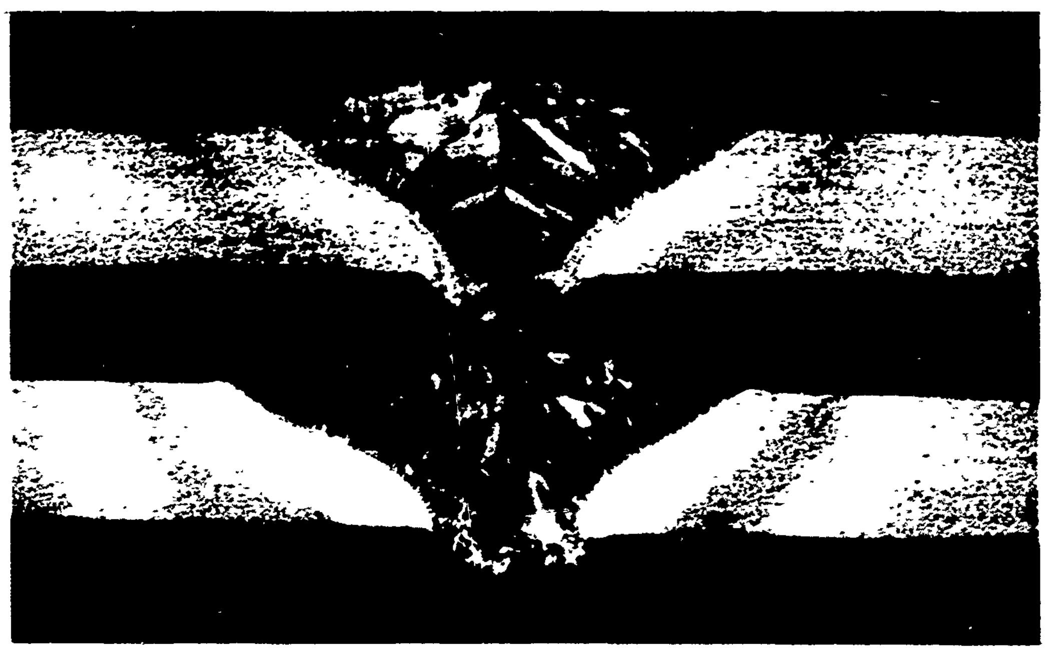

Naturally aged

Artificially aged

S-118A and 109A 139012A 10X Keller's Etch

Made on a room temperature backing bar

Figure 39 - Frankford DCRP-GMA welds in .090-in. 2014-T6 sheet

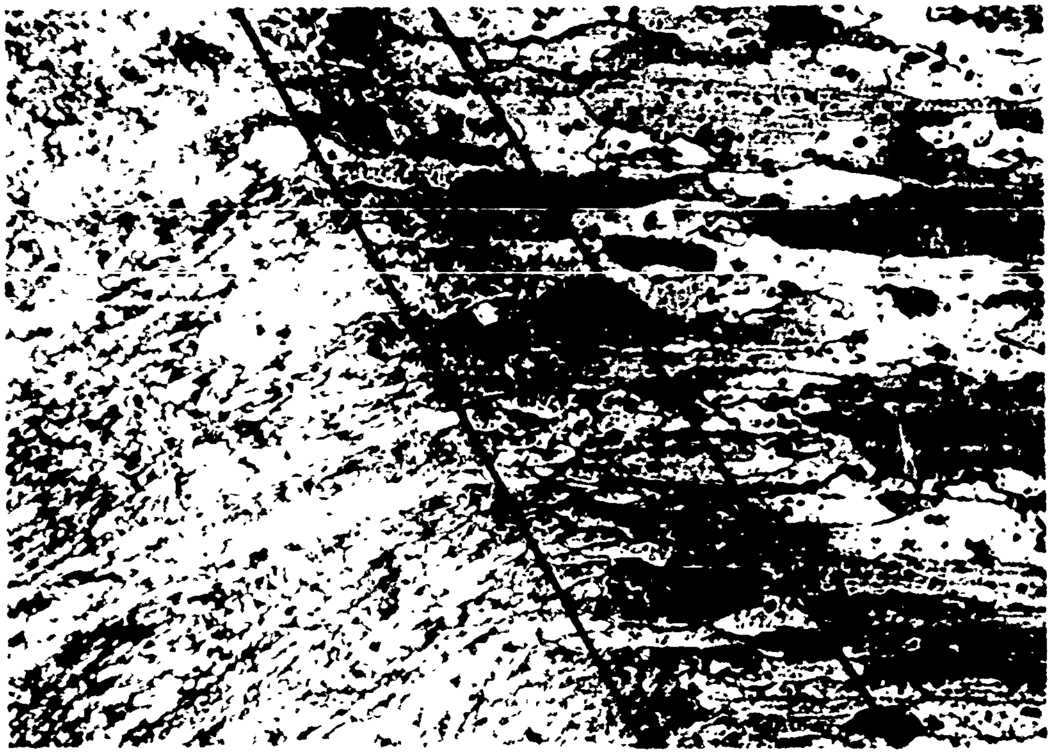

Liquid nitrogen cooled

S-93B 139053-A 300X Keller's Etch

RT

S-121B 139054-B 300X Keller's Etch

Figure 40 - Shows the difference in cell size in the weld nugget and in the width of the partially melted zone between welds in .090-in. 2024-T86 made on liquid nitrogen-cooled and room-temperature backing bars.

S-95B 139055-A 300X Keller's Etch

Made on a liquid nitrogen cooled backing bar

S-116A 139056-A 300X Keller's Etch

Made on a room temperature backing bar

Figure 41 - DCRP-GMA welds in .090-in. 2014-T6 sheet showing the smaller cell size and narrower partially melted zone in a liquid nitrogen-cooled weld than in a weld made on a room-temperature backing bar.